

Fabrication of Cold Spray Ti-O Coatings Engineered from  
Agglomerated Powders

(凝集粉末作製技術によるコールドスプレーTi-O 皮膜の創  
製)

July, 2016

Doctor of Engineering

Toibah Binti Abd. Rahim

トイバ ビンティ アブドラヒム

Toyohashi University of Technology

## Abstract

Current attention has focused on the preparation of thick ceramic coating using nanostructured materials as feedstock materials using thermal spray process. Cold spray method has appeared as a promising process to form ceramic nanostructured coating without significantly changing the microstructure of the initial feedstock materials whereas many conventional thermal spray processes do due to its low processing temperature. However, deposition of ceramic powders by cold spray is not easy due to brittle characteristics of the material. Moreover, the bonding mechanism on how the ceramic coating was formed on the substrate is still unclear as this method requires plastic deformation of particles upon the impact onto the substrate.

Therefore, in this study, focused have been made on the TiO<sub>2</sub> nanostructured feedstock materials which were synthesized throughout of the study. The properties of the powders also have been altered by several conditions in order to make it suitable for cold spray deposition. The mechanism of coating deposition and properties of the feedstock powders were investigated in this study. The following results which obtained by this study were summarized as below:

1. In this work, the synthesis of agglomerated TiO<sub>2</sub> powders, which are ready to be used as feedstock materials for a cold spray process after synthesis via a simple hydrolysis (TiO<sub>2</sub>-H) and hydrothermal (TiO<sub>2</sub>-HT) process, is described. The XRD patterns showed that single phase anatase TiO<sub>2</sub> was able to be produced using a low temperature process for the hydrolysis and hydrothermal methods. However, the results showed that TiO<sub>2</sub>-H powders have a smaller crystallite size and broader peaks compared with TiO<sub>2</sub>-HT powders. SEM and TEM analysis confirmed that the TiO<sub>2</sub>-H powders were built up from nano-sized particles, and were further agglomerated into micrometer-size, which is a preferable size for the cold spray process. On the other hand, TiO<sub>2</sub>-HT powders showed a formation of agglomerated particles with minimal particle agglomeration which was revealed by the SEM image and the particle size analyzer. A preliminary study on coating

deposition using cold spray showed that TiO<sub>2</sub>-H powders can be deposited onto ceramic tile substrate with a ~50µm thickness. Meanwhile for TiO<sub>2</sub>-HT powders, only particle embedment can be observed on the surface of the substrate. The results reveal that porosity contained in the agglomerated morphology is important in order to build up the coating by cold spray due to the tendency of the porous structure to break easily upon impact onto the substrate.

2. To further clarify the effect of porosity contain in the powder for the cold spray deposition, effect of low calcination on the as-synthesized TiO<sub>2</sub> by hydrolysis method have been conducted. Then, as-synthesized TiO<sub>2</sub> and calcined TiO<sub>2</sub> powders were studied on coating deposition by cold spray process. The results of this study indicated that a post treatment on TiO<sub>2</sub> powder improved powder deposition on ceramic tile substrate via the cold spray method. The cross-section of the obtained coating which was observed using SEM showed that nanoparticles TiO<sub>2</sub> powders in the agglomerated form were able to be deposited on the substrate and formed a thick coating. A stacking of agglomerated TiO<sub>2</sub> powders was found on the cross-section observation which is due to the breaking up of ceramic particles which was induced by porosity in the powder and is believed to be responsible for the formation of the coating. The results of this study also reveal that, when the feedstock powders have denser packing of particles and minimum number of porosity in the powder, breaking of particles during the spraying become more difficult. This hard and dense particle made them resistant to fragmentation and adherence on surface of the substrate.
3. Further study have been conducted by addition of ammonium sulfate; (NH<sub>4</sub>)<sub>2</sub>SO<sub>4</sub> during the powder synthesis. Addition of structure-directing agent, (NH<sub>4</sub>)<sub>2</sub>SO<sub>4</sub> promotes the agglomeration to occur with denser closed packing of particle arrangement which reduce the number of existing porosity in the synthesized powder. The addition of (NH<sub>4</sub>)<sub>2</sub>SO<sub>4</sub> addition was found to be very effective to unite the nano-sized particles together to form agglomeration in order to form the tertiary particles. The preliminary study of coating

formation depicted that the powder obtained could be used as the feedstock powder for cold spray process to make coating as it can be deposited onto the ceramic tile substrate. Once again, porosity in the powders was deduced as one of the crucial factors that contribute to better deposition of TiO<sub>2</sub> coating by cold spray process. Plastic deformation also may contribute to the formation of coating due to the used of nanostructured powders which received high local compact pressure during the spraying process.

4. Further studies on the obtained coating have been investigated. The study reveals that the properties of the coating (hardness, roughness and porosity) also depend on the properties of the initial feedstock powders. Moreover, anatase phase was preserved as revealed by the XRD analysis. This finding proves that cold spray process is suitable process to fabricate TiO<sub>2</sub> coating which can prevent phase transformation to occur due to low processing temperature. Details observation on the surface and cross-section of the coatings show that nanostructured particles from the feedstock powders were well-retained in the coating structure.
  
5. In order to study the individual particle impact morphologies, wipe tests were conducted on aluminum, copper and ceramic tile substrate. From the SEM observation, the results showed that the collided particles were plastically deformed and adhered on the hard ceramic tile substrate during deposition. However, in the case of aluminum and copper substrate, the splat diameters were smaller than the feedstock powder size and both particles and substrates were deformed during the collision. Moreover, many craters were observed on these metal substrates. It was found that the deposition behavior of TiO<sub>2</sub> particle and the crater formation by the cold spray process was affected by the hardness and surface roughness of the substrate materials.

# Table of Contents

Abstract.....	i
Table of Contents.....	iv
List of Figure.....	vii
List of Table.....	xi
1 Introduction .....	1
1.1 Titanium Dioxide (TiO <sub>2</sub> ).....	1
1.1.1 Phase Structure of Titanium Dioxide .....	1
1.1.2 Properties of TiO <sub>2</sub> .....	1
1.1.3 Applications of TiO <sub>2</sub> as Photocatalyst.....	3
1.2 Titanium Dioxide Coatings .....	5
1.2.1 Conventional Coating Processes .....	5
1.2.2 Thermal spray process .....	6
1.3 Current Studies/ Developments of Thermal Spray Titanium Dioxide Coating .....	7
1.3.1 Conventional Thermal Spray Processes .....	7
1.3.2 Low Temperature Process .....	11
1.4 Cold Spray Technology.....	14
1.4.1 Basic Principles.....	14
1.4.2 Bonding Mechanism in Cold Spray .....	16
1.5 Titanium Dioxide as Ceramic Feedstock Materials for Cold Spray Process .....	26
1.5.1 Feedstock Materials for Cold Spray Process .....	26
1.5.2 Conventional TiO <sub>2</sub> Powders .....	27
1.5.3 Nanopowders.....	29
1.6 Objectives.....	33
1.7 Thesis Organization.....	34
1.8 References .....	36
2 Synthesis and Properties of Agglomerated TiO <sub>2</sub> Powder by Hydrolysis and Hydrothermal Methods for Cold Spray Coating .....	41
2.1 Introduction .....	41
2.2 Experimental Procedure .....	43

2.2.1	Synthesis of TiO <sub>2</sub> Powders by Hydrolysis Method .....	43
2.2.2	Synthesis of TiO <sub>2</sub> Powders by Hydrothermal Method .....	43
2.2.3	TiO <sub>2</sub> Coating by Cold Spray Process .....	44
2.2.4	Characterization of TiO <sub>2</sub> Powders and Coating.....	44
2.3	Results & Discussion .....	45
2.3.1	Characterizations of TiO <sub>2</sub> powders .....	45
2.3.2	Microstructure and Crystalline Structure of TiO <sub>2</sub> Coating .....	51
2.3.3	Deposition Mechanism .....	54
2.4	Conclusions .....	56
2.5	References .....	57
3	Cold-Sprayed Titanium Dioxide Coating Using Powders Calcined at Low Temperatures .....	59
3.1	Introduction .....	59
3.2	Experimental Procedures.....	61
3.2.1	Preparation of TiO <sub>2</sub> Powders for Cold Spray Coating.....	61
3.2.2	Cold Spray Process .....	62
3.2.3	Characterization of TiO <sub>2</sub> Powders and Coating.....	62
3.3	Results & Discussion .....	63
3.3.1	Effects of Low Calcination Temperatures on the Properties of TiO <sub>2</sub> Powders .....	63
3.3.2	Coating Development using as-synthesized TiO <sub>2</sub> and Calcined TiO <sub>2</sub> Powders.....	74
3.4	Conclusions .....	79
3.5	References .....	80
4	Cold Sprayed TiO <sub>2</sub> Coating from Nanostructured Ceramic Agglomerated Powders .....	82
4.1	Introduction .....	82
4.2	Experimental Procedure .....	84
4.2.1	Materials .....	84
4.2.2	Cold Spray Process .....	85
4.2.3	Characterization of Feedstock Materials and Cold-sprayed TiO <sub>2</sub> Coatings .....	86
4.3	Results & Discussion .....	87
4.3.1	Characterization of as-synthesized TiO <sub>2</sub> powders with different mol % addition of (NH <sub>4</sub> ) <sub>2</sub> SO <sub>4</sub> .....	87
4.3.2	Characterization of as-synthesized TiO <sub>2</sub> powders used for cold spray process.....	92

4.3.3	Characterization of TiO <sub>2</sub> coatings prepared by cold spray method .....	102
4.4	Conclusions .....	115
4.5	References .....	116
5	Effect of Substrate Material on Cold-Sprayed Titanium Dioxide Coating.....	118
5.1	Introduction .....	118
5.2	Experimental Procedure .....	121
5.2.1	Synthesis of Agglomerated TiO <sub>2</sub> Powders.....	121
5.2.2	TiO <sub>2</sub> Coating Preparation by Cold Spray Process .....	121
5.2.3	Characterization of TiO <sub>2</sub> Powders and TiO <sub>2</sub> Coating .....	123
5.3	Results & Discussion .....	123
5.4	Conclusions .....	135
5.5	References .....	136
6	General Conclusions & Recommendations for Future Work.....	138
6.1	General Conclusions.....	138
6.1.1	Feedstock particle size .....	139
6.1.2	Porosity .....	140
6.1.3	Crystallinity.....	140
6.1.4	Substrate materials.....	141
6.2	Recommendations for Future Work .....	142
7	Contribution of Study.....	143
7.1	Contribution of This Study to the Research/ Academic Field .....	143
7.2	Contribution of This Study to the Industrial Field.....	144
8	Publications List and Oral Presentations .....	145
8.1	List of Papers/Journals and Proceedings with Referee’s Review .....	145
8.1.1	List of Journals.....	145
8.1.2	List of Proceedings .....	145
8.2	Oral presentations .....	146
9	Acknowledgements.....	148

## List of Figure

Figure 1.1: Simplified principle of the conventional thermal spray process using ceramic as feedstock materials. ....	8
Figure 1.2: Schematic diagram showing the phase transformation of anatase TiO <sub>2</sub> to rutile TiO <sub>2</sub> during the conventional thermal spray process. ....	9
Figure 1.3: SEM image of TiO <sub>2</sub> powder (a) and its cross section which shows that the agglomerated particles with solid and dense particles after have been tempered at 600°C.....	18
Figure 1.4: SEM images of cold-sprayed TiO <sub>2</sub> coatings on AlMg <sub>3</sub> substrate. (a) Sprayed as one pass and (b) sprayed with 10 passes. ....	18
Figure 1.5: SEM image of cross-section of polymer coated with TiO <sub>2</sub> using cold spray method. ....	19
Figure 1.6: Proposed mechanism of particle bonding of a cold spray coating on a polymer substrate ...	20
Figure 1.7: SEM image of (a) the spray TiO <sub>2</sub> powder agglomerated from nanoparticles using polymer binder and (b) the cross-section of TiO <sub>2</sub> coating deposited by cold spray process.....	21
Figure 1.8: Cross section microstructure of coatings sprayed with He. Spraying with gas temperature of (a) 200 °C, (b) 300 °C, and (c) 400 °C.....	22
Figure 1.9: Cross section microstructure of coatings sprayed with N <sub>2</sub> . Spraying with gas temperature of (a) 200 °C, (b) 300 °C, and (c) 400 °C.....	22
Figure 1.10: Morphology of TiO <sub>2</sub> feedstock powder; (a) SEM image, (b) FE-SEM image, (c) TEM image and schematic image of adhesion mechanism of cold-sprayed TiO <sub>2</sub> particle . ....	23
Figure 1.11: The cold spray result of (a) as-synthesized, (b) annealed, and (c) hydrothermal treated TiO <sub>2</sub> powders deposited on copper substrates. ....	24
Figure 1.12: SEM micrograph of the cold spray coating cross-sectional area: (a) cold sprayed nano-TiO <sub>2</sub> layer, (b) APS TiO <sub>2</sub> - coating, and (c) steel substrate. ....	25
Figure 1.13: SEM image of (a) conventional fused and crushed titania feedstock particle and (b) particle of (a) observed at higher magnification; absence of nanostructural character. ....	28
Figure 1.14: (a) Typical morphology of agglomerated spray-dried titania powders. (b) High magnification view of (a)—agglomeration of individual nanosized titania particles and (c) Nanotexture formed by a semi-molten agglomerate on the surface of an HVOF-sprayed nanostructured titania coating. ....	31
Figure 2.1: Schematic diagram of cold spray system.....	44



Figure 2.2: TEM images of TiO <sub>2</sub> powders that synthesized by hydrolysis (a) and hydrothermal (b) method. .....	46
Figure 2.3: SEM images of TiO <sub>2</sub> powders that synthesized by hydrolysis (a & c) and hydrothermal (b & d) methods. ....	47
Figure 2.4: FESEM images of TiO <sub>2</sub> powders that synthesized by (a) hydrolysis and (b) hydrothermal method.....	48
Figure 2.5: Particle size distribution profile of starting agglomerated TiO <sub>2</sub> powders synthesized by (a) hydrolysis and (b) hydrothermal method.....	49
Figure 2.6: XRD pattern of TiO <sub>2</sub> powders that were synthesized by (a) hydrolysis (TiO <sub>2</sub> -H) and (b) hydrothermal (TiO <sub>2</sub> -HT). ....	51
Figure 2.7: Cross-sectional view of TiO <sub>2</sub> coating deposited by cold spray using powder synthesis by (a) hydrolysis (TiO <sub>2</sub> -H) and (b) hydrothermal (TiO <sub>2</sub> -HT). ....	52
Figure 2.8: XRD pattern of (a) TiO <sub>2</sub> -H powder and (a) TiO <sub>2</sub> -H coating deposited by cold spay process.....	53
Figure 2.9: Possible mechanism of bonding between TiO <sub>2</sub> powders and the substrates using powder synthesized by (a) hydrolysis and (b) hydrothermal method. ....	55
Figure 3.1: DTA curve recorded in air with a 10°C/ min heating rate for as-synthesized TiO <sub>2</sub> . ....	64
Figure 3.2: XRD patterns of TiO <sub>2</sub> powders that calcined at different temperatures; (a) as-synthesized powder (TiO <sub>2</sub> -0), (b) TiO <sub>2</sub> powder calcined at 200°C (TiO <sub>2</sub> -2), (c) TiO <sub>2</sub> powder calcined at 300°C (TiO <sub>2</sub> -3) and (d) TiO <sub>2</sub> powder calcined at 400°C (TiO <sub>2</sub> -4).....	66
Figure 3.3: The XPS spectra of (a) wide scan spectra of TiO <sub>2</sub> powders that calcined at different temperatures and narrow scan spectra of TiO <sub>2</sub> powders that calcined at different temperatures corresponds to (b) Ti 2 <i>p</i> , (c) O 1 <i>s</i> , and (d) S2 <i>p</i> .....	69
Figure 3.4: SEM micrographs of TiO <sub>2</sub> powders calcined at different temperatures: (a) as-synthesized powder (TiO <sub>2</sub> -0), (b) TiO <sub>2</sub> powder calcined at 200°C (TiO <sub>2</sub> -2), (c) TiO <sub>2</sub> powder calcined at 300°C (TiO <sub>2</sub> -3) and (d) TiO <sub>2</sub> powder calcined at 400°C (TiO <sub>2</sub> -4).....	71
Figure 3.5: SEM images taken at high magnification of TiO <sub>2</sub> powders calcined at different temperatures: (a) as-synthesized powder (TiO <sub>2</sub> -0), (b) TiO <sub>2</sub> powder calcined at 200°C (TiO <sub>2</sub> -2), (c) TiO <sub>2</sub> powder calcined at 300°C (TiO <sub>2</sub> -3) and (d) TiO <sub>2</sub> powder calcined at 400°C (TiO <sub>2</sub> -4).....	72
Figure 3.6: TEM micrographs of TiO <sub>2</sub> powders calcined at different temperatures: (a) as-synthesized powder (TiO <sub>2</sub> -0), (b) TiO <sub>2</sub> powder calcined at 200°C (TiO <sub>2</sub> -2), (c) TiO <sub>2</sub> powder calcined at 300°C (TiO <sub>2</sub> -3) and (d) TiO <sub>2</sub> powder calcined at 400°C (TiO <sub>2</sub> -4).....	73

Figure 3.7: Cross-sectional view of the nanostructured TiO <sub>2</sub> coating deposited on a ceramic tile substrate by a CS process using: (a) as-synthesized powder (TiO <sub>2</sub> -0), (b) TiO <sub>2</sub> powder calcined at 200°C (TiO <sub>2</sub> -2), and (c) TiO <sub>2</sub> powder calcined at 300°C (TiO <sub>2</sub> -3). .....	75
Figure 3.8: Cross-sectional view of TiO <sub>2</sub> coating using powder calcined at 300°C revealing coatings that were formed by the stacking of TiO <sub>2</sub> agglomerates: (a) low magnification (x 300) and (b) & (c) higher magnification (x 3000). .....	78
Figure 4.1: Synthesis of TiO <sub>2</sub> powders with different mol% addition of (NH <sub>4</sub> ) <sub>2</sub> SO <sub>4</sub> by simple hydrolysis method.....	85
Figure 4.2: SEM images of the TiO <sub>2</sub> powders synthesized with different mol% addition at different magnifications: (a, f & j) 0, (b, g & l) 0.1, (c, h & m) 0.5, (d, i & n) 1 and (e, j & o) 5. ....	89
Figure 4.3: X-ray diffraction patterns of as-synthesized TiO <sub>2</sub> : (a) without addition of (NH <sub>4</sub> ) <sub>2</sub> SO <sub>4</sub> and (b) with 1 mol% addition of (NH <sub>4</sub> ) <sub>2</sub> SO <sub>4</sub> . ....	94
Figure 4.4: SEM image and EDX elemental mapping of Ti, O and S in TiO <sub>2</sub> powders synthesized with 1 mol% addition of (NH <sub>4</sub> ) <sub>2</sub> SO <sub>4</sub> . .....	96
Figure 4.5: XPS spectra of the S 2p region for the as-synthesized TiO <sub>2</sub> powders: (a) without addition of (NH <sub>4</sub> ) <sub>2</sub> SO <sub>4</sub> and (b) with 1 mol% addition of (NH <sub>4</sub> ) <sub>2</sub> SO <sub>4</sub> . ....	97
Figure 4.6: SEM micrograph of as-synthesized TiO <sub>2</sub> : (a & c) without addition of (NH <sub>4</sub> ) <sub>2</sub> SO <sub>4</sub> and (b & d) with addition of (NH <sub>4</sub> ) <sub>2</sub> SO <sub>4</sub> . ....	99
Figure 4.7: High-resolution TEM pictures of crystalline grains for the as-synthesized TiO <sub>2</sub> : (a) without addition of (NH <sub>4</sub> ) <sub>2</sub> SO <sub>4</sub> and (b) with addition of (NH <sub>4</sub> ) <sub>2</sub> SO <sub>4</sub> . The red arrows show some of the single size of 1° nano-particles. ....	100
Figure 4.8: DTA curved of as-synthesized TiO <sub>2</sub> via hydrolysis method.....	102
Figure 4.9: Cross-sectional view of TiO <sub>2</sub> coating deposited on ceramic tiles by cold spray process, respectively: (a) without addition of (NH <sub>4</sub> ) <sub>2</sub> SO <sub>4</sub> and (b) with addition of (NH <sub>4</sub> ) <sub>2</sub> SO <sub>4</sub> . ....	104
Figure 4.10: XRD patterns of powder and coating using different type of TiO <sub>2</sub> powder, respectively: (a) without addition of (NH <sub>4</sub> ) <sub>2</sub> SO <sub>4</sub> and (b) with addition of (NH <sub>4</sub> ) <sub>2</sub> SO <sub>4</sub> . ....	105
Figure 4.11: SEM images of single impact morphologies of TiO <sub>2</sub> powders on substrate using TiO <sub>2</sub> powders synthesized (a) without addition of (NH <sub>4</sub> ) <sub>2</sub> SO <sub>4</sub> and (b) with addition of (NH <sub>4</sub> ) <sub>2</sub> SO <sub>4</sub> .....	107
Figure 4.12: Details of SEM images of existing porosity of as-synthesized TiO <sub>2</sub> with arrows show some of the existing porosity in the obtained TiO <sub>2</sub> powder; (a) TiO <sub>2</sub> powders without addition of (NH <sub>4</sub> ) <sub>2</sub> SO <sub>4</sub> and (b)with addition of (NH <sub>4</sub> ) <sub>2</sub> SO <sub>4</sub> , respectively. ....	110

Figure 4.13: SEM images of cross-section of coating and surface of coating, respectively: (a) & (c) TiO<sub>2</sub> without addition of (NH<sub>4</sub>)<sub>2</sub>SO<sub>4</sub> and (b) & (d) TiO<sub>2</sub> with addition of (NH<sub>4</sub>)<sub>2</sub>SO<sub>4</sub>. ..... 111

Figure 4.14: High magnification SEM micrographs of (a) TiO<sub>2</sub> feedstock powders synthesized with (NH<sub>4</sub>)<sub>2</sub>SO<sub>4</sub> addition and (b-d) cross-sectional views of TiO<sub>2</sub> coating prepared by cold spray process at different magnifications..... 112

Figure 4.15: SEM micrographs of surface topography of TiO<sub>2</sub> coating prepared by cold spray process at different magnification using TiO<sub>2</sub> feedstock powders synthesized with (NH<sub>4</sub>)<sub>2</sub>SO<sub>4</sub> addition; (a) 5000 X, (b) 50 000 X, (c) 200 000 X and (d) 300 000 X. .... 113

Figure 5.1: Characteristics of the starting TiO<sub>2</sub> powder for cold spray process: (a) and (b) are SEM images at low magnification, (c) FESEM image at higher magnification and (d) TEM image of the starting TiO<sub>2</sub> powder..... 125

Figure 5.2: Particle size distribution profile of starting agglomerated TiO<sub>2</sub> powders synthesized via simple hydrolysis method. .... 126

Figure 5.3: Single impact morphologies of TiO<sub>2</sub> particles and cross-sectional view of TiO<sub>2</sub> coating on different types of substrates: (a & b) ceramic tile, (c & d) copper and (e & f) aluminum, respectively. Pores and craters on the surface of substrates for single impact morphologies are indicated by white and black arrows, respectively..... 128

Figure 5.4: Schematic diagram of possible deposition mechanism of agglomerated TiO<sub>2</sub> on different substrate: (a) soft substrate; copper and aluminum and (b) hard ceramic tile substrate. .... 131

Figure 5.5: XRD pattern of as-synthesized TiO<sub>2</sub> and the coating deposited on ceramic tile substrate by cold spray process..... 132

Figure 5.6: Fractured cross-section of TiO<sub>2</sub> coating on ceramic tile substrate at high magnification. The inset in (a) and (b) are the evidence of presence of different size of fractured TiO<sub>2</sub> particles after cold-sprayed coating..... 134

## List of Table

Table 1.1: Properties of TiO <sub>2</sub> based on Crystal Structure .....	2
Table 1.2: Summary of surface modification technologies to prepare TiO <sub>2</sub> coatings using conventional method for photocatalyst applications.....	5
Table 1.3: Summary of preparation method to deposit TiO <sub>2</sub> coatings using conventional method for photocatalyst applications.....	10
Table 1.4: Summary of comparison between cold spray process and aerosol deposition process . .....	13
Table 3.1: Calculated crystallite size using the Scherrer equation of TiO <sub>2</sub> powders calcined at different temperatures. ....	67
Table 4.1: Cold spray conditions .....	86
Table 4.2: The correlation between (NH <sub>4</sub> ) <sub>2</sub> SO <sub>4</sub> addition during the synthesis and the crystallite size and particle size. ....	91
Table 4.3: Lattice strain, primary particle size and lattice parameters of as-synthesized TiO <sub>2</sub> powders. .	95
Table 4.4: Chemical composition analysis by EDS for as-synthesized TiO <sub>2</sub> powders synthesized by hydrolysis method. ....	95
Table 4.5: Properties of TiO <sub>2</sub> coating prepared by cold spray process.....	114
Table 5.1: Cold spray conditions. ....	122

# **1 Introduction**

## **1.1 Titanium Dioxide (TiO<sub>2</sub>)**

### **1.1.1 Phase Structure of Titanium Dioxide**

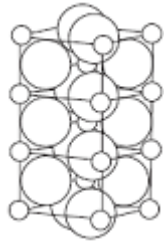

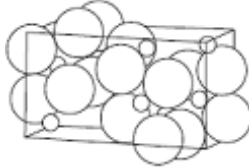
There are three types of crystal structures of TiO<sub>2</sub> that exist naturally and mainly sourced from ilmenite ore which are known as rutile, anatase and brookite. All these types are known as TiO<sub>2</sub> which using the same chemical formula, but their crystal structures are different. However, brookite type is less common using in the industry as it can transform into rutile phase at very low temperatures. Meanwhile, rutile is well known as a very stable phase compared to anatase type. The anatase type can convert irreversibly to the equilibrium rutile phase upon heating above temperatures in the range 600°- 800 °C. Generally, anatase and brookite are more common phase exists in nanoscale natural and synthetic samples, but conversely rutile is the stable phase at high temperatures [1,2].

### **1.1.2 Properties of TiO<sub>2</sub>**

The properties of TiO<sub>2</sub> depend largely on its particle size, crystal structure, morphology and crystallinity [3]. Titanium dioxide (TiO<sub>2</sub>) is widely known as a crucial material in photocatalysts, gas sensors, water and air purification, electrochromic devices, solar cells, and many more [4–15]. TiO<sub>2</sub> is well known as a wide gap semiconductor oxide. It works based on the UV light; electron and hole pair is generated by the UV irradiation, inducing chemical

reactions at the surface. Hence, the most promising characteristic of  $\text{TiO}_2$  lies in its photochemical properties such as high photocatalytic activity. In terms of solubility,  $\text{TiO}_2$  is insoluble in dilute alkali, dilute acid. Though, this oxide material is soluble in hot concentrated sulfuric acid, hydrochloric acid, nitric acid. The solubility of titanium dioxide is related to solutes.  $\text{TiO}_2$  also has excellent electrical properties as it has high dielectric constant. It can be transformed into rutile when anatase and plate  $\text{TiO}_2$  are at high temperatures, so melting and boiling points of the board of rutile and anatase  $\text{TiO}_2$  actually does not exist. Only rutile  $\text{TiO}_2$  has a melting point and boiling point.  $\text{TiO}_2$  has hydroscopicity, but not too strong. The hydrophilic is related to surface area. When the surface area is large, the moisture absorption is high. The moisture absorption of  $\text{TiO}_2$  is relevant to the surface treatment and the nature too. Moreover,  $\text{TiO}_2$  has a good thermal stability. Table 1 summarizes the characteristics of each types of these  $\text{TiO}_2$ .

Table 1.1: Properties of  $\text{TiO}_2$  based on Crystal Structure

Type of $\text{TiO}_2$	Rutile	Anatase	Brookite
<b>Properties</b>			
Crystal system	Tetragonal 	Tetragonal 	Orthorhombic 

No. of unit cell	2 $a = 0.459 \text{ nm}$ $c = 0.296 \text{ nm}$	4 $a = 0.379 \text{ nm}$ $c = 0.951 \text{ nm}$	8 $a = 0.917 \text{ nm}$ $b = 0.546 \text{ nm}$ $c = 0.514 \text{ nm}$
Density ( $\text{g/cm}^3$ )	4.13	3.79	3.99
Melting Point ( $^{\circ}\text{C}$ )	$1840 \pm 10$	change to rutile	change to rutile
Refractive Index	2.605–2.616, 2.890–2.903	2.561, 2.488	2.583, 2.700
Band gap value (eV)	3.0	3.2	-

### 1.1.3 Applications of $\text{TiO}_2$ as Photocatalyst

Environmental pollution has drawn attention in the world today due to the need of safe and clean environment. Industrial activities and transportation are some examples that contribute to the unhealthy surroundings especially in the urban areas. Of the technologies recently use to reduce the pollution in our environment are by the applications of photocatalysts.  $\text{TiO}_2$  have attracted much attention to be used as photocatalyst materials among the photocatalytically active materials due to its availability, low cost, chemical stability and nontoxic properties [16–22].  $\text{TiO}_2$  is the widely studied photocatalyst for waste water purification owing to its biological and chemical inertness, strong oxidizing power, nontoxicity and long term stability against chemical and photochemical corrosion [23].

The brookite phase has not been used and studied widely as a photocatalyst due to presents of many defects in its crystal structure [24]. Moreover, the brookite structure is more difficult to obtain as compared to anatase and rutile structure [25]. Among these three structures of TiO<sub>2</sub>, anatase phase with fine particles are more preferable for high photoactivity with the absence of rutile phase which has lower photoactivity than anatase [2,5,24,26]. There are several studies reported that the properties of the as-synthesized TiO<sub>2</sub> including its polymorphic transformation from anatase to rutile was likely dependent upon on the precursor and the preparation method [1,2].

TiO<sub>2</sub> is an effective photocatalyst for water and air purification, treatment of indoor air and for self-cleaning surfaces. Moreover, it can be used as an antibacterial agent because of its strong oxidation activity and superhydrophilicity [27]. It has been reported that for the photocatalytic applications, TiO<sub>2</sub> can be used in powder form (slurry) or coating deposited by several methods [28,29]. Despite the fact that TiO<sub>2</sub> powders have an outstanding photocatalytic activity compared to the coating due to their higher specific surface area, separation of powder from the liquid state used in water treatments and recycling processes can reduce their effectiveness [30]. Coating of TiO<sub>2</sub> on various materials as substrates can be one of the solution to this problem. Therefore, coating of TiO<sub>2</sub> for photocatalyst applications are the main focused in this study.



## 1.2 Titanium Dioxide Coatings

### 1.2.1 Conventional Coating Processes

Moreover, many attempts have been made to prepare TiO<sub>2</sub> coatings, such as chemical vapor deposition, (CVD), pulsed laser deposition, sputtering, electrodeposition, hydrothermal crystallization, chemical spray pyrolysis, sol gel and also thermal spray process. The photocatalytic activity of the coating depends on several factors such as crystal size, surface area, crystal structure and also coating thickness [31]. These factors are largely affected by the preparation methods and deposition conditions. Table 1.2 is a summary of the TiO<sub>2</sub> coating or film deposited on different substrates using different methods for photocatalytic applications. Major drawbacks using these conventional coating techniques are difficulties to deposit thick coating. Moreover, coating techniques such as PVD and CVD requires large and complicated equipment. Therefore, a more simpler and economic coating method such as thermal spray process can be used to prepare thick coating on large surface substrates.

Table 1.2: Summary of surface modification technologies to prepare TiO<sub>2</sub> coatings using conventional method for photocatalyst applications.

<b>Method</b>	<b>Substrate materials</b>	<b>Typical coating thickness</b>	<b>Ref.</b>
<b>CVD</b>	Steel sheet	Less than 5 $\mu\text{m}$	[32]
<b>Dip coating</b>	Stainless steel mesh	155 nm	[33]

<b>Sol-gel</b>	Soda lime glass or quartz plates	Less than 300 nm	[31]
<b>Magnetron sputtering</b>	Stainless steel mesh	165 nm	[33]
<b>Spray pyrolysis</b>	Stainless steel	Less than 2.5 $\mu\text{m}$	[34]

### 1.2.2 Thermal spray process

Nowadays, surface treatments of engineering materials have become significant for serviceable engineering components. Recently, thermal spray processes have been used for industrial surface treatment application due to coating properties such as adhesion strength to substrate, low porosity-oxide content and microstructural characteristics. Thermal spray coatings have become an important part of modern industry, offering customized surface properties for a variety of industrial applications ranging from thermal barrier coatings for high tech turbine blades to erosion resistant coatings for boiler tubes.

Thermal spraying is a coating process where the metallic and non-metallic materials are deposited in a molten or semi-molten condition to form a coating using a thermal source. Metals, alloys, carbides, ceramics, plastic, composites, blended materials and cermets are the most widely used coating materials for this process. The initial coating material for thermal spray process which usually in the form of rods, wires, or powders is heated, generally to a molten state and projected onto a substrate thereby forming a coating.

Usually, the surface of the substrate is degreased, masked, and roughened prior the coating process in order to activate the surface by increasing the free surface energy which will lead to increase of surface area for bonding of the sprayed particles. In principle, any material that can withstand blasting procedures to roughen the surface can be used as thermal spray coating base material. One of inherent advantages of thermal spraying is the process covers diverse range of substrate materials and substrate sizes. Moreover, thermal spray process also having the greatest range of coating materials. Basically, any material that does not decompose to other material once melted when expose to heat generated during the thermal spray process can be used as the coating feedstock material. Thermal spray process also known as a faster rate coating process and it is also possible to do coating on-site work. Furthermore, the coating can be done in a dry process thus less environmental impact.

### **1.3 Current Studies/ Developments of Thermal Spray Titanium Dioxide Coating**

#### **1.3.1 Conventional Thermal Spray Processes**

Thermal spraying is an effective and low cost process to prepare thick and large coatings to modify the surface properties of the component. During the conventional thermal spray process, some parts of the feedstock powders will melt to assure coating integrity, i.e., adhesion and cohesion. Therefore, the processing temperature use is usually above the melting temperature of the spray particles. Figure 1.1 shows the simplified principle of conventional thermal spray process using agglomerated ceramics powder from nanostructured materials as

spray materials. Since the use of nanostructured materials show superior properties in various applications when compared to their conventional powders, it opens remarkable possibilities to be used as feedstock materials in agglomerated form to prepare coating by thermal spray process. Moreover, when nanostructured materials have been used as spray particles to prepare coating by thermal spray process, the molten particles will act as a binder to the non-molten spray particles during the spraying process [35]. It is important to point out that during the thermal spraying; the molten particles have loss the characteristics or properties of nanostructured materials as it experienced grain growth. This will reduce the performance of the coating as compared to its powder when uses for real application. Therefore, the preservation of the small grain size which originally from the nanostructured powder is very crucial as the  $\text{TiO}_2$  photocatalytic reaction depends strongly on its grain size. Photodecomposition of nanostructured  $\text{TiO}_2$  coating can be higher than the microstructured coating prepared with similar process and conditions.

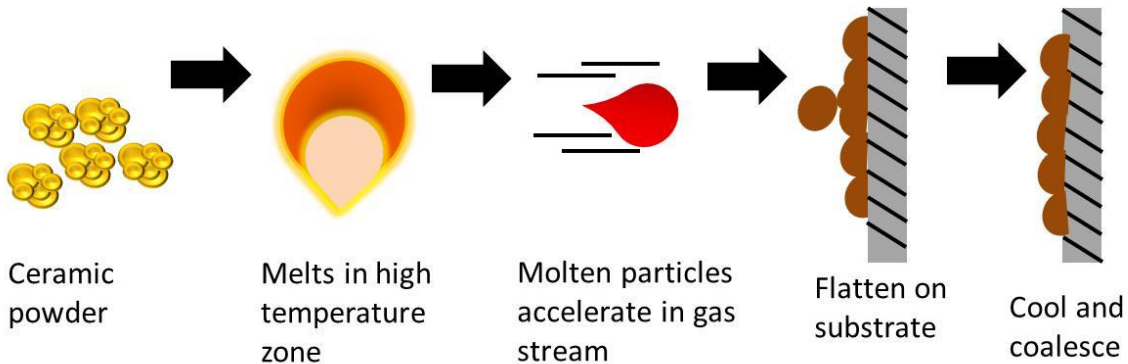


Figure 1.1: Simplified principle of the conventional thermal spray process using ceramic as feedstock materials.

While thermal spraying have significant progress in preparing coating for wide area with more cost effective and minimum operation time, challenges still exist in various aspect especially when it involves ceramic materials such as  $\text{TiO}_2$ . The drawback of the conventional thermal spray process to prepare  $\text{TiO}_2$  coating is the irreversible phase transformation of  $\text{TiO}_2$  structure from anatase to a less photocatalytic rutile phase at  $500\text{-}600^\circ\text{C}$  under normal conditions [36] as shown in Fig. 1.2. Moreover, Table 1.3 shows the summary of some thermal spray methods that have been used to prepare  $\text{TiO}_2$  coating. The results show that, it is quite challenging to preserve the anatase phase in the as-prepared coating by conventional thermal spray method.

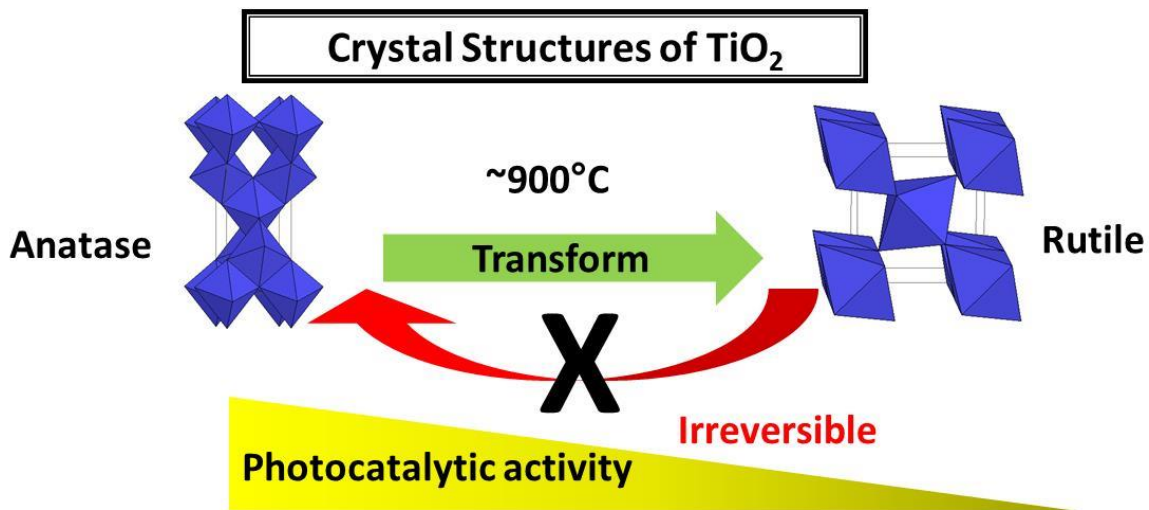


Figure 1.2: Schematic diagram showing the phase transformation of anatase  $\text{TiO}_2$  to rutile  $\text{TiO}_2$  during the conventional thermal spray process.

Table 1.3: Summary of preparation method to deposit TiO<sub>2</sub> coatings using conventional method for photocatalyst applications.

<b>Spray technique</b>	<b>Size of agglomerated feedstock material</b>	<b>Substrate</b>	<b>Coating thickness</b>	<b>Phase structure in the obtained coating</b>	<b>Reference</b>
<b>Air Plasma Spraying</b>	10 to 50 $\mu$ m (from 7 nm)	Stainless steel	~30 $\mu$ m	Anatase, rutile & different titanium suboxides	[30]
<b>High Velocity Oxygen Fuel</b>	10 to 50 $\mu$ m (from 7 nm)	Stainless steel	~20 $\mu$ m	Rutile & anatase	[30]
<b>Suspension Spraying</b>	10 to 50 $\mu$ m ( ranging from 6-12 nm)	Stainless steel	~20 $\mu$ m	Anatase and small amount of rutile	[37]
<b>Flame Spraying</b>	20-50 $\mu$ m (from 20 nm)	Stainless steel & Carbon steel	150 $\mu$ m	Rutile	[38]

Therefore, a proper selection of coating process is crucial due to the goal to obtain coatings with higher photocatalytic activity. Anatase and rutile has differences of photocatalytic properties. Several studies suggested that anatase is more efficient as photocatalyst and this structure can be preserved if only the processing temperature of the thermal spray process is below the transformation temperature of anatase to rutile. Moreover, low processing temperature

of thermal spray process also can maintain the initial grain size of the feedstock materials which also has significant effect on the catalytic activity of  $\text{TiO}_2$ . This might due to the characteristics of smaller crystallites size which can promote the photocatalytic activity of  $\text{TiO}_2$ . Preservation of the anatase phase after the thermal spray is desirable for photocatalytic applications. Consequently coating process of a high temperature which above the transformation temperature of anatase to rutile phase is one of the major challenges in conventional spray thermal spray.

The results obtained to date, strongly indicated there is necessity for development of thermal spray coating of  $\text{TiO}_2$  or any other ceramic materials that can avoid phase transformation to occur during the process. Due to this problem, it encourage new discoveries of new process of thermal spray which utilize kinetic energy instead of thermal energy by increase particle velocity to project the feedstock powders to the substrate. The kinetic energy will transform to thermal energy upon impact on the substrate in order to permit sticking of particles. There are two new technologies of thermal spray methods that utilize low processing temperature during the process and working based on the kinetic energy of the particles for deposition. The processes are cold spray and aerosol deposition method.

### **1.3.2 Low Temperature Process**

Aerosol deposition method (ADM) and cold spray deposition is the low energy consumption processes dissimilar to conventional deposition processes. The aerosol deposition method is a room temperature process which has been used to coat ceramics materials on metal, ceramic and polymer substrates. This process uses an aerosol mixture of nano-sized ceramic

particles and a carrier gas which will be accelerated by the carrier gas through a nozzle. For the acceleration of the particles, pressure difference is required. For this reason, the ADM method consists of two vacuum chambers; an aerosol-generation chamber and deposition chamber which were connected by a tube. During the process, the ceramic particles were aerosolized by aerosol-generation chamber which has a carrier gas system and a vibration system to mix the powder with the carrier gas and conveyed to the deposition chamber. The kinetic energy of the particles is used for bonding during the impact [40]. This process is widely used as it can be carried out at low temperature. Therefore, thermal damage of the substrate can be minimized. Despite of these advantages, ADM process requires vacuum condition during the process and the deposited coating only limited to several micrometer of thickness.

Meanwhile, cold spray process is deposition technique to deposit micro-sized particles using a high pressure gas. This process does not require vacuum condition. During the process, the particles are accelerated to supersonic velocities and impact onto a substrate surface without melting before the impact. This technique can produce thicker coating thickness as compared to ADM process. Unfortunately, this process does not permit the direct spraying of nanostructured powder which can cause blockage in the feeding system during the powder supply to the nozzle. However, the use of nano-powders as spray materials for this process can be achieved by modification of the size of feedstock powders by agglomeration of the particles. Moreover, since deformability is important for cold spray coating to build up, this method shows more potential to deposit metal materials rather than ceramic materials. However, ceramic coatings are possible to be deposited by cold spray process. This part will be discussed in details in Chapter 1.4.2. Therefore, in summary, based on the principle of particle collisions by utilizing kinetic energy at a low-process temperature, ADM and cold spray process can be used to fabricate ceramic



coating. Table 1.4 shows the summary comparison between these two methods to produce ceramic coating.

Table 1.4: Summary of comparison between cold spray process and aerosol deposition process [39].

<b>Method/ Properties</b>	<b>Cold spray</b>	<b>ADM</b>
<b>Type of powder</b>	Metallic, cermet, metal matrix composites and ceramic powders	Mainly ceramic powder
<b>Size of powder</b>	Micro-sized particles (10-50 $\mu\text{m}$ )	Nano-sized ceramic particles (0.5-1.5 $\mu\text{m}$ )
<b>Type of carrier gas</b>	Helium, Nitrogen	Helium, Air
<b>Pressure of Gas</b>	High-pressure gas (0.3-5.0 MPa)	Low-pressure gas (0.01-0.3 MPa)
<b>Temperature</b>	Below melting temperature of the feedstock material	Room temperature
<b>Vacuum condition</b>	Do not require vacuum condition	Medium vacuum condition
<b>Deposition rate</b>	High deposition rate	Low

Therefore, from these observations, ceramic coating can be deposited at low temperature by ADM or cold spray process. In this study, we reporting the deposition of ceramic coating by

cold spray process by synthesizing the nanoparticles TiO<sub>2</sub> powder that agglomerated up to micrometer ranged which suitable for direct spraying of the powder in the conventional powder feeder.

## **1.4 Cold Spray Technology**

### **1.4.1 Basic Principles**

Cold spray is an emerging coating technique where the spray materials in a solid state are deposited by plastic deformation on the substrate. A coating is formed when powder particles in solid state at high velocities (high kinetic energy) impact onto the substrate, deform, and adhere to it or to other particles. In addition, good bonding between cold spray powder particles requires a high plastic deformation during particle impact by converting the kinetic energy to thermal energy upon impact on the substrate [15,40]. Since this process is spraying the feedstock materials below the melting temperature of the materials, some drawbacks that occur while preparing large and thick coating using traditional thermal spray can be reduced or eliminated. The most advantages of this process are [41]:

- a. The amount of heat distributed to the coated part is relatively small. Hence, the microstructural alterations in the substrate material are minimal or negligible.
- b. Material degradation can be avoided to occur when thermally and oxygen-sensitive depositing materials (e.g. copper or titanium) are cold sprayed due to the absence of in-flight oxidation and other chemical reactions.

- c. Nanophase, intermetallic and amorphous materials, which are not amenable to traditional thermal spray processes due to a major degradation of the depositing material also can be deposited by cold spray process.
- d. The formation of embrittling phases can be avoided.
- e. Macro- and micro-segregations of the alloying elements during solidification which usually occurs during the spraying by the conventional thermal spray methods and can considerably compromise materials properties do not take place during cold spraying. Therefore, good properties of the powder material are preserved in cold-sprayed bulk materials.
- f. Cold spray of the materials like copper, solder and polymeric coatings offers new potentials for cost-effective and environmentally friendly choices to the technologies such as electroplating, soldering and painting.

The success of the ceramic cold spray coating depends on several factors such as the nozzle geometry, characteristics of the feedstock powders (e.g. density, strength, and melting temperature), gas type, gas temperature, standoff distance, substrate and many more. Selection of proper combination of particle temperature, velocity and size of the feedstock materials permit spraying of particles at the minimum temperature possible.

### 1.4.2 Bonding Mechanism in Cold Spray

Cold spraying process involves two stages which is [42]:

1. The spraying of the first layer of particles on a substrate (particle-substrate). During this stage, the particles interact with the substrates. This process will determine the quality of the interface and adhesion. This is the more complicated stage as it depends on particle and substrate parameters such as roughness, hardness, temperature, etc. and also on the state of the surface. The number of particles impacts on the surface of the substrate will change the state of the surface, which result in changes in conditions of interaction between the particle and the substrate and leads to unsteady growth of the coating.
2. The buildup of the coating (particle-particle). This stage depends mainly on the first stage. The first impacting particles that adhere on the substrate leads to rapid increase in the number of attached particles and to formation of continuous coating.

Generally, the bonding mechanism that involve during the cold spraying is significantly difference from the traditional thermal spray process. Furthermore, there are several mechanisms have been suggested by previous researcher that explain the bonding mechanisms operating. The main bonding mechanisms in cold spray that contribute to the attachment of particle to the substrate occur at the particle substrate interface at or exceed the critical velocity of the sprayed particles, whose value depends on the particle impact temperature, chemistry of the powder materials, powder quality, particle size and the thermomechanical properties of the sprayed

material [43,44]. This is recognized to adiabatic shear instability, resulting from the local heating and softening of the material [41,43]. However, there are some other suggested bonding mechanism has been proposed by other researchers and they are includes mechanical interlocking, physical, metallurgical and chemical bonding [45,44,46]. Clarification of bonding mechanisms of the feedstock materials during cold spraying is crucial towards wide applications of the promising coating method. Yet, there is a debate in clarifying the bonding mechanisms of ceramic particles during the cold spray coating. Despite the fact that the bonding involve during the deposition is still questionable and remains controversy as the process itself influenced by several factors.

Kliemann et al. have shown that it is possible to produce  $\text{TiO}_2$  coating by cold spray if there is shear instabilities occur on the ductile substrates [47]. However, they reported that dense agglomerated  $\text{TiO}_2$  particles with nanosized crystallites (Fig. 1.3) which have been tempered for 3 h at  $600^\circ\text{C}$  in air atmosphere before spraying did not contribute to bonding which led to unsuccessful to build up the coating on their own even the particles have been sprayed for 10 spray passes under the same process parameters (Fig. 1.4). However, their finding shows that the ceramic particles break on impact which demonstrates the brittleness of the spray powder under cold spray conditions.

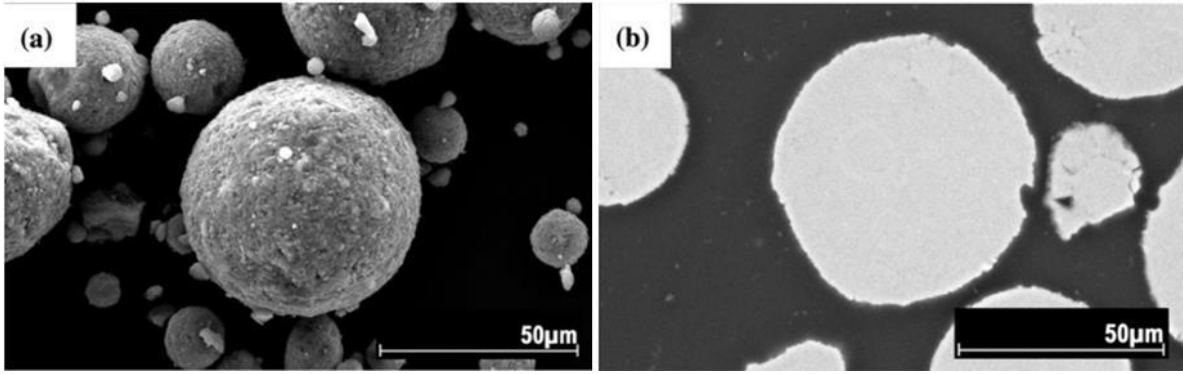


Figure 1.3: SEM image of  $\text{TiO}_2$  powder (a) and its cross section which shows that the agglomerated particles with solid and dense particles after have been tempered at  $600^\circ\text{C}$  [47].

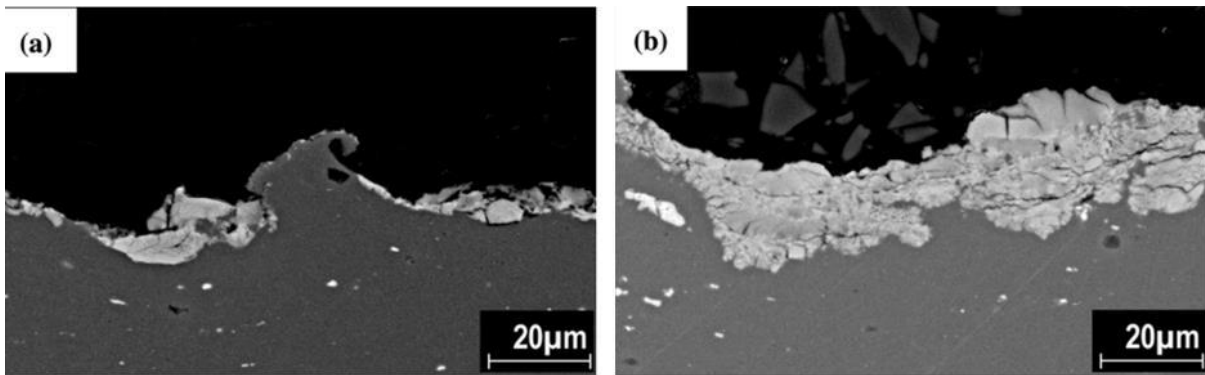


Figure 1.4: SEM images of cold-sprayed  $\text{TiO}_2$  coatings on  $\text{AlMg}_3$  substrate. (a) Sprayed as one pass and (b) sprayed with 10 passes [47].

Burlacov et al. reported that anatase  $\text{TiO}_2$  can be deposited on polymer substrates for photocatalyst applications [48]. They found that most of the cold spray coating that they have prepared showed excellent adhesion to the substrate with suitable surface roughness and also good photocatalytic activity. However, the coating thicknesses that have been produced on the

polymer substrates only limited to about 20  $\mu\text{m}$  thickness (Fig. 1.5). Moreover, they also encountered problems during the deposition of brittle ceramic particles which tend to erode on impact previously deposited material and also caused the polymeric material which act as the substrate to squeeze out of the surface after particle impact (Fig. 1.6). This removed polymer will cover parts of the uppermost  $\text{TiO}_2$  particle layer which in turns reduced the photocatalytic activity of anatase coating.

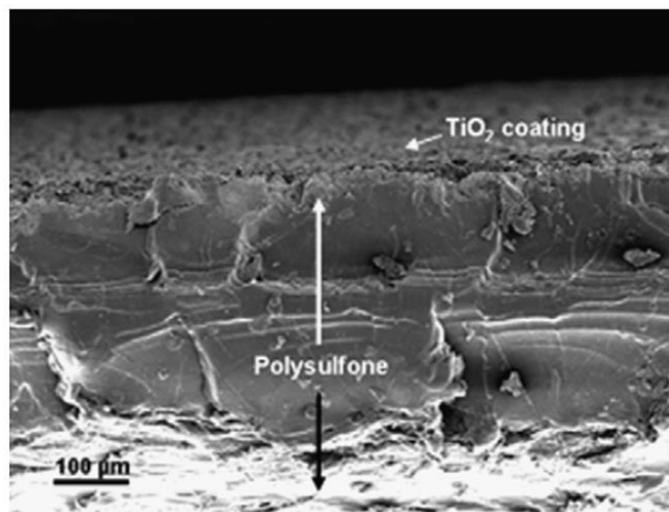


Figure 1.5: SEM image of cross-section of polymer coated with  $\text{TiO}_2$  using cold spray method [48].

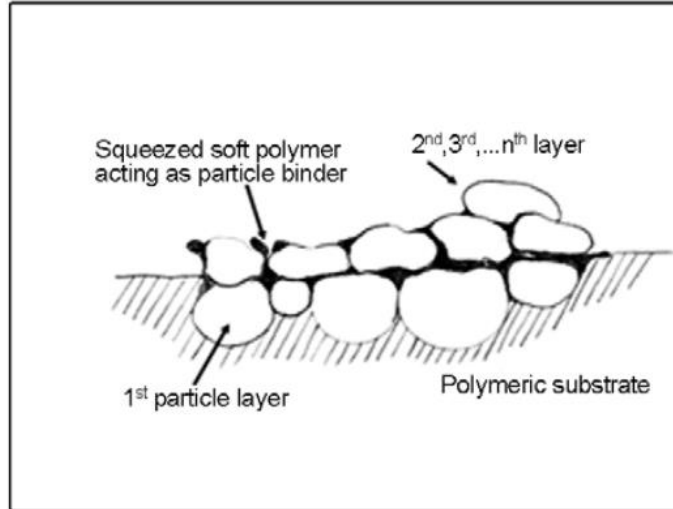


Figure 1.6: Proposed mechanism of particle bonding of a cold spray coating on a polymer substrate [48] .

Moreover, study by Yang et al. proposed that nanoporous  $\text{TiO}_2$  film which about thickness of 10-15  $\mu\text{m}$  was deposited by cold spray method using agglomerated  $\text{TiO}_2$  powder with primary particle size of 200 nm and polyvinyl alcohol was used as a binder during the agglomeration [7]. They suggested that the sprayed  $\text{TiO}_2$  powders was deformed under high transient impact pressure due to the polymeric binder that used during the agglomeration of  $\text{TiO}_2$  nanoparticles, which lead to deformation that comparable to the deformation of metallic powders by cold spray process.



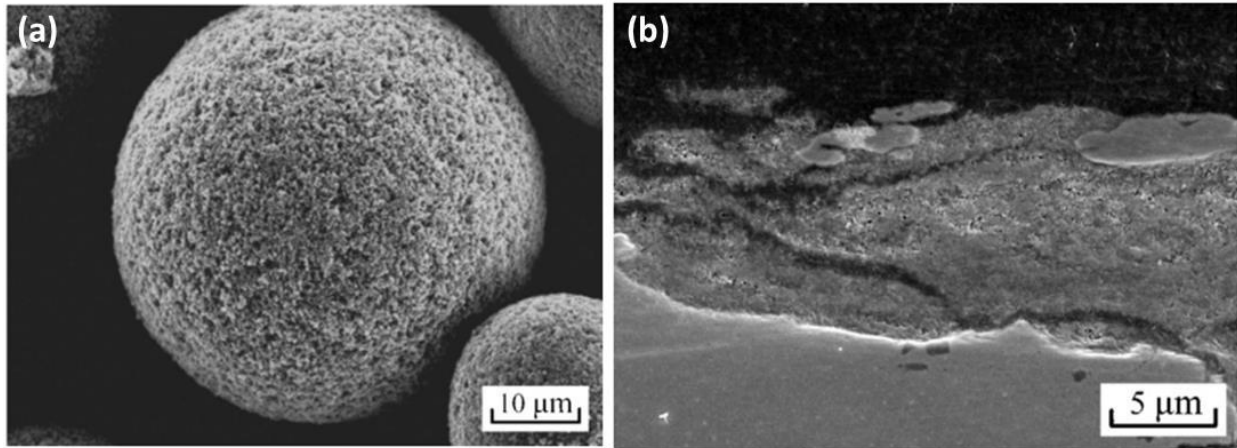


Figure 1.7: SEM image of (a) the spray TiO<sub>2</sub> powder agglomerated from nanoparticles using polymer binder and (b) the cross-section of TiO<sub>2</sub> coating deposited by cold spray process [7].

Later on, study conducted by Yamada et al. shows that process gas conditions, either using helium (He) or nitrogen (N<sub>2</sub>) as the process gas is not the main factor to form TiO<sub>2</sub> coating using cold spray process as both type of the gas was possible to build up coating layer on the substrate [49]. They also reported that deposition efficiency of sprayed particles can be controlled by the temperature of the process gas as shown in Fig. 1.8 and Fig. 1.9 using He and N<sub>2</sub> gas at different temperatures, respectively.

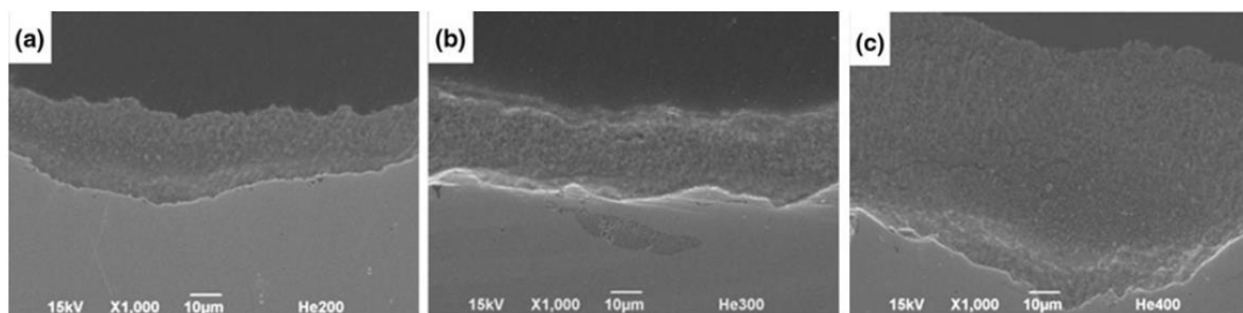


Figure 1.8: Cross section microstructure of coatings sprayed with He. Spraying with gas temperature of (a) 200 °C, (b) 300 °C, and (c) 400 °C [49].

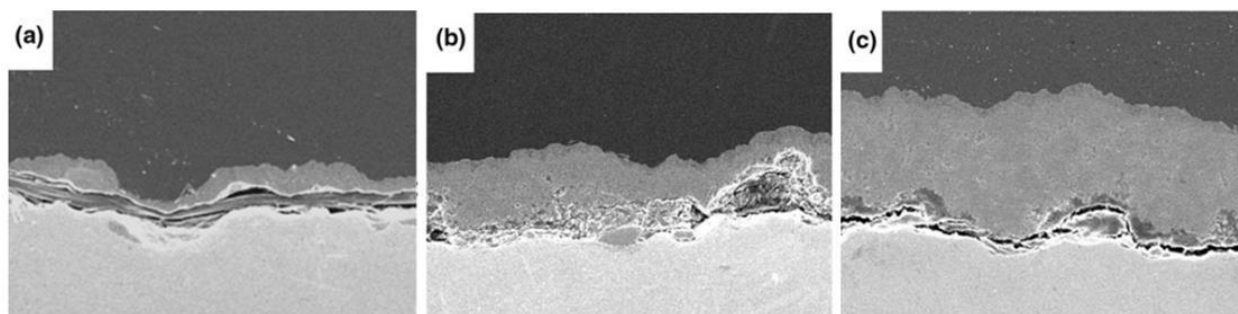


Figure 1.9: Cross section microstructure of coatings sprayed with N<sub>2</sub>. Spraying with gas temperature of (a) 200 °C, (b) 300 °C, and (c) 400 °C [49].

The same authors also reported that a TiO<sub>2</sub> coating was produced from a recombination of broken up crystallites links during the cold spray process, which was initiated by the porous structure of the agglomerated powders [50]. They proposed that chemical bonding may allow thick coatings to be deposited by cold spray process. The authors described that during the process, the agglomerated powder in nano-scale primary particles which also contains nanoporosity were fractured, leaving an unstable surface with a dangling bonds structure. In order to reobtain a stable surface, the fractured particles decoupled and formed a surface with

improved stability, which lead to bonding of the newly impacting particles and in turns building-up of the coating (Fig. 1.10-d). They did believe that starting feedstock materials play important role for the deposition of TiO<sub>2</sub> coating by cold spray process. Fig. 1.10 shows the morphology of the feedstock powders that have been used to prepare TiO<sub>2</sub> coating.

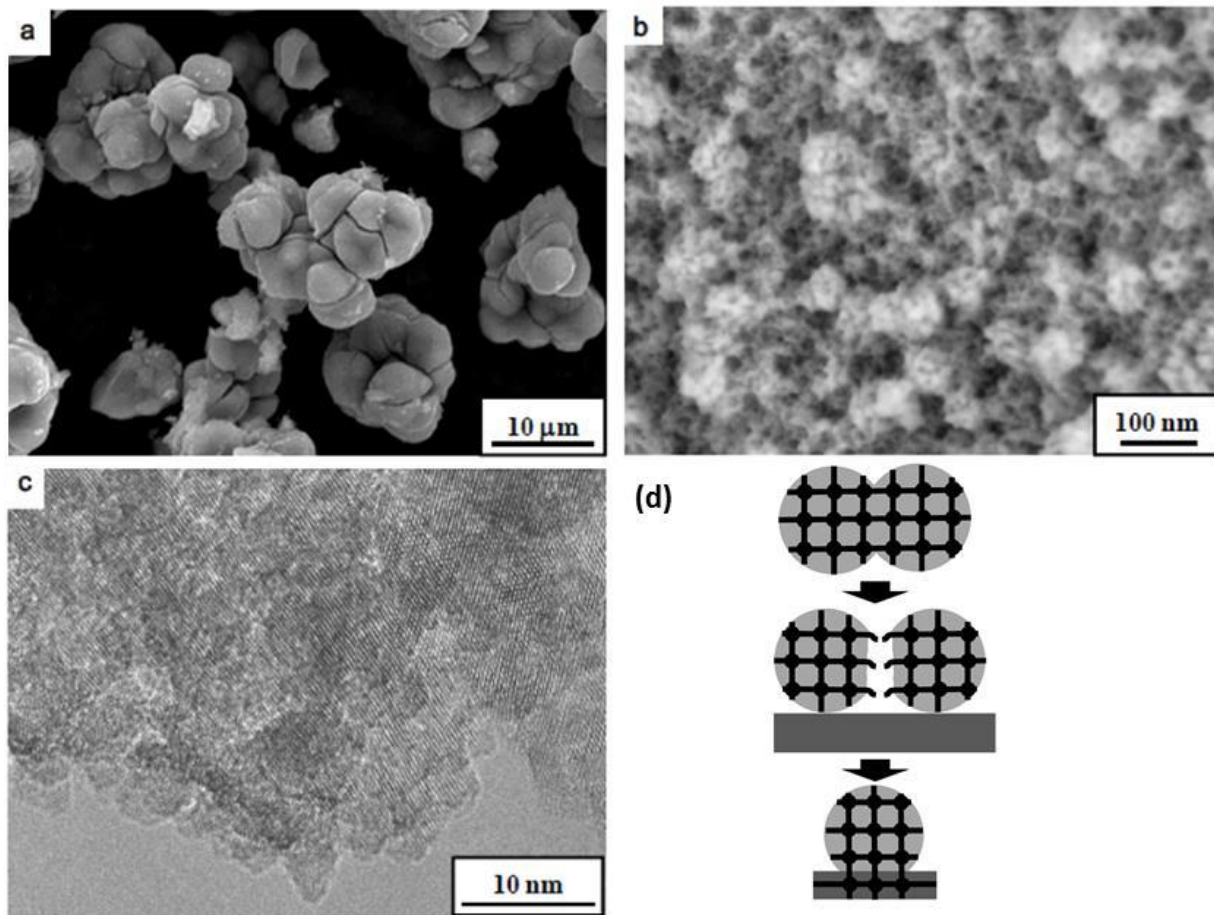


Figure 1.10: Morphology of TiO<sub>2</sub> feedstock powder; (a) SEM image, (b) FE-SEM image, (c) TEM image and schematic image of adhesion mechanism of cold-sprayed TiO<sub>2</sub> particle [49,50].

Study conducted by Salim et al. shows that  $\text{TiO}_2$  coating can be deposited by cold spray process when the feedstock powders were synthesized by simple hydrolysis method and further heat treated by hydrothermal treatment [40]. Their finding also suggested that the initial properties of the ceramic spray particles which contain nanoparticles with some nanoporosity are very crucial for the deposition of  $\text{TiO}_2$  by cold spray method using  $\text{N}_2$  at  $500^\circ\text{C}$  and  $1\text{MPa}$  was used as the process gas. In this work, they successfully deposited thick coating of about  $150\ \mu\text{m}$  using this type of powders (Fig. 1.11-c). Contrary to  $\text{TiO}_2$  powders that did not undergo post heat treatment and  $\text{TiO}_2$  powders that were annealed at  $600^\circ\text{C}$ , only particles embedment was observed and coating of about  $75\ \mu\text{m}$  was deposited on the surface of copper substrate, respectively (Fig. 1.11-a & b)).

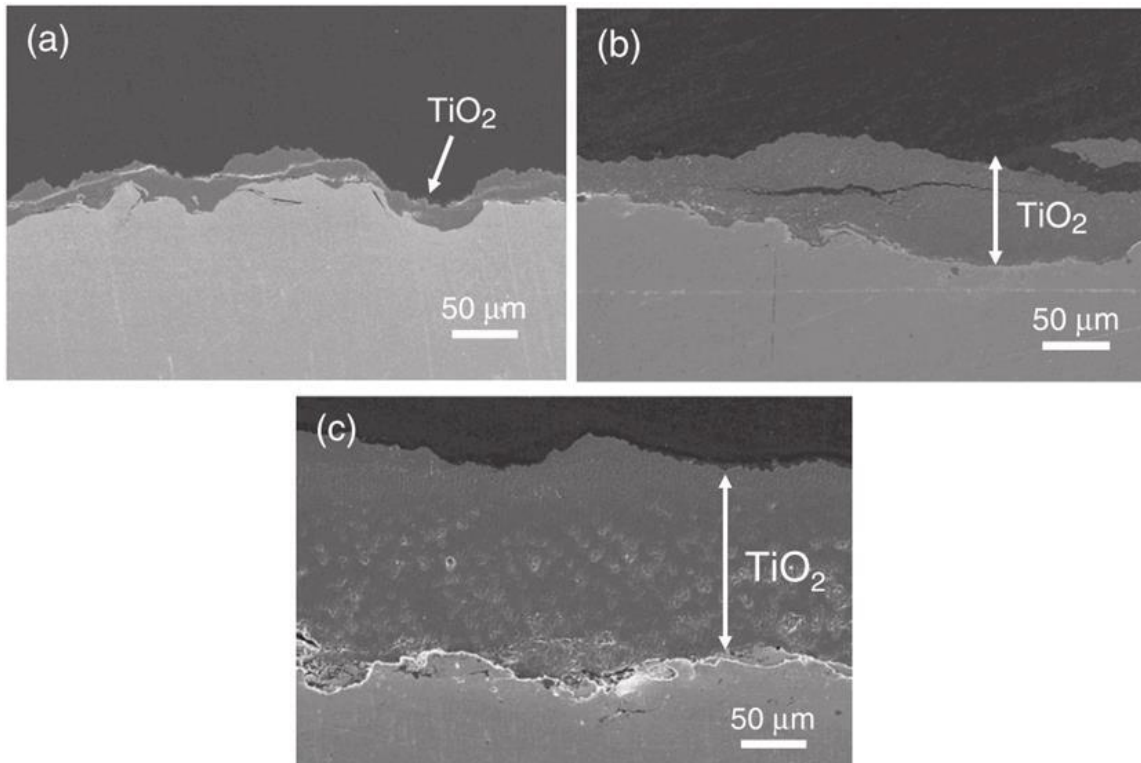


Figure 1.11: The cold spray result of (a) as-synthesized, (b) annealed, and (c) hydrothermal treated  $\text{TiO}_2$  powders deposited on copper substrates [40].

Attempts to deposit nano-anatase  $\text{TiO}_2$  by cold spray on stainless steel and ceramic tiles have been conducted by Gardon et al. met with limited success. Built-up a coating appeared to be challenging on both types of substrates even after altering the operational conditions of the process. While, the study shows that nano-anatase  $\text{TiO}_2$  coating was deposited onto steel substrate only when the substrate was previously coated with titanium sub-oxide layers by atmospheric plasma spray as shown in Fig. 1.12 [45] . They suggested that the layer of titanium sub-oxide coating worked as a surface geometry and composition that preferred for the deposition of anatase particles. They also revealed that the mechanism that responsible for  $\text{TiO}_2$  deposition by cold spray process is the chemical bonding between the particles and substrate. This study indicated that the previous layer of titanium sub-oxide would prepare the substrate with an appropriate surface roughness that needed for deposition of  $\text{TiO}_2$  particles. Moreover, substrate composition also important for deposition as it can provide chemical affinities during the interaction of the particles after the impact. In addition, hardness of the substrate may also ease the interaction between the particle and substrate.

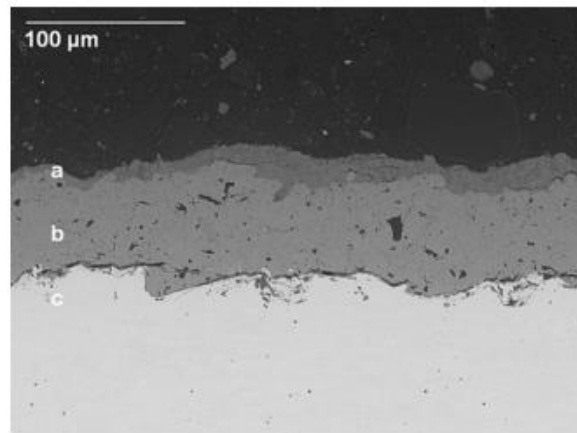


Figure 1.12: SEM micrograph of the cold spray coating cross-sectional area: (a) cold sprayed nano- $\text{TiO}_2$  layer, (b) APS  $\text{TiO}_2$ - coating, and (c) steel substrate [45].

Besides this, Sayyar et al. reported that limited thickness of about few microns were coated onto ceramic substrate by cold spray process at the pressure of 4 bar at room temperature using TiO<sub>2</sub> translucent colloid synthesized by sol-gel method [51]. Recently, Herrmann-Geppert et al. used cold spray to prepare TiO<sub>2</sub> coating using powder with primary particle size of about 25 nm and have been agglomerated to micro sized ranged by spray drying. The TiO<sub>2</sub> powders were sprayed by three different types of carrier gas which are nitrogen, helium and argon on titanium plate. However, they reported that in all cases, the average thickness of about 5 to 10 μm was deposited onto the substrate which resulting from the diameter of the initial feedstock powder.

Therefore, from the previous discussed studies conducted the results show that cold spray coating of TiO<sub>2</sub> is not easy to be obtained but it is not impossible. This is one of the driving forces for pursuing research on cold spray coating using TiO<sub>2</sub> ceramic powders as spray material.

## **1.5 Titanium Dioxide as Ceramic Feedstock Materials for Cold Spray Process**

### **1.5.1 Feedstock Materials for Cold Spray Process**

The main characteristic of feedstock materials to be used for cold spray process is the ability of that material to be deformed upon impact onto the substrate. Moreover, particle impact velocities which requires for deposition depend on its powder properties which include its particle size, morphology, density, hardness and etc. Ductility of the feedstock materials seems

very important for the deposition in order to form shear deformation on the contacting surfaces which in turns, resulting the bonding and lead the coating to build up by receiving multiple collision of newly arrived particles upon the impact. Therefore, it seems quite difficult to deposit ceramic materials which possess brittle characteristic by cold spray process. However, at some extends ceramic material may plastically deform under certain conditions which are [52–54]:

1. Under confining pressure (e.g. high pressure compression and indentation) fracture of the material is hindered, and, instead, plastic deformation can occur.
2. An inertial force can replace the role of confining pressure under a dynamic loading of high strain rate. Therefore, deformation processes such as slip, twin and etc can be observed.
3. Nanosized ceramics can undergo plastic deformation. The study shows that small particles of 40 nm in diameter can undergo plastic deformation without failure by compression test at ambient temperature.

From the mention above conditions, brittle to ductile transition of ceramic materials is possible to occur when preparing ceramic coating by cold spray as the process utilize the dynamic loading and nanoscale materials have been used as feedstock powders.

### **1.5.2 Conventional TiO<sub>2</sub> Powders**

Previously, in order to produce ceramic coatings by thermal spray process, conventional ceramic feedstock powders have been used. This feedstock powders are typically fused and

crushed before further use as feedstock materials [15,35,55–60]. Fig. 1.13 shows the example of conventional  $\text{TiO}_2$  powders that have been used to prepare thermal spray coating. There are two methods were used to prepare  $\text{TiO}_2$  powders for industrial applications which are the chloride and sulfate process [15,61,62]. After the synthesis process, different components of the powder are mixed and melted in furnace and the resulting block is crushed by several ways such as hammer mills, stamping mills, jaw crushers and gyratory crushers [63]. Dense, blocky and angular with an irregular shape is the typical characteristics of the resulting powders.

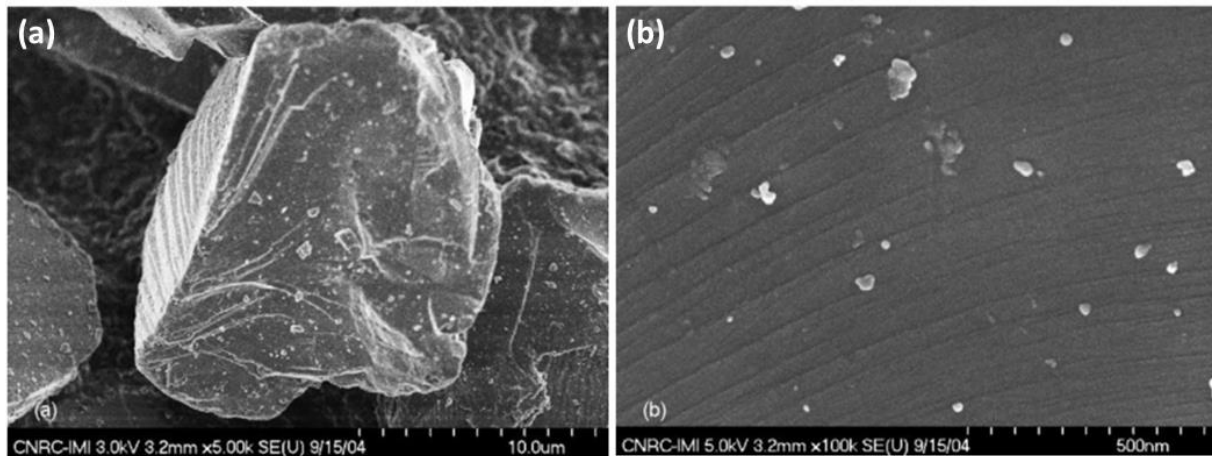


Figure 1.13: SEM image of (a) conventional fused and crushed titania feedstock particle and (b) particle of (a) observed at higher magnification; absence of nanostructural character [62].

There are some drawbacks that contribute to use of conventional  $\text{TiO}_2$  powders to prepare coating by cold spray process. One of the major problems is regarding the properties of the conventional powder itself which are dense and large then the kinetic energy exceeds the adhesion energy. Thus the impact particles rebound rather than deposit on the substrate.



Moreover, grain size affects the photo decomposition efficiency of organic pollutants for the TiO<sub>2</sub> photocatalysts. Normally, the reactions of the TiO<sub>2</sub> photocatalytic take place on the powder surface. When the grain size becomes smaller, the specific surface area becomes larger and the degradation efficiency of organic pollutants also increases. In turns, photodecomposition efficiency of coatings with nano size TiO<sub>2</sub> powder can be higher than that of normal micro size powder [24].

### **1.5.3 Nanopowders**

Current attention has focused on the preparation of TiO<sub>2</sub> coating using nanostructured materials including using ceramic powders as feedstock materials. Nanostructured materials has been drawn considerable attention to be used as feedstock materials for thermal spray coating method due to superior properties of nanostructured materials in terms of its physical and mechanical properties [35,59,64]. The improvement of the properties resulted from finer grain sizes of nanostructured materials when compared to existing engineering materials with conventional sizes level. Deposition of finely structured coatings from nanomaterials can be achieved by spraying of liquid feedstock consisting either of submicrometer-sized or nanometer-sized particles dispersed in a suspension or solution and also by spraying of agglomerated nanometer-sized particles. Spraying of fine anatase phase can be preserved by spraying dispersing solid particles in a liquid medium by using suspension plasma spraying. This method allows particles to be fed with diameters ranging from several nanometers to 10 μm into the feeding system and allows formation of nanostructured [29]. However, this process has some

drawbacks such as the tendency of the solid particles in liquid suspensions settle over time and undergo formation of large particles by agglomeration, which can contribute to formation of clustered sediments which can cause clogging problem in the feeding system, and also possibility to form only thin coatings [15,29,37].

Typically, powder feedstock materials are used for thermal spray of ceramic coating. However, the feeding system of thermal spray, does not allow the direct spraying of a fine particles especially in nano-sized due to clogging problem experiences by the conventional powder feeder system during the powder supply to the nozzle and also problems encounter on low bow shock layer during the impact onto the substrate due to small size of individual nanoparticles [65–67]. Moreover, the handling of fine particles during the coating process is more difficult than the bigger particles and this opens an issues that related to environmental and health concern [15,37,68].

Therefore, typically prior the coating process, nanostructured feedstock powders is agglomerated up to microsized ranges by spray-drying, ball milling and sintering to improve the flowability of the powders during cold spray process [7,15,47,69–72]. Moreover, the agglomeration of nanosized particles into microscopic particle is advantageous over micro-sized particles for cold spray deposition due to higher particle velocity can be achieved when the same gas velocity is used [73]. The agglomerated morphology is crucial as it involves the use of very fine particles which coupled with pores, which promote easy material flow and a so-called fragmented bonding mechanism [74]. Porous agglomerates has tendency to break easily upon impact onto the substrate, which leads to better densification and promote to build up the coating. Figure 1.14 shows the example of morphology of agglomerated spray-dried titania powders at

low and high magnification and also the surface of an HVOF-sprayed nanostructured titania coating.

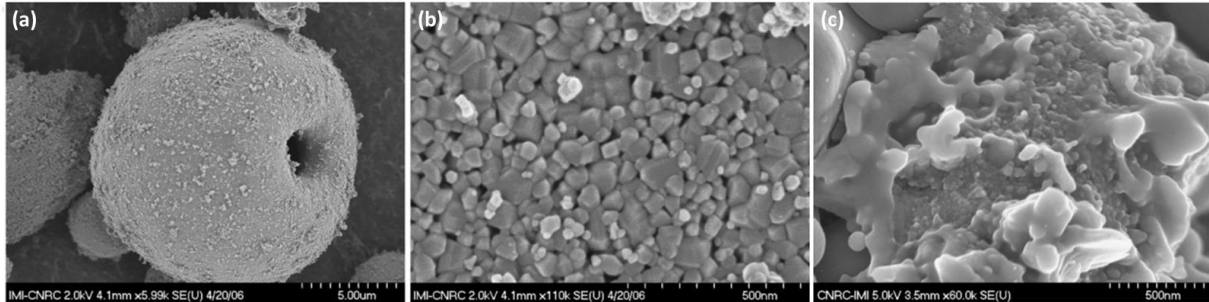


Figure 1.14: (a) Typical morphology of agglomerated spray-dried titania powders. (b) High magnification view of (a)—agglomeration of individual nanosized titania particles and (c) Nanotexture formed by a semi-molten agglomerate on the surface of an HVOF-sprayed nanostructured titania coating [72].

However, spray-drying process that used to agglomerate the fine particles into microsized range particles might contribute to the loss of the nanosized grains especially after the heat exposure during the sintering process [75]. Therefore, other alternative methods to prepare powder feedstock materials for cold spray coating are crucial to preserve the properties of the original properties of the feedstock powders. Natural agglomeration of fine powders into submicron particles can be achieved by selecting an appropriate synthesis method which also includes the precursors, reaction time, structure directing agent and some other parameters. Suitable synthesis process with control parameters not only can produce agglomerated structure but also can produce powders with desired properties, size, morphology, porosity, crystallinity and etc [3].

Sol-gel technique is one of the method that has been used to produce TiO<sub>2</sub> powders with notable advantages including controllability, reliability, low temperature synthesis, good uniformity of the microstructure and reproducibility which in turns in high quality and high purity materials [3,76]. Though, due to polycondensation reaction of the sol-gel method materials, this technique usually produces a powder in an amorphous phase or a poor crystallinity. Hence, it is necessary to carry out post heat treatment to improve the crystallization of the powders [3].

Among the synthesis methods that can be used to produce TiO<sub>2</sub> powders, hydrolysis and hydrothermal method is among the simplest, cost-effective and scalable one. Generally, hydrolysis process is a method that involves reaction between the precursor and the solution. The mixture is then hydrolyzed for some time to allow the nucleation to occur by heat the mixture at certain temperature. Typically, in hydrothermal synthesis, the precursor and solution are mixed together and the reaction will take place in a pressure vessel by applying pressure and temperature during the reaction. A better control of processing parameters can be done by using this method due to the close system during the reaction. Therefore, in this study, these two methods were chosen to prepare the TiO<sub>2</sub> powders as feedstock materials for cold spray process. These two methods also possible to produce nanostructured TiO<sub>2</sub> powders with good properties of the as-synthesized powders by controlling the synthesis parameters. The possibilities to produce nanostructured powder is due to very low synthesis temperature which usually below 200°C and by a single-step process where post heat treatment which usually will cause growth of particle size is not required.

## 1.6 Objectives

Every successful thermal spray application starts with the right material choice. Therefore, the foremost objective of this work is to synthesis titanium dioxide ( $\text{TiO}_2$ ) ceramic materials as feedstock powders for cold spray process. To accomplish this objective, six sub-objectives are addressed. This study embarks on the following objectives:

1. To synthesize ceramic powders of  $\text{TiO}_2$  to be used as feedstock material for cold spray process. Two simple methods, hydrolysis and hydrothermal were chosen to synthesize the powders. The synthesis procedures accomplished were directed to produce the nanoparticles powders which were naturally agglomerated to microscopic range to ensure acceptable to be used as feedstock powders using conventional powder feeders of cold spray system.
2. To characterize the properties of the synthesized powders. In order to investigate the properties of the feedstock materials that required to build up the coating during the cold spray deposition, as-synthesized  $\text{TiO}_2$  powders were analyzed by several methods such as XRD, TEM, FESEM, particle size analyzer and etc.
3. To investigate the influence of low calcination temperatures of as-synthesized  $\text{TiO}_2$  powders by hydrolysis method on the deposition of cold spray coating. In order to avoid progressive grain growth and also the existence of internal pores within the particles, study on the effect of low calcination temperatures on the as-synthesized  $\text{TiO}_2$  powders were also explored in this work.

4. To examine the effects of ammonium sulfate;  $(\text{NH}_4)_2\text{SO}_4$  addition on the morphology and properties of  $\text{TiO}_2$  powders, through hydrolysis method.
5. To investigate the mechanism of single particle bonding by wipe test using different types of powder and also different types of substrates. Factors that contribute to the formation of the cold spray  $\text{TiO}_2$  coating has been investigated based on the material and substrate properties. Mechanism of the deposition has been discussed based on the feedstock materials and substrates used to form the  $\text{TiO}_2$  coating by cold spray method.
6. To study the cold spray coating morphology, crystal structure, hardness, porosity and surface roughness of prepared coatings using ceramic  $\text{TiO}_2$  feedstock material.

## 1.7 Thesis Organization

This thesis consists of 7 chapters, which include the introduction, 4 content chapters, the overall conclusion and also chapter on the contribution of this study to the research/ academic and industrial field. Chapter 1 discusses brief idea, philosophy and the objectives of the study which that lead to this research focus. This chapter also focuses on the review of main theories and describes previous works related to this research, including the material and process that chosen in this study to fabricate the coating in order to achieve the objectives of this study. Chapter 2 presents the synthesis methods that have been used to prepare the feedstock powders for cold spray process. Generally, this chapter describe the simplest method that can be used to synthesize agglomerated powders in micrometer sized that contains nanoparticles as the primary particles. This chapter includes the synthesis method, the characterization of the as-synthesized

powders in order to determine the properties that contribute to coating formation and last but not least the coating formations by cold spray method. Chapter 3 is the continuation work based on the results that obtain in Chapter 2. In this chapter, as-synthesized TiO<sub>2</sub> powders that prepared by hydrolysis method that shows superior property as compared to hydrothermal method as reveal in Chapter 2 was calcined at low calcination temperature ranging from 200-400°C. The effect of the calcination has been studied in terms of the properties of the powder and also the possibility of the powders to be deposited by cold spray process. Chapter 4 describes the synthesis of agglomerated TiO<sub>2</sub> powders with the addition of inorganic salt; ammonium sulfate (NH<sub>4</sub>)<sub>2</sub>SO<sub>4</sub>. This chapter discussed in details the different between the powder synthesized with and without the addition of (NH<sub>4</sub>)<sub>2</sub>SO<sub>4</sub> which includes their deposition on substrate by cold spray and also the properties of the obtained coating. Chapter 5 looks into the preparation of TiO<sub>2</sub> coating using TiO<sub>2</sub> powders synthesized with addition of (NH<sub>4</sub>)<sub>2</sub>SO<sub>4</sub> on different types of substrates. The factors that influenced by substrate materials used to prepare the cold spray coating and mechanism involved during the deposition depending on type of substrate are discussed in detail throughout this chapter. General conclusions and recommendation of further work are summarized in Chapter 6. Contribution of the study to the research/ academic and industrial field have been discussed briefly in Chapter 7. Finally, publications list and oral presentations and also acknowledgements for this study have been written in Chapter 8 and 9, respectively.

## 1.8 References

- 1) X. Chen, S.S. Mao: *Chem. Rev.* 107 (2007) 2891–959
- 2) M. Toyoda: *Appl. Catal. B Environ.* 49 (2004) 227–232.
- 3) E.S. Junior, F.A. La Porta, M.S. Liu, J. Andrés, J.A. Varela, E. Longo: *Dalton Trans.* (2015) 3159–3175.
- 4) S. Bakardjieva, J. Šubrt, V. Štengl, M.J. Dianez, M.J. Sayagues: *Appl. Catal. B Environ.* 58 (2005) 193–202.
- 5) D. Verhovšek, N. Veronovski, U. Lavrenčič Štangar, M. Kete, K. Žagar, M. Čeh: *Int. J. Photoenergy.* 2012 (2012) 1–10.
- 6) H.-G. Jung, Y.S. Kang, Y.-K. Sun: *Electrochim. Acta.* 55 (2010) 4637–4641.
- 7) G.-J. Yang, C.-J. Li, F. Han, W.-Y. Li, A. Ohmori: *Appl. Surf. Sci.* 254 (2008) 3979–3982.
- 8) S. Hu, A. Wang, X. Li, H. Löwe: *J. Phys. Chem. Solids.* 71 (2010) 156–162.
- 9) S.S. Mali, H. Kim, C.S. Shim, P.S. Patil, J.H. Kim, C.K. Hong: *Sci. Rep.* 3 (2013) 3004.
- 10) J. Yu, J. Fan, L. Zhao: *Electrochim. Acta.* 55 (2010) 597–602.
- 11) X.-L. He, G.-J. Yang, C.-J. Li, C.-X. Li, S.-Q. Fan: *J. Power Sources.* 251 (2014) 122–129.
- 12) X. Jin, J. Xu, X. Wang, Z. Xie, Z. Liu, B. Liang, et al.: *RSC Adv.* 4 (2014) 12640.
- 13) H.-G. Jung, S.W. Oh, J. Ce, N. Jayaprakash, Y.-K. Sun: *Electrochem. Commun.* 11 (2009) 756–759.
- 14) R. Klaysri, S. Wichaidit, T. Tubchareon, S. Nokjan, S. Piticharoenphun, O. Mekasuwandumrong, et al.: *Ceram. Int.* 41 (2015) 11409–11417.
- 15) M. Gardon, J.M. Guilemany: *J. Therm. Spray Technol.* 23 (2014) 577–595.
- 16) J.C. Colmenares, R. Luque, J.M. Campelo, F. Colmenares, Z. Karpiński, A.A. Romero: *Materials (Basel).* 2 (2009) 2228–2258.
- 17) D. Sannino, V. Vaiano, G. Sarno, P. Ciambelli: *Chemical Engineering Transactions* 32 (2013) 355–360.
- 18) F.-L. Toma, L.M. Berger, D. Jacquet, D. Wicky, I. Villaluenga, Y.R. de Miguel, et al.:



- Surf. Coatings Technol. 203 (2009) 2150–2156.
- 19) M. Muniz-miranda, A. Di Fabio, S. Parmeggiani, A. Zoppi, C. Giolli, G. Rizzi, et al., *La Metallurgia Italiana* (2008) 27-36.
  - 20) C. Han, J. Andersen, V. Likodimos, P. Falaras, J. Linkugel, D.D. Dionysiou: *Catal. Today*. 224 (2014) 132–139.
  - 21) B. Yu, K.M. Leung, Q. Guo, W.M. Lau, J. Yang: *Nanotechnology* 22 (2011) 1-9.
  - 22) M. Bozorgtabar, M. Rahimipour, M. Salehi: *Mater. Lett.* 64 (2010) 1173–1175.
  - 23) L.G. Devi, R. Kavitha: *Mater. Chem. Phys.* 143 (2014) 1300–1308.
  - 24) K. Akira, J. Wei: *Transactions of JWRI*, 34 (2005) No. 1.
  - 25) M. Farahmandjou: *Int. J. Fundam. Phys. Sci.* 3 (2013) 54–56.
  - 26) M. Yamada, Y. Kandori, K. Sato, M. Fukumoto: *J. Solid Mech. Mater. Eng.* 3 (2009) 210–216.
  - 27) A.N. Banerjee: *Nanotechnol. Sci. Appl.* 4 (2011) 35–65.
  - 28) F.-L. Toma, D. Sokolov, G. Bertrand, D. Klein, C. Coddet, C. Meunier: *J. Therm. Spray Technol.* 15 (2006) 576–581.
  - 29) F.-L. Toma, G. Bertrand, D. Klein, C. Coddet, C. Meunier: *J. Therm. Spray Technol.* 15 (2006) 587–592.
  - 30) F. Toma, G. Bertrand, D. Klein, C. Meunier, S. Begin: *Journal of Nanomaterials*, 2008 (2008) 1-8.
  - 31) C. Wu, Y. Lee, Y. Lo, C. Lin, C. Wu: *Applied Surface Science* 280 (2013) 737– 744
  - 32) F. Maury, J. Mungkalasiri: *Key Eng. Mater.* 415 (2009) 1–4.
  - 33) B.-H. Moon, Y.-M. Sung, C.-H. Han: *Energy Procedia*. 34 (2013) 589–596.
  - 34) J. Dostanić, B. Grbić, N. Radić, S. Stojadinović, R. Vasilić, Z. Vuković: *Appl. Surf. Sci.* 274 (2013) 321–327.
  - 35) R.S. Lima, B.R. Marple: *Surf. Coatings Technol.* 200 (2006) 3428–3437.
  - 36) P. Periyat, D.E. McCormack, S.J. Hinder, S.C. Pillai: *J. Phys. Chem. C.* 113 (2009) 3246–

3253.

- 37) B.W. Robinson, C.J. Tighe, R.I. Gruar, A. Mills, I.P. Parkin, A. K. Tabecki, et al.: *J. Mater. Chem. A*. 3 (2015) 12680–12689.
- 38) P. Ctibor, V. Stengl, Z. Pala: *Journal of Advance Ceramic* 2(3) (2013) 218–226.
- 39) H. Kim, S. Yang, R.C. Pawar, S.-H. Ahn, C.S. Lee: *Ceram. Int.* 41 (2015) 5937–5944.
- 40) N.T. Salim, M. Yamada, H. Nakano, K. Shima, H. Isago, M. Fukumoto: *Surf. Coatings Technol.* 206 (2011) 366–371.
- 41) M. Grujicic, C. Zhao, W. DeRosset, D. Helfrich: *Mater. Des.* 25 (2004) 681–688.
- 42) A. Papyrin: *Cold Spray technology* 159 (2001) 49–51.
- 43) H. Assadi, F. Gärtner, T. Stoltenhoff, H. Kreye: *Acta Mater.* 51 (2003) 4379–4394.
- 44) Y. Liu, Y. Wang, X. Suo, Y. Gong, C. Li, H. Li: *Ceram. Int.* 42 (2016) 1640–1647.
- 45) M. Gardon, C. Fernández-Rodríguez, D. Garzón Sousa, J.M. Doña-Rodríguez, S. Dosta, I.G. Cano, et al.: *J. Therm. Spray Technol.* 23 (2014) 1135–1141.
- 46) R. Drehmann, T. Grund, T. Lampke, B. Wielage, K. Manygoats, T. Schucknecht, et al.: *J. Therm. Spray Technol.* 23 (2014) 68–75.
- 47) J.-O. Kliemann, H. Gutzmann, F. Gärtner, H. Hübner, C. Borchers, T. Klassen: *J. Therm. Spray Technol.* 20 (2010) 292–298.
- 48) I. Burlacov, J. Jirkovský, L. Kavan, R. Ballhorn, R.B. Heimann: *J. Photochem. Photobiol. A Chem.* 187 (2007) 285–292.
- 49) M. Yamada, H. Isago, H. Nakano, M. Fukumoto: *J. Therm. Spray Technol.* 19 (2010) 1218–1223.
- 50) M. Yamada, H. Isago, K. Shima, H. Nakano, M. Fukumoto, T. J., Deposition of TiO<sub>2</sub> Ceramic Particles on Cold Spray Process, in: and G.M. B.R. Marple, A. Agarwal, M.M.

- Hyland, Y.-C. Lau, C.-J. Li, R.S. Lima (Ed.), *Therm. Spray Glob. Solut. Futur. Appl.*, Eds., Singapore, 2010, 2010: pp. 172 – 176.
- 51) Z. Sayyar, A.A. Babaluo, J.R. Shahrouzi: *Appl. Surf. Sci.* (2015) 1–10.
  - 52) H. Park, J. Kwon, I. Lee, C. Lee: *Scr. Mater.* 100 (2015) 44–47.
  - 53) F. Cao, H. Park, G. Bae, J. Heo, C. Lee: *J. Am. Ceram. Soc.* 96 (2013) 40–43.
  - 54) K.M. Kim, S.J. Song, J.Y. Seok, J.H. Yoon, K.M. Kim, G.H. Kim, et al.: *Sci. Rep.* 3, 3443 (2013).
  - 55) R.S. Lima, B.R. Marple: *Mater. Des.* 29 (2008) 1845–1855.
  - 56) L. Pawlowski, M. Bigan, R. Jaworski, M. Martel: *Surf. Coat. Technol.* 204 (2010) 1236–1246.
  - 57) J.M. Shockley, S. Descartes, P. Vo, E. Irissou, R.R. Chromik: *Surf. Coat. Technol.* 270 (2015) 324–333.
  - 58) J. Qiao, R. Bolot, H. Liao: *Surf. Coat. Technol.* 220 (2013) 170–173.
  - 59) A. Ibrahim, R.S. Lima, C.C. Berndt, B.R. Marple: *Surf. Coat. Technol.* 201 (2007) 7589–7596.
  - 60) R.S. Lima, B.R. Marple: *Mater. Sci. Eng. A.* 395 (2005) 269–280.
  - 61) C. Tian, J. Du, X. Chen, W. Ma, Z. Luo, X. Cheng, et al.: *Trans. Nonferrous Met. Soc. China.* 19 (2009) 829–833.
  - 62) B. Grzmil, D. Grella, B. Kic, Hydrolysis of titanium sulphate compounds, *Chem. Pap.* 62 (2008) 18–25. doi:10.2478/s11696-007-0074-8.
  - 63) P. Fauchais, G. Montavon, G. Bertrand: *J. Therm. Spray Technol.* 19 (2010) 56–80.
  - 64) L. Marcinauskas: *MATERIALS SCIENCE (MEDŽIAGOTYRA)* 16 (No. 1) ( 2010) 47-51.

- 65) R. Gadow, F. Kern, A. Killinger: *Mater. Sci. Eng. B Solid-State Mater. Adv. Technol.* 148 (2008) 58–64.
- 66) M. Fukumoto, H. Terada, M. Mashiko, K. Sato, M. Yamada, E. Yamaguchi: *Mater. Trans.* 50 (2009) 1482–1488.
- 67) H. Koivuluoto, P. Vuoristo, J. Therm. Spray Technol. 18(4) (2009) 555–562.
- 68) V.K. Champagne, D.J. Helfrich: *Surf. Eng.* 30 (2014) 396–403.
- 69) Z. Yi, C. Guofeng, W. Ma, W. Wei: *Prog. Org. Coatings.* 61 (2008) 321–325.
- 70) C.Y. Su, C.T. Lu, W.T. Hsiao, W.H. Liu, F.S. Shieu: *Thin Solid Films.* 544 (2013) 170–174.
- 71) R.S. Lima, B.R. Marple: *J. Therm. Spray Technol.* 16 (2007) 40–63.
- 72) M. Gaona, R.S. Lima, B.R. Marple: *J. Mater. Process. Technol.* 198 (2008) 426–435.
- 73) A. Moridi, S.M. Hassani-Gangaraj, M. Guagliano, M. Dao: *Surf. Eng.* 30 (2014) 369–395.
- 74) M. Jeandin, G. Rolland, L.L. Descurninges, M.H. Berger: *Surf. Eng.* 30 (2014) 291–298.
- 75) F.-L. Toma, L.-M. Berger, T. Naumann, S. Langner: *Surf. Coatings Technol.* 202 (2008) 4343–4348.
- 76) C. Sung, J. Ho, D. Kim, S. Cho, W. Oh: *Journal of Ceramic Processing Research* 11(No. 6) (2010) 736-741.

## **2 Synthesis and Properties of Agglomerated TiO<sub>2</sub> Powder by Hydrolysis and Hydrothermal Methods for Cold Spray Coating**

### **2.1 Introduction**

The ability to produce ceramic powders with controlled physical and chemical properties offers great benefits for various applications which require this material. Titanium dioxide (TiO<sub>2</sub>) is well known as one type of photocatalyst material that has been used as a self-cleaning coating for the external surfaces of buildings, houses, monuments, road tunnels, air and water purification from organic pollutants, anti-bacterial applications and many more [1-3]. A thick and large area coating, especially for photocatalytic application using TiO<sub>2</sub>, is more economically produced using a thermal spray method [2, 4]. However, conventional thermal spraying of ceramic materials such as TiO<sub>2</sub> suffers from a notable drawback where the high processing temperature causes phase transformation to occur.

Anatase phase is a metastable phase which will transform to rutile phase once it is above its melting temperature. This transformation is irreversible and should be avoided as rutile phase has lower photocatalytic activity when compared to anatase as a photocatalyst [4-6]. The cold spray [4, 5] process is a thermal spray process that operates below the melting temperature of the feedstock materials. Therefore, the properties of the powder material can be preserved even after the coating process.

In cold spraying, many factors contribute to coating formation and one of the dominant factors is the nature of the feedstock powder. Recently, significant attention has been paid to the

use of nanostructured ceramic material in a cold spray process. Feedstock materials from nanostructured powders can not only enhance the photocatalytic performance of  $\text{TiO}_2$  but also can promote ductility of the fine powder [7]. This characteristic is important for powder deformation on substrate by the cold spray method.

However, cold spray deposition using ceramic powders as feedstock materials is considered challenging due to their brittle characteristics and small size which can be the cause of hose clogging problems during the process [8, 9]. Therefore, agglomeration of the fine powder up to micrometer size by means of spray drying is preferable and is usually undertaken prior to the coating process [8, 10]. Yet, it is possible to synthesis nanostructured powder into micrometer sized particles due to the tendency of the nanoparticles to agglomerate as a result of the van der Waals attraction.

There are two synthesis methods that can be used to synthesis nanometer sized  $\text{TiO}_2$  powders. They are the chloride and sulfate processes [11]. In the case of the chloride method it is challenging, especially in the presence of atmospheric moisture, to control the hydrolysis rate. On the other hand, the sulfate process offers an easily controlled process and also benefits from low cost raw materials. Among these methods, hydrolysis and hydrothermal methods require simple equipment and no strict control of the process parameters.

In this study,  $\text{TiO}_2$  powders were synthesized via the hydrolysis and hydrothermal methods using similar raw materials. The properties of the obtained powders were characterized by transmission electron microscopy (TEM), scanning electron microscopy (SEM), field emission scanning electron microscope (FESEM), particle size analyzer and X-ray diffraction (XRD). A preliminary study on coating deposition was studied by using a cold spray process.

## **2.2 Experimental Procedure**

### **2.2.1 Synthesis of TiO<sub>2</sub> Powders by Hydrolysis Method**

In the current work, the TiO<sub>2</sub> powder used was prepared using 10 wt.% of titalyl sulfate (TiOSO<sub>4</sub> · nH<sub>2</sub>O, Chameleon Reagent, Japan) which was mixed with distilled water to perform the hydrolysis reaction and hereafter is known as TiO<sub>2</sub>-H. The solution was stirred on a hot plate at 120 °C for 8 h. During the reaction, the white solution transformed into a clear solution. Upon completion of the synthesis, a white precipitate formed. The precipitate was washed with distilled water several times and collected by decantation. The precipitate was then dried in an oven at 120 °C.

### **2.2.2 Synthesis of TiO<sub>2</sub> Powders by Hydrothermal Method**

The TiO<sub>2</sub> powder synthesized by the hydrothermal method in this work was prepared using 10 wt% of titalyl sulfate (TiOSO<sub>4</sub> · nH<sub>2</sub>O, Chameleon Reagent, Japan) and is hereafter known as TiO<sub>2</sub>-HT. The starting material was dissolved in distilled water by magnetic stirring for 30 minutes. The resultant transparent solution was then transferred to a Teflon- lined autoclave. The hydrothermal reaction was carried out at 150°C for 8h. Upon completion of the hydrothermal synthesis, the autoclave was allowed to cool naturally at room temperature. The obtained white precipitate was washed several times with distilled water and oven dried at 120°C.

### 2.2.3 TiO<sub>2</sub> Coating by Cold Spray Process

The deposition of TiO<sub>2</sub> coatings was performed using a custom-made suction nozzle using a CGT KINETIKS 4000 (Cold Gas Technology, Germany). Ceramic tiles (INAX ADM-155M) were used as the substrate which had been grit blasted prior to their use. The gas temperature and pressure were 500°C and 3 MPa, respectively. Nitrogen gas was used as the process gas. Fig. 2.1 shows the schematic diagram of the cold spray system used in this experiment.

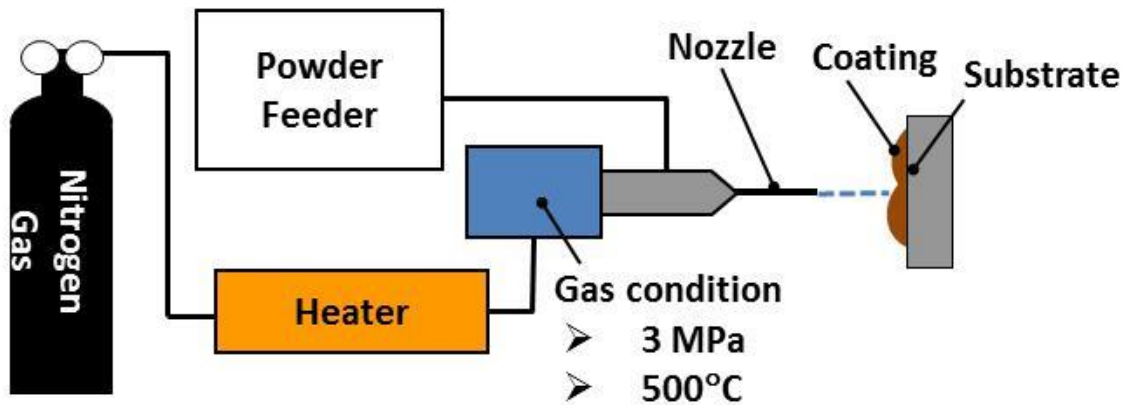


Figure 2.1: Schematic diagram of cold spray system.

### 2.2.4 Characterization of TiO<sub>2</sub> Powders and Coating

The morphology of the resulting powders and the obtained fractured cross-sections of the coating samples were examined using a scanning electron microscope (SEM: JSM-6390, JEOL)



and a field emission scanning electron microscope (FESEM: SU8000, Hitachi). A transmission electron microscope (TEM: JEM-2100F, JEOL) was used to measure the primary particles size of the as-synthesized TiO<sub>2</sub>. The agglomerate size of the synthesized TiO<sub>2</sub> powders was measured using a Nano Particle Size Analyzer SALD-7100 (Shimadzu). The phase purity and crystallinity of the as-synthesized powders were characterized by X-ray diffraction (XRD: RINT 2500, Rigaku) with Cu-K $\alpha$  radiation ( $\lambda = 1.5406 \text{ \AA}$ ) over the  $2\theta$  range of 10-80°. The Scherrer equation [12] was used to calculate the crystal size of the TiO<sub>2</sub>.

## **2.3 Results & Discussion**

### **2.3.1 Characterizations of TiO<sub>2</sub> powders**

Powder morphology and distributions correlated strongly with the synthesis method. From the results obtained in this study, hydrolysis and hydrothermal methods can produce nanometer sized TiO<sub>2</sub> powders as observed by TEM and shown in Fig. 2.2 (a) and (b) for TiO<sub>2</sub>-H and TiO<sub>2</sub>-HT, respectively. There is no significant difference in the primary images of the particles for both processes. Both methods show that the as-synthesized TiO<sub>2</sub> powders have a high tendency to agglomerate naturally. On the contrary, SEM observation showed that the morphology and powder distribution for these two processes were not similar. From the SEM images, it can be seen that the TiO<sub>2</sub>-H powders have a relatively uniform distribution of powder and are agglomerated in the range from 5-20  $\mu\text{m}$  as revealed in Fig. 2.3 (a). Meanwhile for the TiO<sub>2</sub> powders, which were synthesized by the hydrothermal method, agglomerated powder, with an aggregated particle size, is in the range of 0.5-25  $\mu\text{m}$  and random distribution was observed as shown in Fig. 2.3 (b). In comparison to TiO<sub>2</sub>-H powders, SEM analysis as shown in Fig. 2.3 (d)

also shows that TiO<sub>2</sub>-HT powders were of a larger size with a more pronounced formation of secondary particles. Furthermore, Fig. 2.4 depicts that TiO<sub>2</sub>-H contains more pores as compared to TiO<sub>2</sub>-HT which shows that TiO<sub>2</sub>-H has a more porous and loose structure between the fine particles.

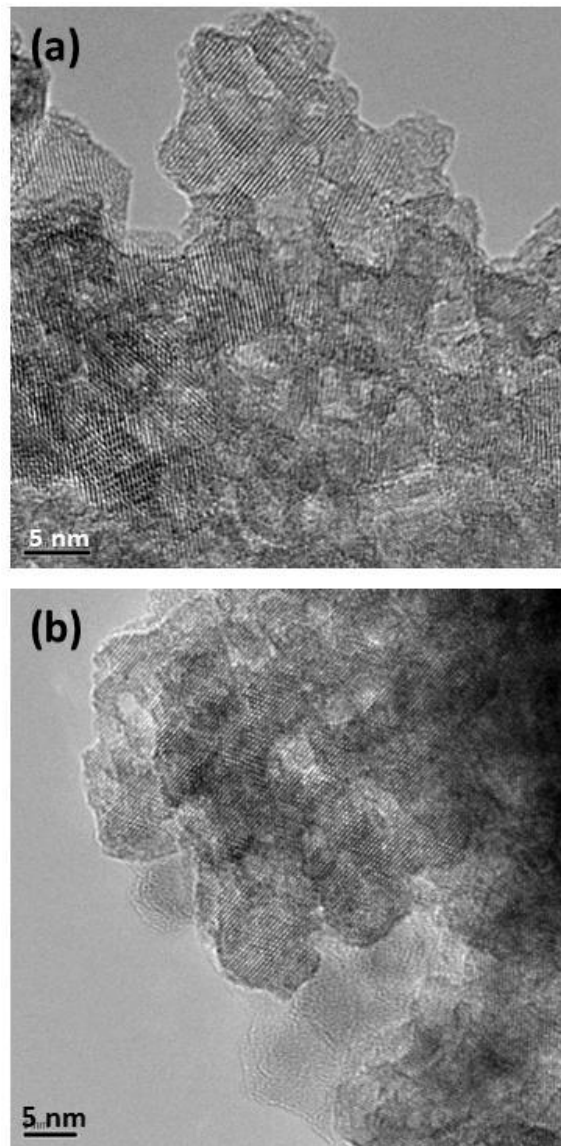


Figure 2.2: TEM images of TiO<sub>2</sub> powders that synthesized by hydrolysis (a) and hydrothermal (b) method.

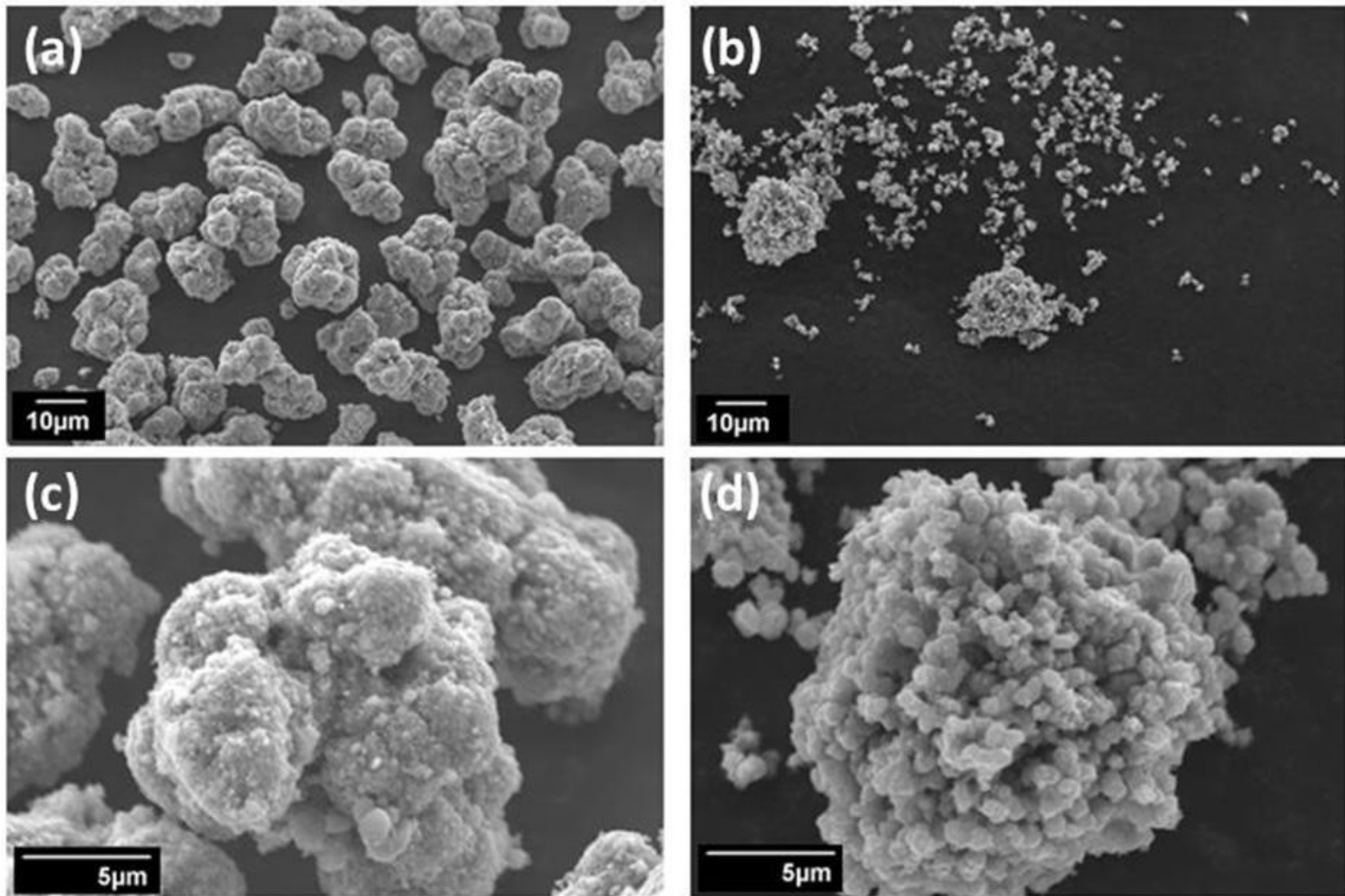


Figure 2.3: SEM images of  $\text{TiO}_2$  powders that synthesized by hydrolysis (a & c) and hydrothermal (b & d) methods.

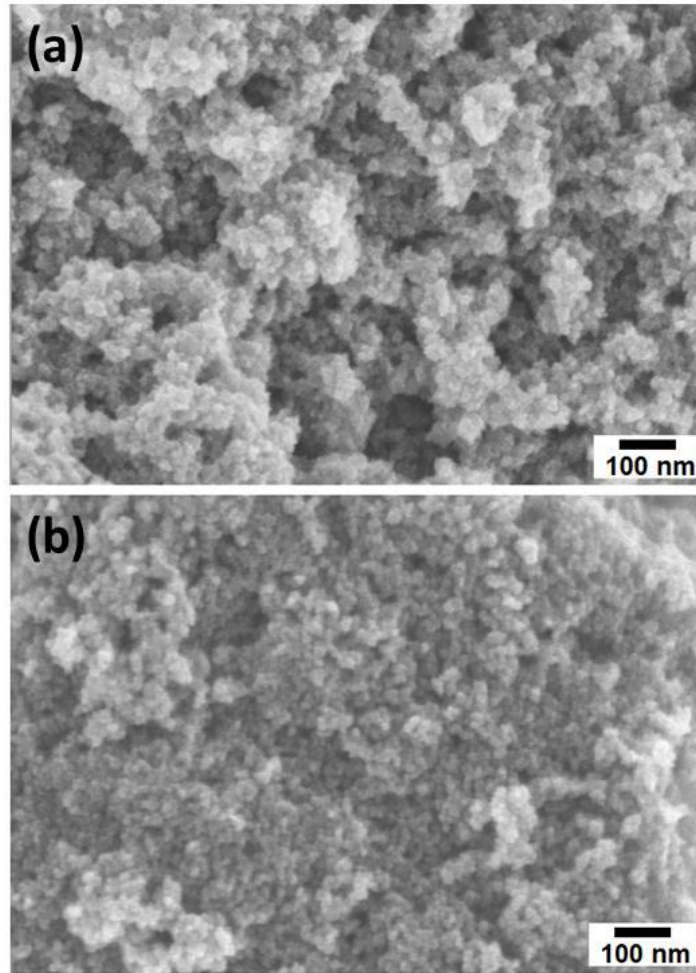


Figure 2.4: FESEM images of  $\text{TiO}_2$  powders that synthesized by (a) hydrolysis and (b) hydrothermal method.

The particle size distribution of each powder which were synthesized by different routes was obtained using a Nano Particle Size Analyzer SALD-7100 (Shimadzu) which is shown in Fig. 2.5. The size distribution of TiO<sub>2</sub> powders synthesized by hydrolysis method is  $d_{10} = 4.92 \mu\text{m}$ ,  $d_{50} = 10.70 \mu\text{m}$ , and  $d_{90} = 19.72 \mu\text{m}$ . However, unlike the TiO<sub>2</sub>-H, TiO<sub>2</sub> powders, that were synthesized by the hydrothermal method, they show a wide range of particle size with their size distributions of  $d_{10} = 4.18 \mu\text{m}$ ,  $d_{50} = 19.85 \mu\text{m}$ , and  $d_{90} = 46.76 \mu\text{m}$ . The results show that both synthesis methods can produce powders that readily agglomerate due to van der Waals force which in turn eliminates the need for spray drying to agglomerate the nano-sized primary particles to micro-sized feedstock powders for the cold spray process.

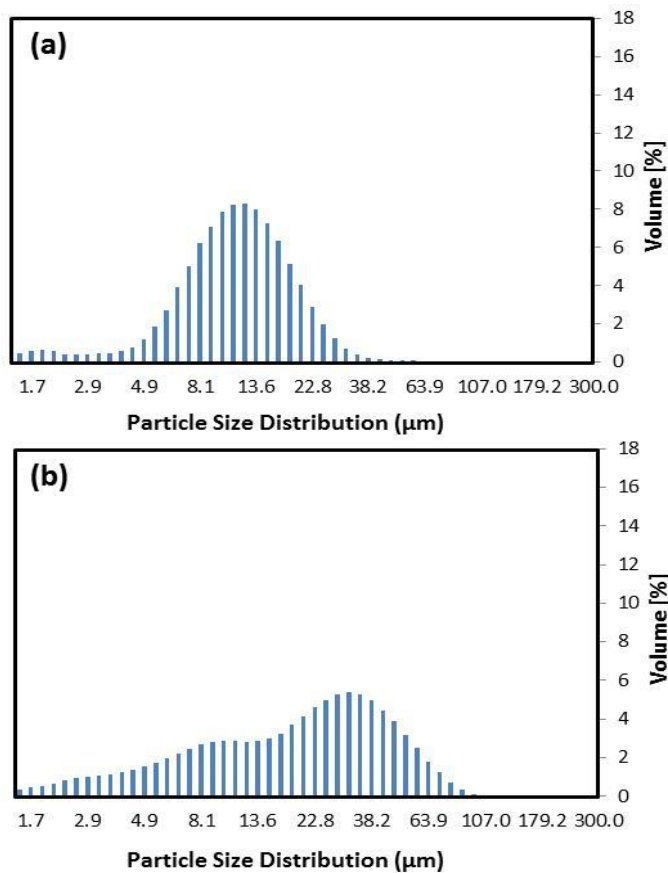


Figure 2.5: Particle size distribution profile of starting agglomerated TiO<sub>2</sub> powders synthesized by (a) hydrolysis and (b) hydrothermal method.

A significant difference in crystallinity can be observed between the TiO<sub>2</sub>-H and TiO<sub>2</sub>-HT powders as shown by the XRD patterns in Fig.2.6. Both patterns show the characteristics of the anatase phase of TiO<sub>2</sub> and are in good agreement with PDF card No. 21-1272. The disappearance of a rutile structure in TiO<sub>2</sub>-H and TiO<sub>2</sub>-HT powders showed that with this method, it is possible to produce only anatase TiO<sub>2</sub> powders at a low synthesis temperature. Figure 2.6 also revealed that the hydrothermal process produced TiO<sub>2</sub> powder with higher crystallinity compared to the hydrolysis method. From the result obtained, the sharp peaks of TiO<sub>2</sub>-HT powders were due to a higher temperature during synthesis as compared to the TiO<sub>2</sub>-H powders. Meanwhile, TiO<sub>2</sub>-H powders have a broader peak than the TiO<sub>2</sub>-HT powders which indicates that TiO<sub>2</sub>-H is of a smaller crystallite size. The crystallite sizes of both particles, which were calculated using the Scherrer equation from the (101) planes, were 11.09 nm and 24.65 nm for TiO<sub>2</sub>-H and TiO<sub>2</sub>-HT powders, respectively.

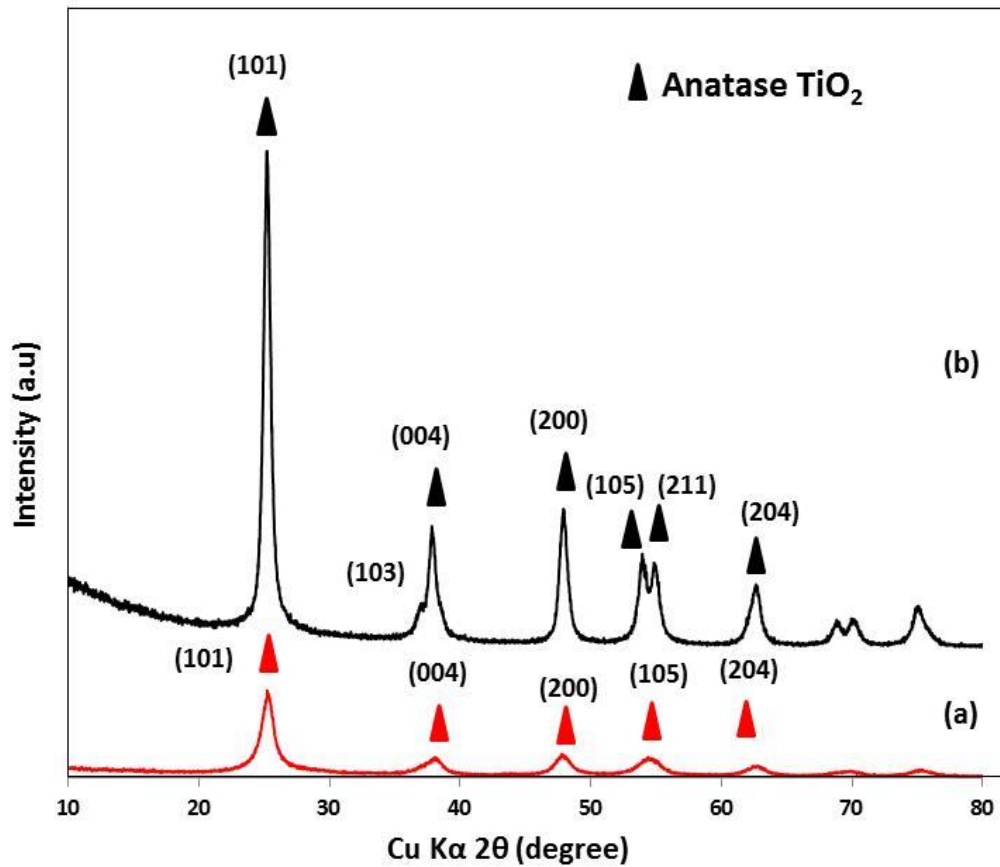


Figure 2.6: XRD pattern of TiO<sub>2</sub> powders that were synthesized by (a) hydrolysis (TiO<sub>2</sub>-H) and (b) hydrothermal (TiO<sub>2</sub>-HT).

### 2.3.2 Microstructure and Crystalline Structure of TiO<sub>2</sub> Coating

Figure 2.7 shows the cross-section of the TiO<sub>2</sub> coating that was obtained using the synthesized TiO<sub>2</sub> powders for both methods. It can be seen that the TiO<sub>2</sub>-H powders can be deposited on the ceramic tiles substrate and form a coating of about 50 μm thickness as shown in Fig. 2.7 (a). Meanwhile, in the case of the TiO<sub>2</sub>-HT powders, only particle embedment, with very

few particles attached to the surface of the substrate, was observed (Fig. 2.7 (a)). The results obtained in this study revealed that only  $\text{TiO}_2\text{-H}$  powders were successful in building-up the coating due to the continuous stacking of agglomerated  $\text{TiO}_2\text{-H}$  powders on the previously-deposited particles.

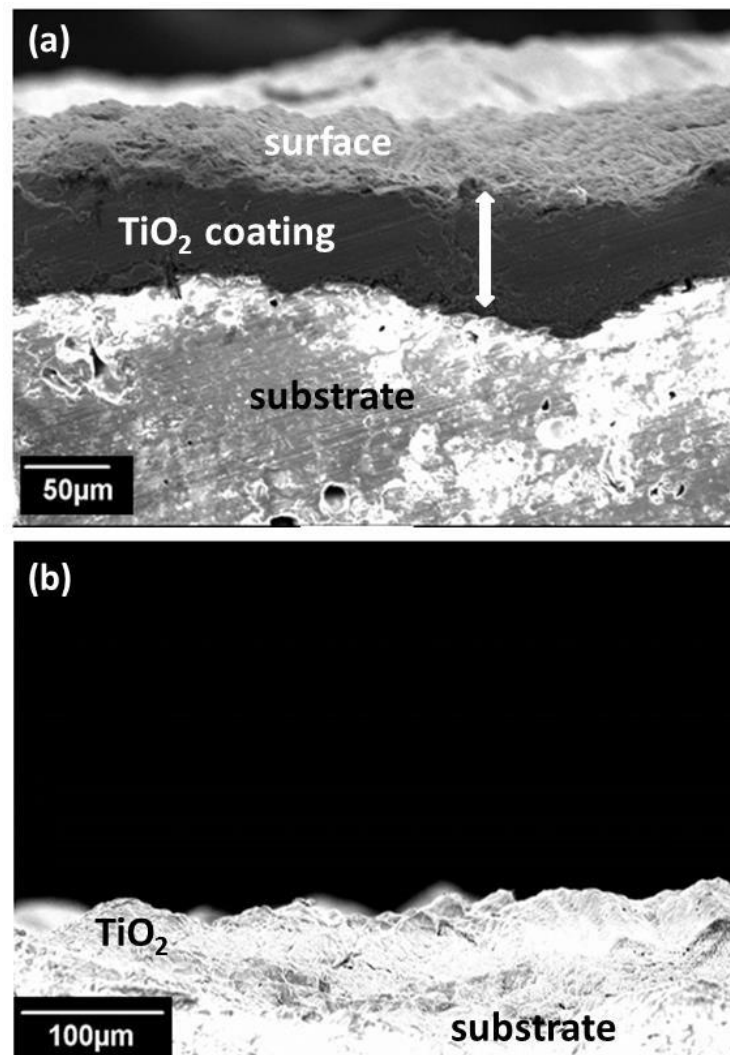


Figure 2.7: Cross-sectional view of  $\text{TiO}_2$  coating deposited by cold spray using powder synthesis by (a) hydrolysis ( $\text{TiO}_2\text{-H}$ ) and (b) hydrothermal ( $\text{TiO}_2\text{-HT}$ ).



Figure 2.8 presents the XRD patterns of anatase TiO<sub>2</sub> coatings in comparison with the feedstock powders for TiO<sub>2</sub>-H. The results revealed that anatase phase was preserved for cold-sprayed coating using TiO<sub>2</sub>-H powders. In cold spraying, the processing temperature is below the melting temperature of the feedstock materials. It is concluded that no phase transformation occurs during the coating process as no other phase; i.e. rutile phase was observed. The absence of rutile phase is expected to increase the photocatalytic activity of the as-sprayed coating [4].

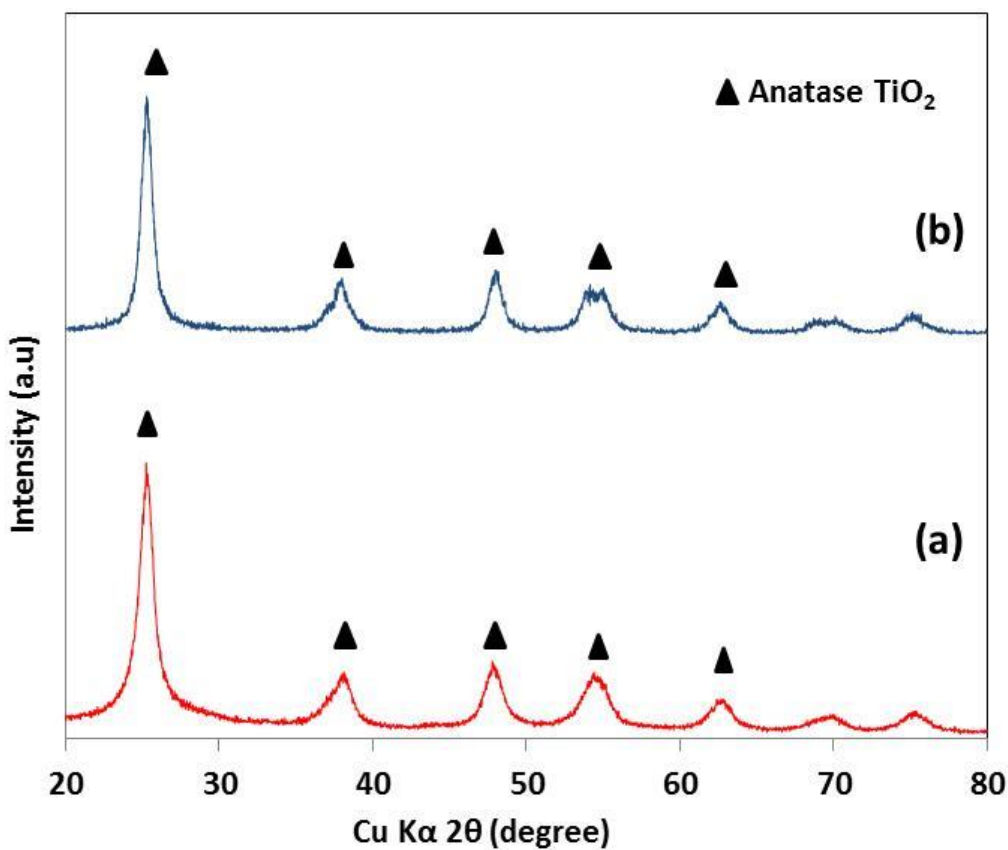


Figure 2.8: XRD pattern of (a) TiO<sub>2</sub>-H powder and (a) TiO<sub>2</sub>-H coating deposited by cold spray process.

### 2.3.3 Deposition Mechanism

From the results obtained, it was concluded that the morphology and property of the feedstock materials play very important roles in order to successfully deposit the powder onto the substrate via the cold spray process. A different synthesis route has produced different properties for the synthesized powder. The deposition mechanism of ceramic feedstock materials by kinetic spraying can be varied depending on the particle size, shape, agglomeration, porosity, grain size, interphase, and more [14, 15]. Kim et al. reported the role of TiO<sub>2</sub> nanoparticles in the dry deposition of NiO micro-sized particles at room temperature. A NiO coating was only achieved when TiO<sub>2</sub> particles were mixed with micro-sized NiO prior to deposition. TiO<sub>2</sub> powders were used in assisting the deposition of NiO due to the ability of nano-TiO<sub>2</sub> to deform and the tendency of the feedstock powders to break up their agglomerates upon impact with the substrate. The finding of this study suggested that coating of ceramic material by kinetic spraying is affected by the size and shape of the starting feedstock materials.

Figure 2.9 shows the possible mechanism on how the coating formed onto the substrate using TiO<sub>2</sub> powders that were synthesized by the hydrolysis and hydrothermal methods. In this study, TiO<sub>2</sub>-H with smaller diameter agglomerates was successfully deposited onto the substrate. The TiO<sub>2</sub>-H suffers from a harsh condition during the impact onto the substrate which led to the breaking up of its agglomerates initiated by the porosity that is contained in the powder. Low crystallinity with some porosity that is contained in the TiO<sub>2</sub>-H powders, indicates that the binding force which holds the agglomerate particles together may be weaker than the force in the TiO<sub>2</sub>-HT. Moreover, Yamada et. al [12] reported that a TiO<sub>2</sub> coating was produced from a recombination of broken up crystallite links during the cold spray process, which was initiated

by the porous structure of the agglomerated powders. The authors described that during the process, the nano-scale primary particles in the agglomerated powder were fractured, leaving an unstable surface with a dangling bond structure. In order to reobtain a stable surface, the fractured particles recombined and formed a surface with improved stability. This was achieved by the adhesion of the fractured particles with the substrate upon collision and with the previously-deposited  $\text{TiO}_2$  coating layer.

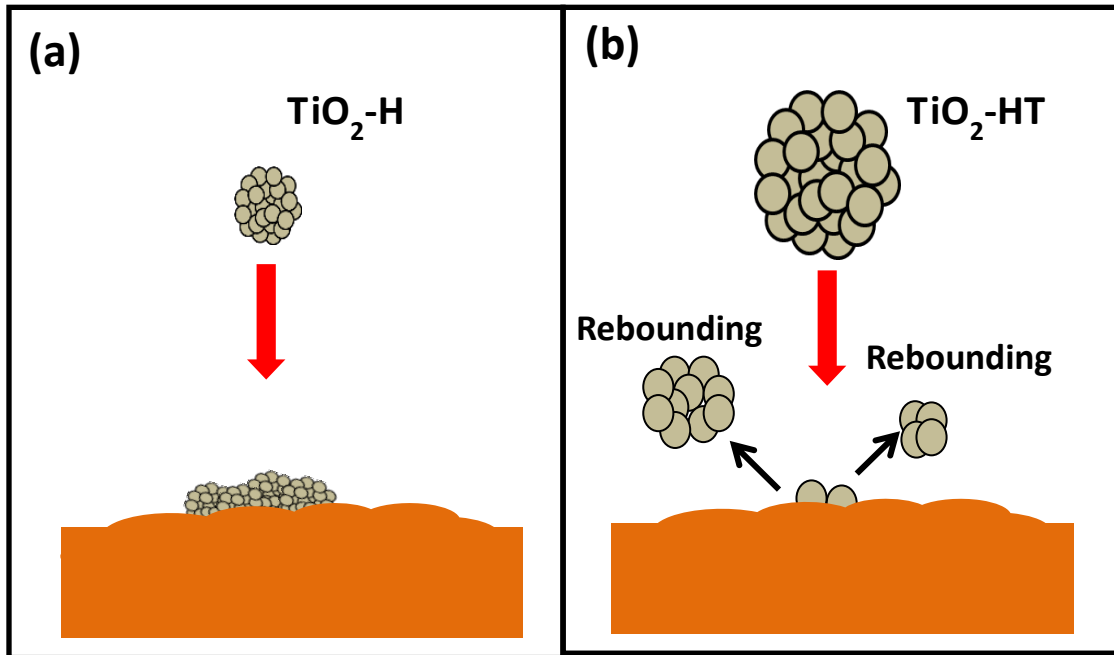


Figure 2.9: Possible mechanism of bonding between  $\text{TiO}_2$  powders and the substrates using powder synthesized by (a) hydrolysis and (b) hydrothermal method.

Contrary to TiO<sub>2</sub>-HT, it seems that TiO<sub>2</sub>-HT particles were not deformed or broke up on impact with the substrate during cold spray due to the harder and larger size of the particles compared to TiO<sub>2</sub>-H. Hence, the density of TiO<sub>2</sub>-HT was expected to be higher than TiO<sub>2</sub>-H and TiO<sub>2</sub>-HT experienced an excess of kinetic energy which led to a rebound of the incident TiO<sub>2</sub>-HT particles as shown in Fig. 2.9 (b). In addition, TiO<sub>2</sub>-HT powders have a higher degree of crystallinity (as shown in Fig. 2.6) due to a higher synthesis temperature which led to a higher rate of precipitation during the reaction; thereby resulting in the formation of stronger agglomerated particles with bigger sized secondary particles. Therefore, in this case, TiO<sub>2</sub>-HT powders proved to be difficult to fracture and an unstable surface was not obtained. Since the collided particles were hard and possess a stable surface, only evidence of particle embedment was observed on the surface of the substrate due to a lower number of pores that were coupled with the particles which led to fracture resistance upon impact onto the substrate (Fig. 2.7 (a)) .

## 2.4 Conclusions

The feasibility of synthesizing anatase TiO<sub>2</sub> powders specifically for a cold spray process was studied by hydrolysis and hydrothermal methods at low synthesis temperatures. Low-cost starting materials, TiOSO<sub>4</sub> and distilled water were used as the precursor and solvent, respectively. XRD analysis revealed that TiO<sub>2</sub>-H powders have a broader diffraction peak than TiO<sub>2</sub>-HT powders which indicates that TiO<sub>2</sub>-H are of smaller crystallite size and have lower crystallinity. The results showed that both synthesized processes produced nanometer sized primary particles which were agglomerated into micrometer sized tertiary particles. However,

SEM observation showed that TiO<sub>2</sub>-H powders have a more uniform powder distribution compared to TiO<sub>2</sub>-HT. Coating deposition showed that only agglomerated TiO<sub>2</sub>-H powders could be used as feedstock material for the CS process. This study shows that selection of appropriate morphology together with the crystallinity of the feedstock powders is important to produce a ceramic coating on the substrate by cold spray. This study indicates that a successful deposition depends on the tendency of the feedstock powders to break up the agglomerates upon collision with the substrate which is promoted by the porous structure of the agglomerated powders.

## 2.5 References

- 1) D. Verhovšek, N. Veronovski, U. Lavrenčič Štangar, M. Kete, K. Žagar, M. Čeh: *Int. J. Photoenergy*. 2012 (2012) 1–10.
- 2) F.-L. Toma, G. Bertrand, D. Klein, C. Meunier and S. Begin: *J. Nanomater.* 2008 (2008) 1–8.
- 3) Y.-N. Chang, X.-M. Ou, G.-M. Zeng, J.-L. Gong, C.-H. Deng, Y. Jiang, J. Liang, G. Yuan, H. Liu and X. He: *Appl. Surf. Sci.* 343 (2015) 1–10.
- 4) M. Yamada, H. Isago, H. Nakano, M. Fukumoto: *J. Therm. Spray Technol.* 19 (2010) 1218–1223.
- 5) M. Gardon, C. Fernández-Rodríguez, D. Garzón Sousa, J.M. Doña-Rodríguez, S. Dosta, I.G. Cano and J. M. Guilemany: *J. Therm. Spray Technol.* 23 (2014) 1135–1141.
- 6) N.T. Salim, M. Yamada, H. Nakano, K. Shima, H. Isago and M. Fukumoto: *Surf. Coatings Technol.* 206 (2011) 366–371.
- 7) L. Pawlowski: *Surf. Coatings Technol.* 202 (2008) 4318–4328.
- 8) M. Gardon and J.M. Guilemany: *J. Therm. Spray Technol.* 23 (2014) 577–595.

- 9) R.S. Lima and B.R. Marple: *J. Therm. Spray Technol.* 16 (2007) 40–63.
- 10) I. Herrmann-Geppert, P. Bogdanoff, T. Emmler, Th. Dittrich, J. Radnik, T. Klassen, H. Gutzmann and M. Schieda: *Catal. Today.* 260 (2016) 140-147.
- 11) B. Grzmil, D. Grela, B. Kic: *Chem. Pap.*, 62 (2008) 18–25.
- 12) S. Ngamta, N. Boonprakob, N. Wetchskun, K. Ounnunkad, S. Phanichphant and B. Inceesungvorn: *Mater. Lett.* 105 (2013) 76–79.
- 13) M. Yamada, H. Isago, K. Shima, H. Nakano and M. Fukumoto: in *Proc. ITSC 2010, Thermal spray: Global Solutions for Future Applications*, May 2010, Singapore, DVS-Berichte 264, DVS Media GmbH, Dusseldorf, Germany, (2010), pp. 187-191.
- 14) H. Kim, S. Yang, R.C. Pawar, S.-H. Ahn and C.S. Lee: *Ceram. Int.* 41 (2015) 5937–5944.
- 15) H. Park, J. Kim and C. Lee: *Scr. Mater.* 108 (2015) 72–75.

### **3 Cold-Sprayed Titanium Dioxide Coating Using Powders Calcined at Low Temperatures**

#### **3.1 Introduction**

Titanium dioxide ( $\text{TiO}_2$ ) has been reported to be widely used for photocatalyst to degrade harmful and toxic organic pollutants [1]. This material has been used for a self-cleaning application on the external surfaces of buildings [2, 3].  $\text{TiO}_2$  also known as road warrior as to clean the nitrogen oxide ( $\text{NO}_x$ ) in the air that was produced by vehicles emissions [4]. Various techniques have been used to fabricate  $\text{TiO}_2$  coating for photocatalyst applications including chemical vapor deposition (CVD), physical vapor deposition (PVD), dip-coating and sol gel method [5-8]. However, these methods have some restrictions such as high production cost and complex large-scale equipment [5]. In the case of CVD and PVD, vacuum condition is needed during the fabrication of the coating. Meanwhile for dip-coating technique, the process requires long production time, careful manufacturing process and also high temperatures for post-deposition treatment [8]. Moreover, these techniques are limited to produce thin and small scale coatings.

Thermal spray is an alternative method to fabricate large scale thick  $\text{TiO}_2$  photocatalyst coating with less time consumption and more cost effective. However, a significant challenge in the conventional thermal spray techniques including atmospheric plasma-spray (APS) process and high-velocity oxy fuel (HVOF) is high processing temperature uses during the process to melt the feedstock powders for coating deposition [7, 8]. The high process temperature may lead

to the phase transformation of TiO<sub>2</sub> from anatase to rutile and also increase the initial crystallite size of the TiO<sub>2</sub> powders. The change in crystal structure and crystallite size is not favorable as it reduces the photocatalytic property of the coatings [9]. A lower temperature process, such as cold spraying, offers a great advantage in the deposition process as this process generally operates below the melting temperature of the feedstock materials [8, 10-13]. Thus, this technique can prevent phase changes after the coating process.

Cold spraying is a thermal spray process that uses supersonic gas stream to accelerate the feedstock particles below its melting temperature. Therefore, cold spray process is one of the suitable processes to fabricate thick and large scale of anatase TiO<sub>2</sub> coating [7]. Generally, in cold spray process, the feedstock materials are usually plastically deformed on the substrate upon impact, forming layer of coating. TiO<sub>2</sub> is a ceramic material which has a brittle characteristic, making it difficult to be deposited by this method. However, several studies have been conducted and demonstrated that TiO<sub>2</sub> coating can be produced by cold spray method. Anatase TiO<sub>2</sub> coating was deposited by cold spraying when the surface of steel substrate was coated with titanium sub-oxide layers [8]. The titanium sub-oxide layer was prepared by APS method provides rough and hard surface on the substrate which ease the adherence of TiO<sub>2</sub> powders when impacting onto the substrate due to chemical bonding. A cold-sprayed coating with 150 μm thickness was fabricated using agglomerated TiO<sub>2</sub> powders synthesized with addition of ammonium sulfate and hydrothermally treated prior to the coating process [12]. The NH<sub>4</sub><sup>+</sup> and SO<sub>4</sub><sup>2-</sup> ions adsorptions on surface of TiO<sub>2</sub> and post hydrothermal treatment have contributed to the formation of an oriented agglomerated structure in a single crystal axis were believed as the factors that lead to the building-up of the coating. Moreover, cold-sprayed TiO<sub>2</sub> film about 15 μm with rough and porous structure was also achieved when the ultra-fine TiO<sub>2</sub> powders were



agglomerated into micrometer sized using polyvinyl alcohol as binder [14]. In that study, the deformation of TiO<sub>2</sub> powders was assisted by ductility of the binder during the particles impact under high transient impact pressure.

In this work, a low temperature process method has been utilized to obtain the TiO<sub>2</sub> powders used as the feedstock materials for cold spray. The powders were synthesized via a simple hydrolysis method for photocatalyst application. In order to avoid progressive grain growth and also the existence of internal pores within the particles, study on the effect of low calcination temperatures on the as-synthesized TiO<sub>2</sub> powders were also explored in this work. The as-synthesized TiO<sub>2</sub> and calcined TiO<sub>2</sub> powders were used to study the possibility to produce TiO<sub>2</sub> coating by cold spray process.

## **3.2 Experimental Procedures**

### **3.2.1 Preparation of TiO<sub>2</sub> Powders for Cold Spray Coating**

The TiO<sub>2</sub> powder synthesized by the hydrolysis method in this work was prepared by simple hydrolysis method. Titanyl sulfate solution was prepared by mixing TiOSO<sub>4</sub> · *n*H<sub>2</sub>O (Chameleon Reagent, Japan) in distilled water. The ratio of TiOSO<sub>4</sub> with respect to distilled water was 1:9. The white solution was stirred on a hot plate to maintain the temperature of the solution at ~80 °C. The precipitate was then oven dried at 120 °C for 10 h. The dried powder was crushed to obtain a well-defined TiO<sub>2</sub> powder, hereafter referred to as TiO<sub>2</sub>-0. In order to study the effect of heat treatment at low calcination temperatures on the morphology,

crystallinity and powder deposition of the TiO<sub>2</sub> coating, as-synthesized powders were calcined at 200°C, 300°C and 400°C for 1 h, hereafter designated as TiO<sub>2</sub>-2, TiO<sub>2</sub>-3 and TiO<sub>2</sub>-4 respectively.

### **3.2.2 Cold Spray Process**

The coatings were deposited on a grit-blasted ceramic tile substrate (INAX ADM-155M). Prior to spraying, the ceramic tiles were rinsed with acetone. The spray powders were deposited via the cold spray process using CGT KINETIKS 4000 (Cold Gas Technology, Ampfing, Germany) with a custom made suction nozzle. Nitrogen was used as the process gas with an operating temperature of 500°C and at a pressure of 3 MPa. The spray distance and traverse speed of the process was 30 mm and 20 mm/s, respectively.

### **3.2.3 Characterization of TiO<sub>2</sub> Powders and Coating**

A Differential Thermal Analyzer (DTA: DTA-50, Shimadzu) was used to investigate the thermal property of the as-synthesized TiO<sub>2</sub> with a 10°C/ min heating rate. An X-ray Photoelectron Spectroscopy (XPS: Quantera SXM-CI, ULVAC-Phi, Inc.) was used to measure the chemical composition of the TiO<sub>2</sub> powders. The X-ray diffraction (XRD) patterns were obtained using a Rigaku RINT 2500 with Cu-K $\alpha$  radiation ( $\lambda = 1.5406 \text{ \AA}$ ) over the  $2\theta$  range of 20-80°. The crystallite size of each powder was calculated from the (101) plane by the Scherrer equation. The morphology of the resulting powders and the obtained fractured cross sections of the coating samples were examined using a Scanning Electron Microscope (SEM: JSM-6390, JEOL) and a Field Emission Scanning Electron Microscope (FESEM: SU8000, Hitachi). A

Transmission Electron Microscope (TEM: JEM-2100F, JEOL) was used to measure the primary particle size of the as-synthesized TiO<sub>2</sub>.

### **3.3 Results & Discussion**

#### **3.3.1 Effects of Low Calcination Temperatures on the Properties of TiO<sub>2</sub> Powders**

Figure 3.1 shows the DTA curve of the as-synthesized TiO<sub>2</sub> powders. The DTA curve of as-synthesized TiO<sub>2</sub> powders indicates that a broad endothermic peak exists at ca. 75°C which attributes to desorption of water molecules. The partial presence of water molecules on the surface of the precursor was expected as the reaction was carried out using distilled water as the aqueous media. There is a small endothermic peak maximum at ca. 180°C due to loss of organic residues and chemisorbed water. An exothermic peak observed at 480°C can be attributed to the progressive growth of crystallites size and crystallinity of the TiO<sub>2</sub> powders. The exothermic peak with a maximum at ca. 950°C is corresponded to the phase transformations from anatase phase to rutile phase.

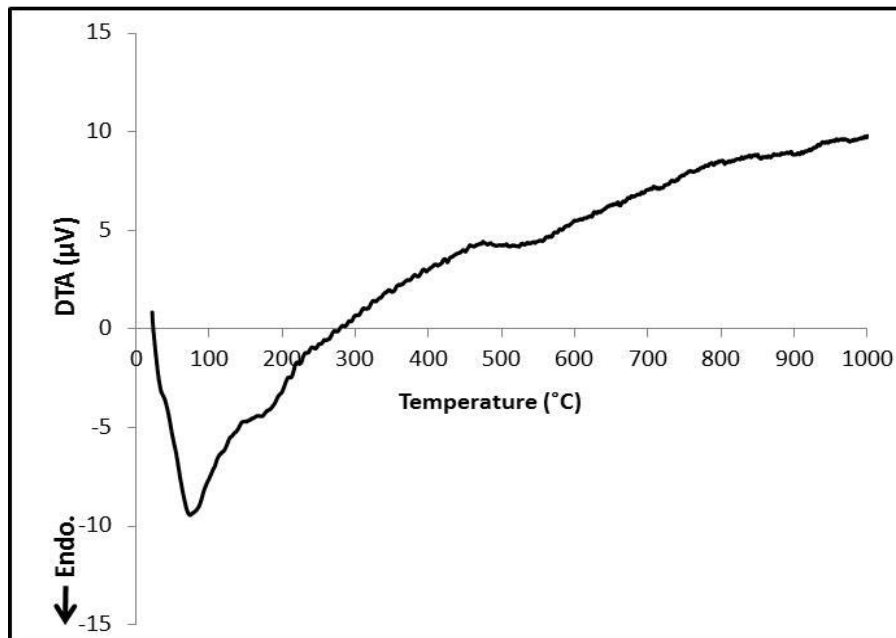


Figure 3.1: DTA curve recorded in air with a 10°C/ min heating rate for as-synthesized TiO<sub>2</sub>.

The XRD pattern of the as synthesized TiO<sub>2</sub> powders at different calcination temperatures is shown in Fig. 3.2. Identification of the phases in the analyzed powders was achieved by comparing the obtained XRD patterns with PDF Card No. 021-1272. The crystallite size on (101) plane was calculated using the Scherrer equation by using the full width at half maximum (FWHM) data of their XRD patterns, and the results showed that increase of crystallite size occurred as the powders were calcined at 200°C, 300°C and 400°C and the obtained results are presented in Table 3.1. This result indicated that the broad diffraction peaks revealed that all of the analyzed powders were in anatase phase with nanometer sized particles. The results indicated that low-temperature calcination can improve crystallinity and crystallite size of the as-synthesized TiO<sub>2</sub> powders. However, only a slight increase of crystallinity and

crystallite sizes were observed for the powders calcined at 200°C, 300°C and 400°C. These results are in good agreement with previous reported studies which shows that only small changes in the crystallinity and the crystallite sizes of the TiO<sub>2</sub> powders were observed when the powders were calcined below 500°C [3, 15]. Moreover, the XRD results were consistent with the DTA result as the curve also revealed that no temperature-induced phase transition occurred when the temperature was increased up to 400°C. Despite the fact that the transformation of anatase to rutile is above 700°C [12, 15, 16] and only anatase phase was identified even after the post-heat treatment.

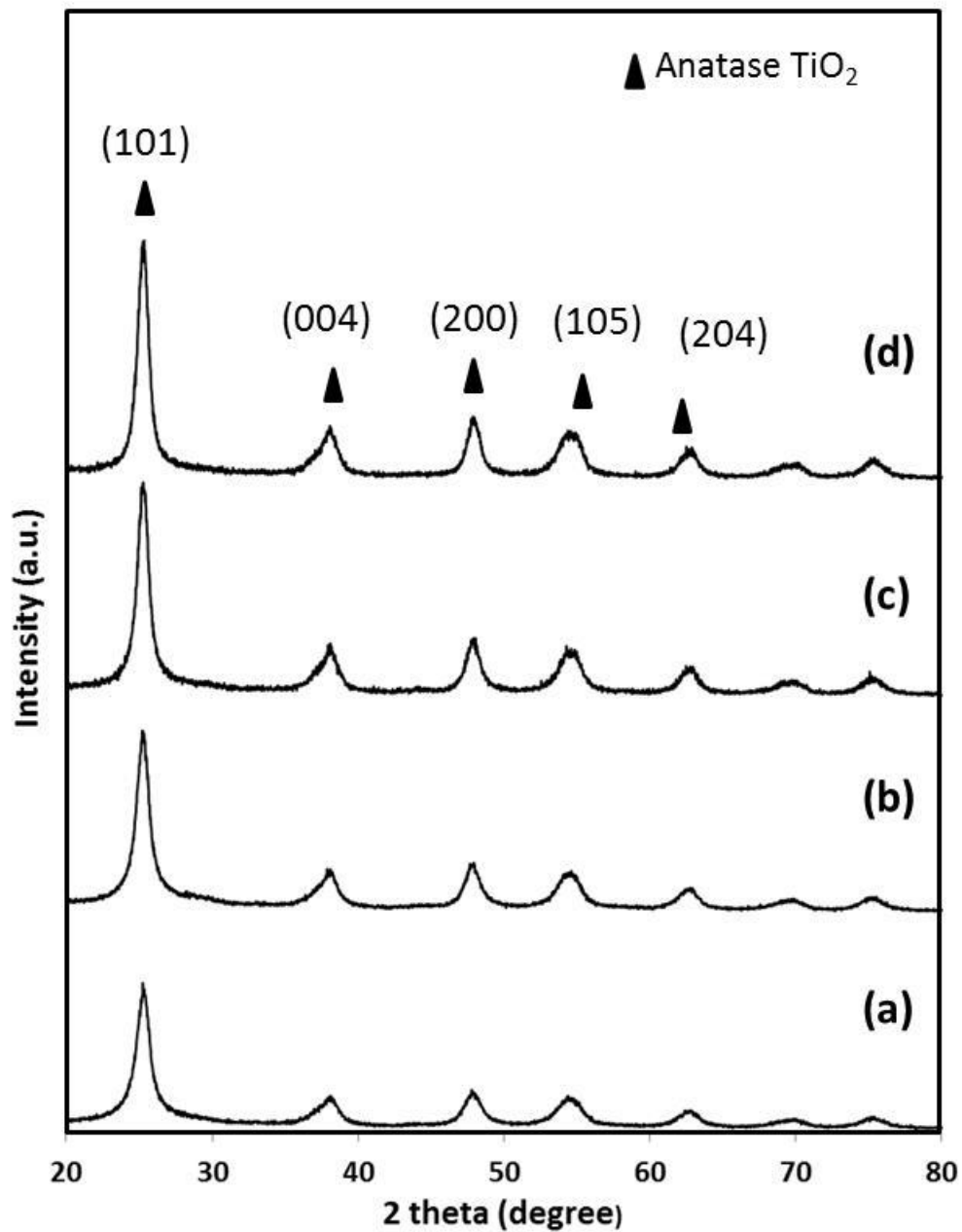


Figure 3.2: XRD patterns of  $\text{TiO}_2$  powders that calcined at different temperatures; (a) as-synthesized powder ( $\text{TiO}_2$ -0), (b)  $\text{TiO}_2$  powder calcined at  $200^\circ\text{C}$  ( $\text{TiO}_2$ -2), (c)  $\text{TiO}_2$  powder calcined at  $300^\circ\text{C}$  ( $\text{TiO}_2$ -3) and (d)  $\text{TiO}_2$  powder calcined at  $400^\circ\text{C}$  ( $\text{TiO}_2$ -4).

Table 3.1: Calculated crystallite size using the Scherrer equation of TiO<sub>2</sub> powders calcined at different temperatures.

<b>Calcination temperature (°C)</b>	<b>Phase</b>	<b>Crystallite size (nm)</b>
As-synthesized	Anatase	11.09
200	Anatase	18.76
300	Anatase	19.33
400	Anatase	21.96

Figure 3.3 shows the XPS spectra of the synthesized TiO<sub>2</sub> powders. The presence of titanium, sulfur, oxygen, and carbon were confirmed by XPS measurement as shown in Fig. 3.3 (a). Carbon peak at ~285 eV originated from the carbon tape which was used during the XPS analysis. Figure 3.3 (b) shows the binding energy of ~459.5 eV and ~465 eV corresponded to Ti 2*p*<sub>3/2</sub> and Ti 2*p*<sub>1/2</sub>, respectively. These binding energies are a characteristic of Ti<sup>4+</sup> in the TiO<sub>2</sub> lattice [17, 18]. A slight shift to lower binding energy was observed when the powder was calcined at 400°C, which can be ascribed to the formation of small amounts of Ti<sup>3+</sup> during the heat treatment [19, 20].

Figure 3.3 (c) shows the O *1s* spectra of as-synthesized TiO<sub>2</sub> and calcined TiO<sub>2</sub> at different temperatures. The binding energy at 530.9 eV is due to the characteristic of the Ti-O band. The peak located at ~532 eV corresponded to the OH groups [21]. This peak appeared in all samples. However, by increasing the calcination temperature, the peak decreased. The results show that the calcined TiO<sub>2</sub> powders contain less hydroxyl groups due to the removal of water during heat treatment which is also an indication of increased crystallinity of the TiO<sub>2</sub> as revealed in the XRD pattern. Moreover, Huang et al [17] reported that the peak that is located with this particular binding energy could be attributed to adsorbed oxygen which in turn is attributed to lattice distortion and porous structure. Meanwhile, Salim et al [12] and Paola et al [16] reported that this peak might also correspond to the sulfate (SO<sub>4</sub><sup>2-</sup>) bonding.

The XPS analysis also revealed the presence of sulfur ion on the surface of TiO<sub>2</sub> powders as illustrated in Fig. 3.3 (d). This result indicates that the presence of SO<sub>4</sub><sup>2-</sup> ions reduced as the calcination temperature increased to 400°C. The SO<sub>4</sub><sup>2-</sup> ions, which originated from the precursor, were also reported after annealing at 600°C [12, 16, and 22]. Sathyamoorthy et al [23] reported that the sulfate ions detached from the surface of anatase TiO<sub>2</sub> particles only when the powder was calcined at 650°C. The removal of the sulfate ions was via the liberation of highly acidic sulfur trioxide fumes. Since our objective is to maintain a small crystallite size at the primary level and to avoid the formation of internal pores in nanoparticles, calcination at a lower temperature of 650°C was conducted. Moreover, Salim et al [12] showed that powder that was annealed at 600°C showed a growth in primary particle size from 3 nm to 25 nm. Also, the thickness of the coating that has been fabricated using annealed TiO<sub>2</sub> powder modified by adding ammonium sulfate during the synthesis was only about 75 μm.



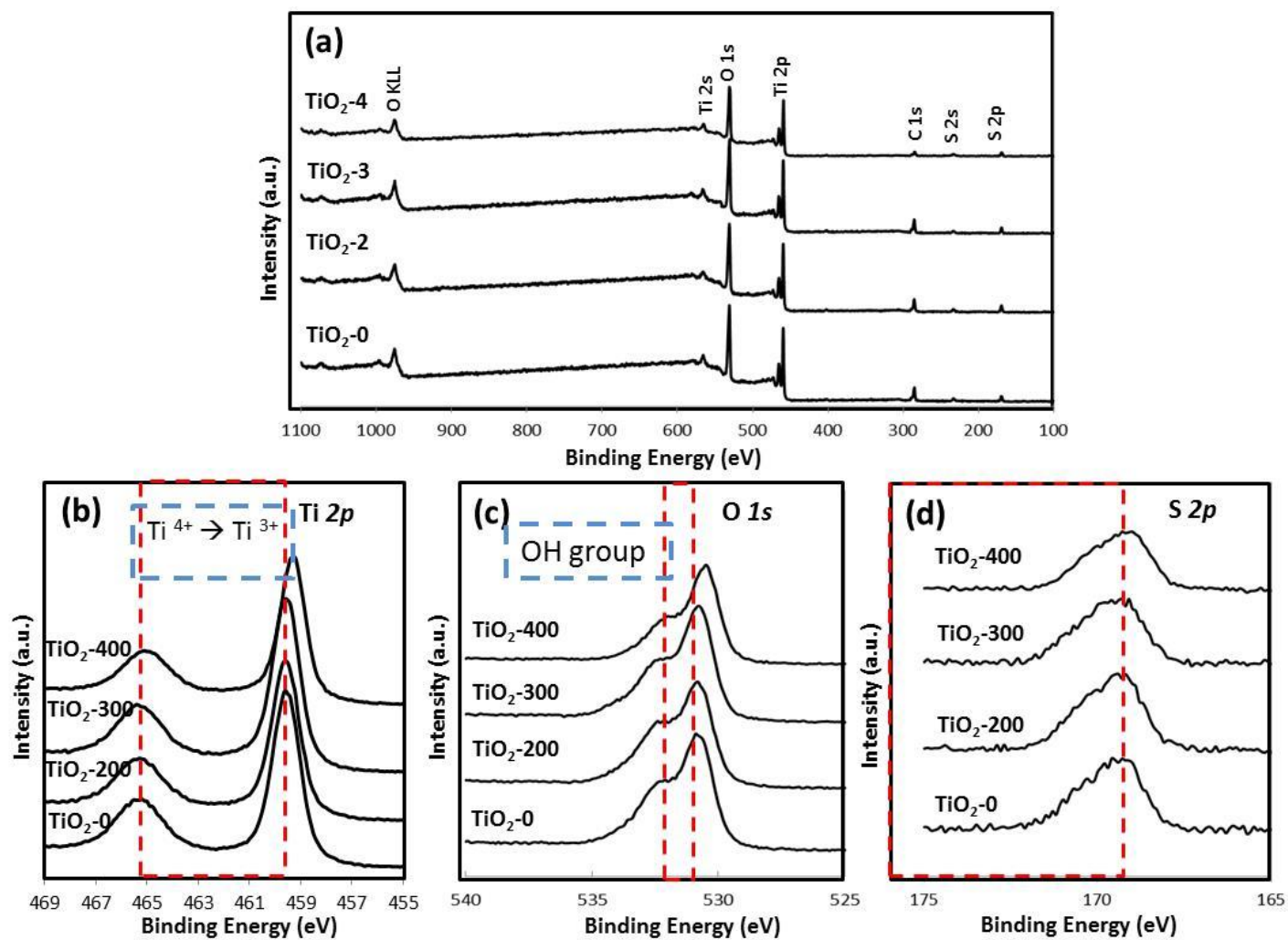


Figure 3.3: The XPS spectra of (a) wide scan spectra of TiO<sub>2</sub> powders that calcined at different temperatures and narrow scan spectra of TiO<sub>2</sub> powders that calcined at different temperatures corresponds to (b) Ti 2*p*, (c) O 1*s*, and (d) S 2*p*.

The particle morphologies of TiO<sub>2</sub> powders after synthesis and calcined at 200°C, 300°C and 400°C were observed by SEM at low and high magnification, as shown in Fig. 3.4 and Fig. 3.5 respectively. No obvious changes were observed in terms of the size of the agglomerated particles even though the powders were calcined up to 400°C. However, the calcination of powders improved the densification of particles by reducing the number of pores which can be seen in Fig. 3.5. TEM image (Fig. 3.6) depicts that the as-synthesized and calcined TiO<sub>2</sub> powders were composed of nanoparticles which were highly agglomerated. A slight increase in the size of the primary particles was observed with TEM when the TiO<sub>2</sub> powders were calcined at 200°C to 400°C which attributed to crystal growth. Previous studies by other researchers also revealed a slight growth of anatase nanocrystallites at low calcination temperatures, such as below 400°C [15, 16, 19, and 24]. Bakardjieva et al [24] reported that slow growth of the anatase nanocrystallites occurred due to the transformation of leftover amorphous parts, together with the growth of existing anatase nanocrystallites during the heat treatment.

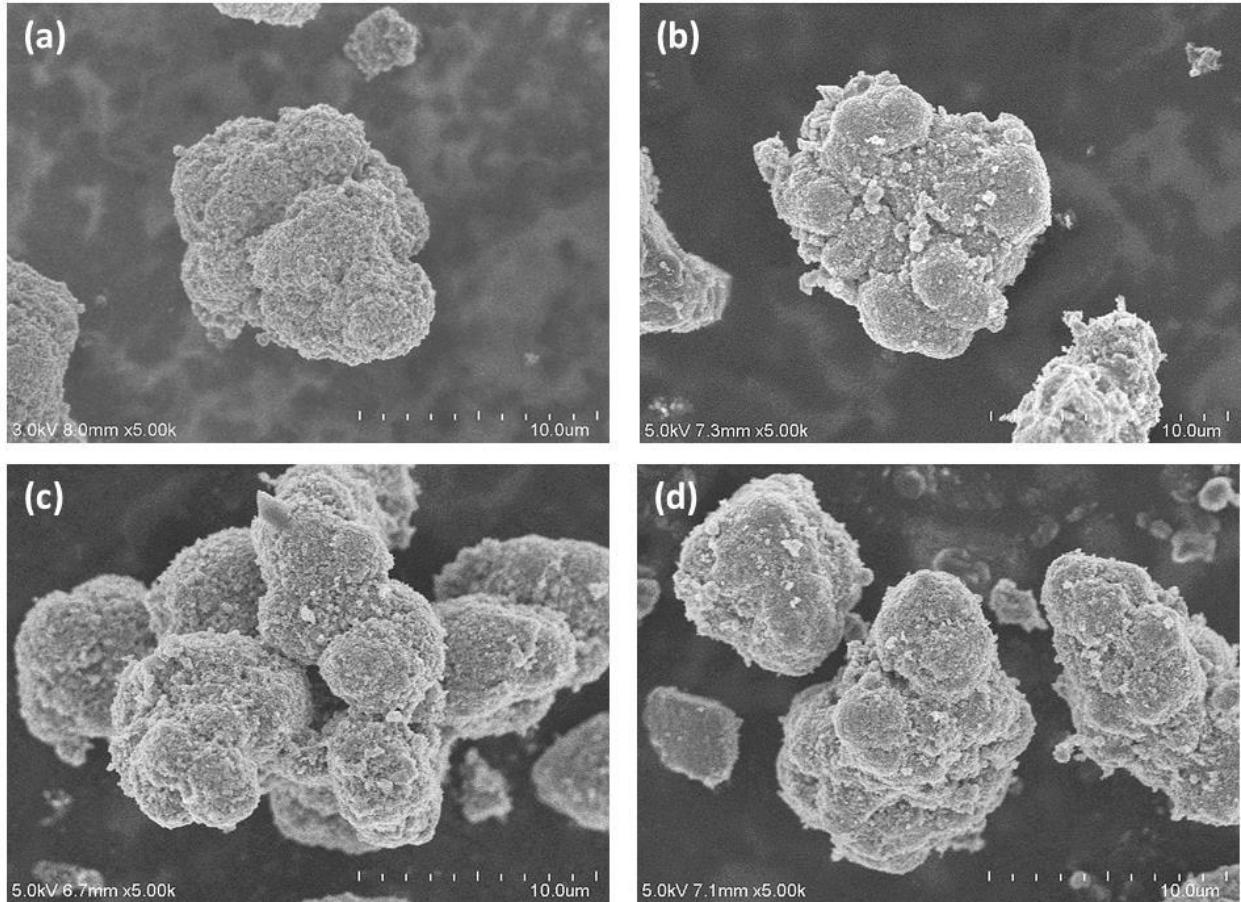


Figure 3.4: SEM micrographs of TiO<sub>2</sub> powders calcined at different temperatures: (a) as-synthesized powder (TiO<sub>2</sub>-0), (b) TiO<sub>2</sub> powder calcined at 200°C (TiO<sub>2</sub>-2), (c) TiO<sub>2</sub> powder calcined at 300°C (TiO<sub>2</sub>-3) and (d) TiO<sub>2</sub> powder calcined at 400°C (TiO<sub>2</sub>-4).

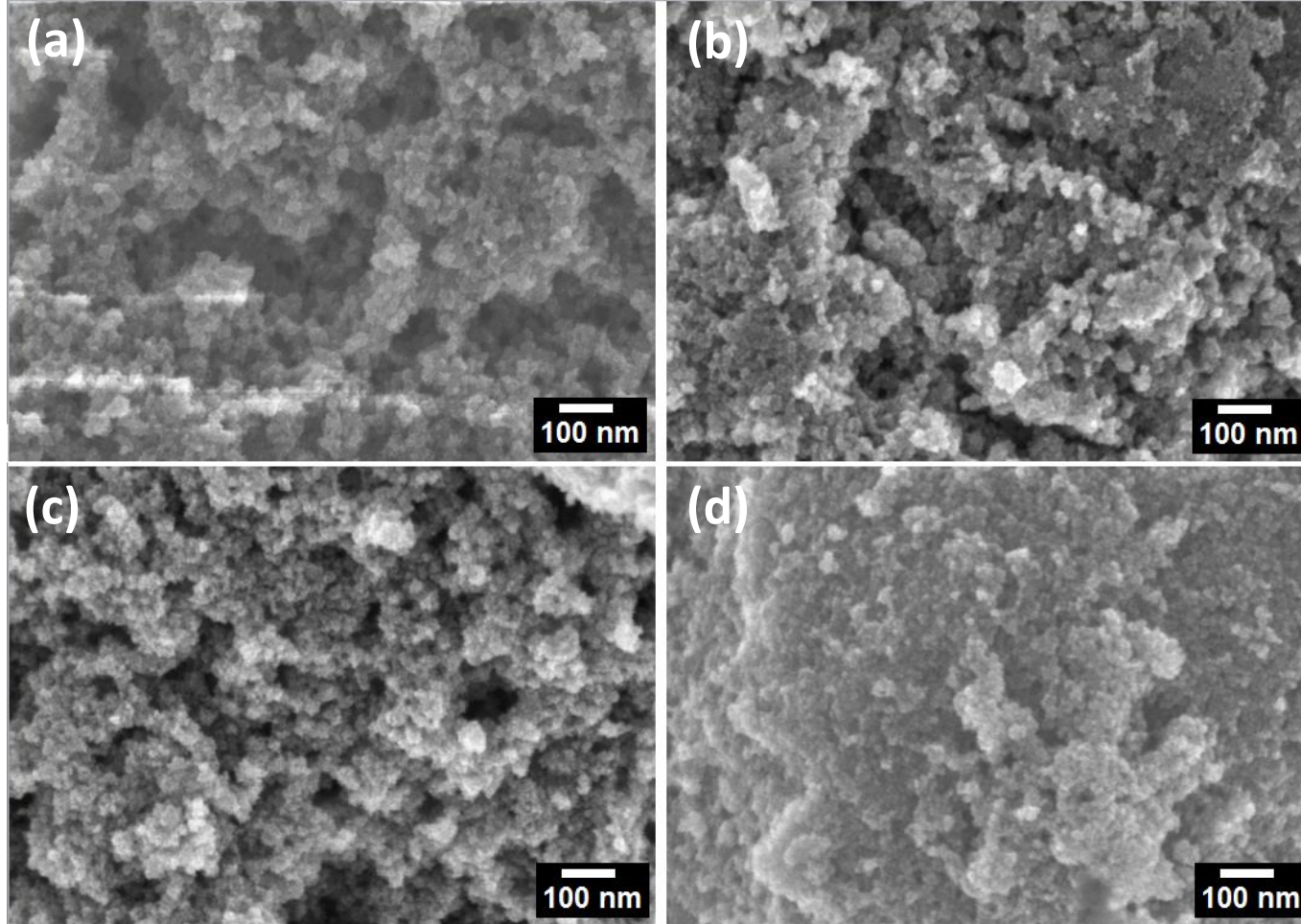


Figure 3.5: SEM images taken at high magnification of  $\text{TiO}_2$  powders calcined at different temperatures: (a) as-synthesized powder ( $\text{TiO}_2$ -0), (b)  $\text{TiO}_2$  powder calcined at  $200^\circ\text{C}$  ( $\text{TiO}_2$ -2), (c)  $\text{TiO}_2$  powder calcined at  $300^\circ\text{C}$  ( $\text{TiO}_2$ -3) and (d)  $\text{TiO}_2$  powder calcined at  $400^\circ\text{C}$  ( $\text{TiO}_2$ -4).

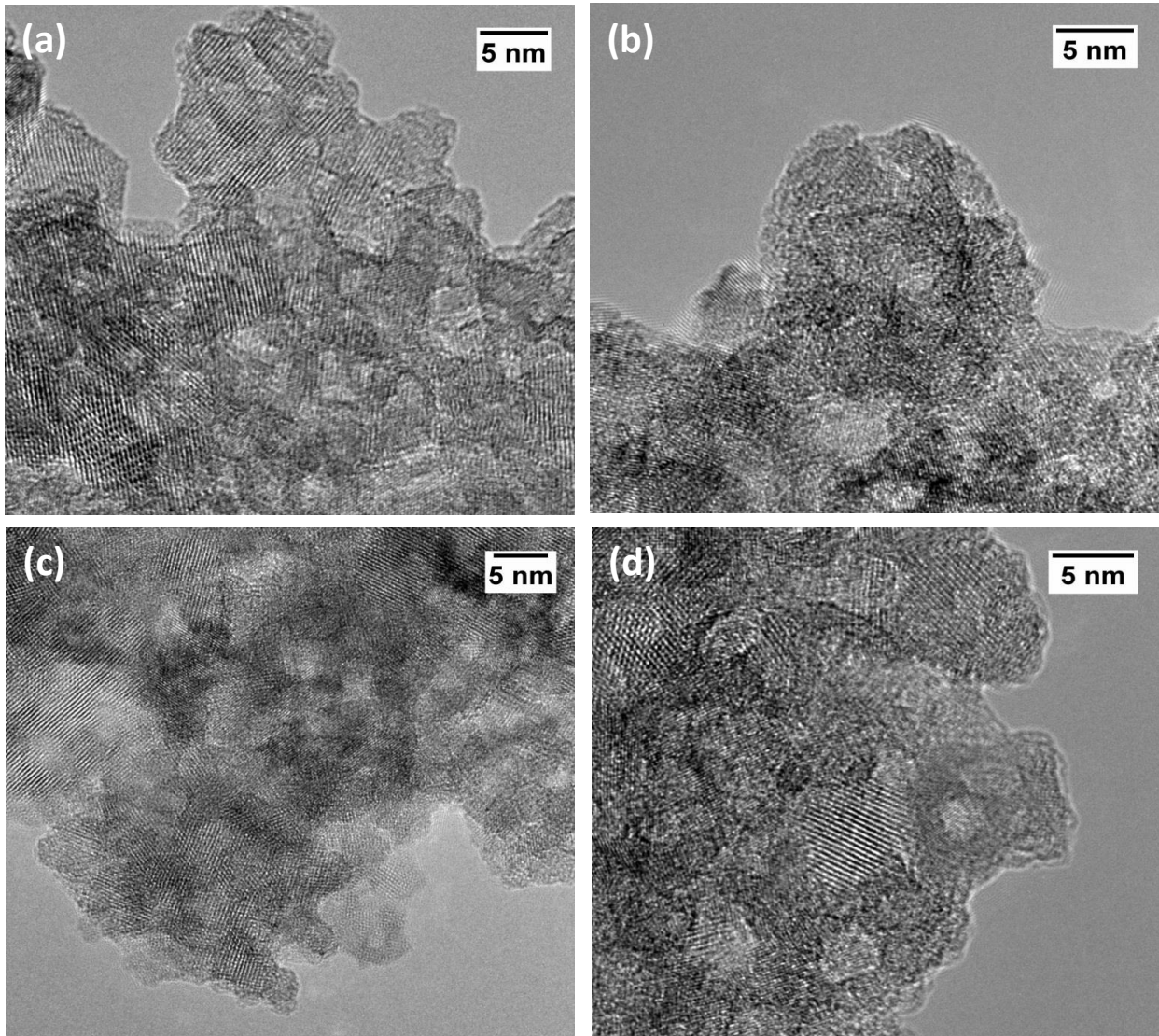


Figure 3.6: TEM micrographs of  $\text{TiO}_2$  powders calcined at different temperatures: (a) as-synthesized powder ( $\text{TiO}_2$ -0), (b)  $\text{TiO}_2$  powder calcined at  $200^\circ\text{C}$  ( $\text{TiO}_2$ -2), (c)  $\text{TiO}_2$  powder calcined at  $300^\circ\text{C}$  ( $\text{TiO}_2$ -3) and (d)  $\text{TiO}_2$  powder calcined at  $400^\circ\text{C}$  ( $\text{TiO}_2$ -4).

### 3.3.2 Coating Development using as-synthesized TiO<sub>2</sub> and Calcined TiO<sub>2</sub> Powders

Coating deposition in this study shows that heat treatment of as-synthesized powder at low temperature not only improved the crystallinity of the as-synthesized TiO<sub>2</sub> slightly which is preferable for photocatalytic activity but also increased the deposition of powder on the ceramic tiles substrate. After cold spraying, the average thicknesses of the TiO<sub>2</sub>-0, TiO<sub>2</sub>-2 and TiO<sub>2</sub>-3 powders were 50 μm, 130 μm and 120 μm, respectively (Fig. 3.7).

The formation of coating can be explained by the tamping effect [25] during the collision between the feedstock powders and the substrate. When a high kinetic energy was supplied during the process via application of pressure and temperature, the particles collide on the substrate. The powders fragmented and formed a coating due to the stacking of the powders during impact. The TiO<sub>2</sub> coating was produced from a recombination of broken crystallite links during the cold spray process, which was initiated by the porous structure of the agglomerated powders. During the process, the loosely agglomerated powders with nano-scale primary particles fractured, leaving an unstable surface with a dangling bond structure [26]. To reobtain a stable surface, the fractured particles recombined and formed a surface with improved stability. These were achieved by the adhesion of fractured particles with the substrate upon collision, and also with the previously-deposited TiO<sub>2</sub> coating layer.

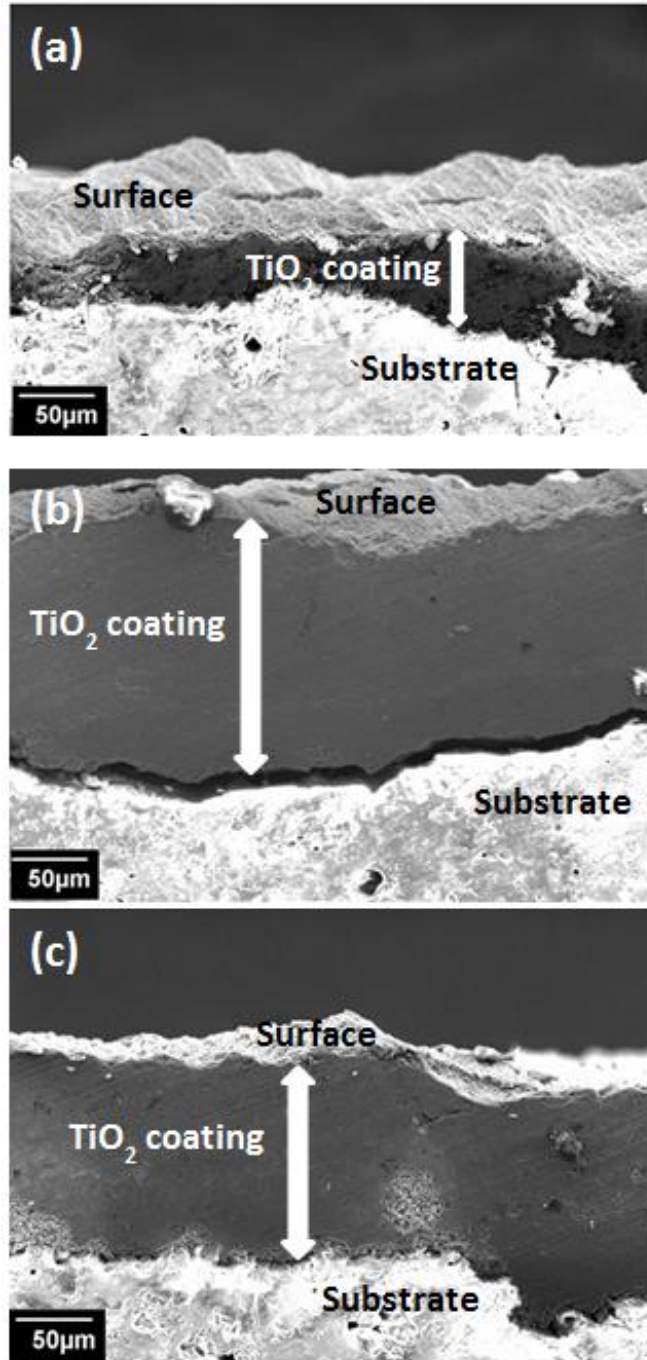


Figure 3.7: Cross-sectional view of the nanostructured TiO<sub>2</sub> coating deposited on a ceramic tile substrate by a CS process using: (a) as-synthesized powder (TiO<sub>2</sub>-0), (b) TiO<sub>2</sub> powder calcined at 200°C (TiO<sub>2</sub>-2), and (c) TiO<sub>2</sub> powder calcined at 300°C (TiO<sub>2</sub>-3).

It is therefore important to note that development of coating using only TiO<sub>2</sub> powders calcined at 400°C was unsuccessful. From the XRD, SEM and TEM results, no significant results found which contributes to the progressive improvement on the crystallinity and densification of the particles when the powders were calcined from 200°C to 400°C. However, it is likely that crystalline bridges became stronger between the primary particles when the calcination temperature was increased up to 400°C. This can be seen by decrease in average size of the pores which play an important role in the particle-particle attraction of the primary particles of TiO<sub>2</sub> powders as shown by SEM image in Fig. 3.5. This might occur due to the higher degree of crystallinity and also the formation of strong/ hard agglomerated particles [27] by a densification of particles during the heat treatment at higher calcination temperature. These hard agglomerated particles, which have less porosity, were difficult to fracture upon impact during the deposition as the particles were strongly bonded together. These strong bonds, which are formed by the crystalline bridges [3] between the particles, made them resistant to fragmentation and adherence on surface of the substrate. This result also shows that a further increase of post heat treatment temperature on as-synthesized TiO<sub>2</sub> powders; at 400°C and above lead to difficulties in building up the coating during collision, and this finding is in good agreement with previous study reported by Salim et al. [12].

It seems that porosity in the ceramic powder has an important role for powder deposition. Conversely, the result of this study shows that the as-synthesized TiO<sub>2</sub> powders which contain more porosity and less crystallinity as comparable to the calcined TiO<sub>2</sub> powders at 200°C and 300°C produced a thinner coating thickness. There are considerable reasons for the as-synthesized TiO<sub>2</sub> powders results in poor deposition using cold spray. Higher magnification image of SEM in Fig. 3.5 shows that as-synthesized TiO<sub>2</sub> powders were composed of highly



porous structure which indicates that the primary particles were loosely bound together by weak attraction force. The SEM image shows that the primary particles were not already in contact with each other as bigger pores were observed. The as-synthesized TiO<sub>2</sub> powders which have the lowest density due to higher amount of porosity and poor crystallinity experienced heavy breakage when exposed to harsh condition during the cold spray process. The tertiary particles tend to fracture into very small particles due to the weak attraction force that hold the primary particles together. Thick coating was difficult to achieve due to low impact energy of smaller particles onto the substrate during the collision. Moreover, higher porosity that was contained in the upcoming particles of as-synthesized TiO<sub>2</sub> led to poor inter-particle contact upon the collisions; producing only thin coating.

The SEM image analysis of TiO<sub>2</sub>-3 confirmed that the TiO<sub>2</sub> powder was not melted during the impact (Fig. 3.8). However, the image has revealed that the collided particles were fragmented as the dimensions of the individual particles on the coating were smaller than the feedstock materials. The figure also shows that the coating had some porosity. This might be due to the porosity which originally existed in the agglomerated particles. This was expected, as the feedstock powder was in an agglomerated form and plastically deformed in cold spray. During the impact of agglomerated TiO<sub>2</sub>, high kinetic energy from the cold spray process initiated the breaking up of agglomerated TiO<sub>2</sub>. Having nanoparticles in ceramic materials make it possible for the feedstock powders to experience dislocation which relates to plastic deformation due to the high kinetic energy and pressure applied during the cold spray process.

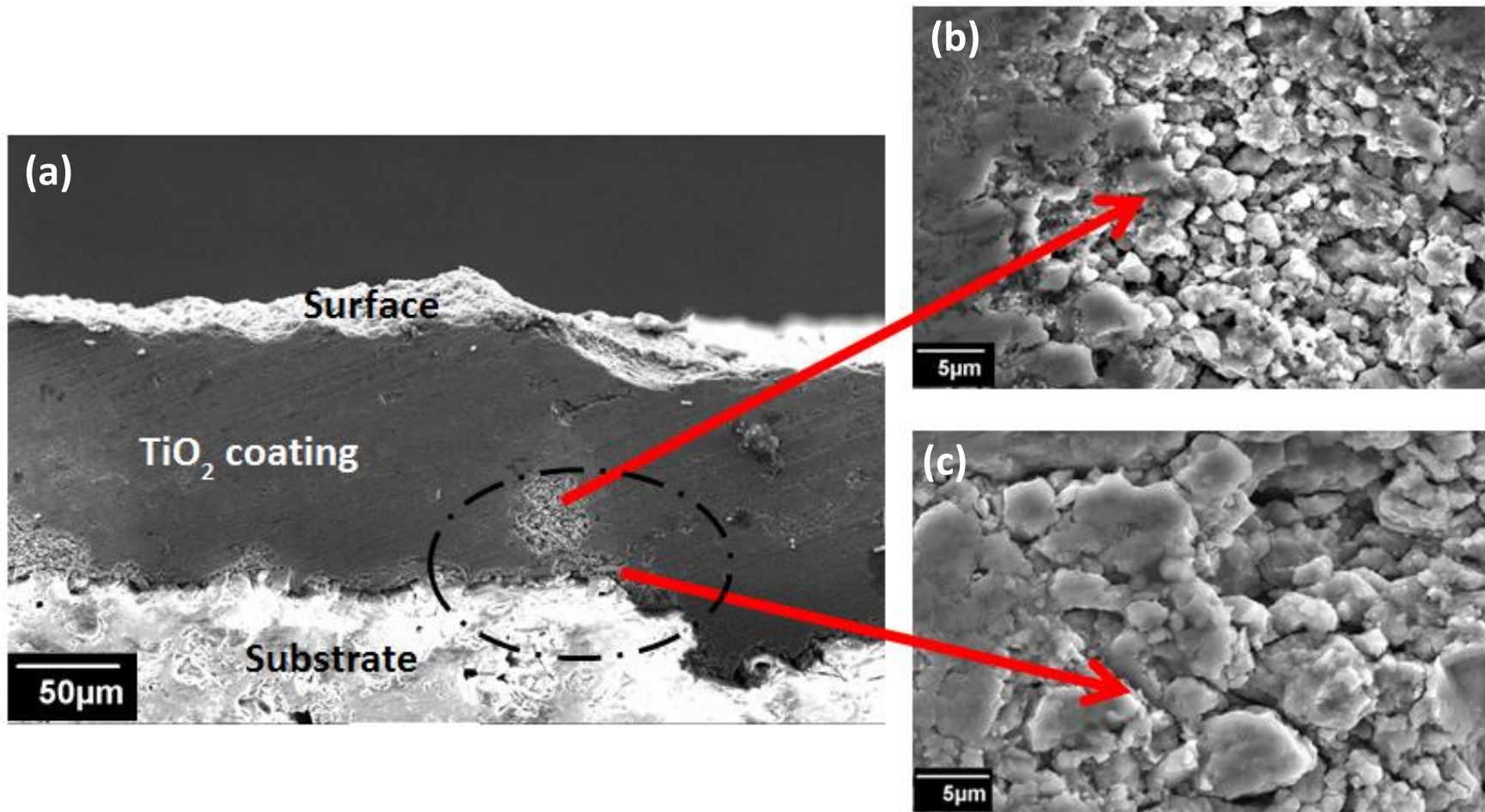


Figure 3.8: Cross-sectional view of TiO<sub>2</sub> coating using powder calcined at 300°C revealing coatings that were formed by the stacking of TiO<sub>2</sub> agglomerates: (a) low magnification (x 300) and (b) & (c) higher magnification (x 3000).

### 3.4 Conclusions

In this study, TiO<sub>2</sub> powders have been successfully synthesized by a simple hydrolysis method without the addition of binder and/or inorganic salt. The method that has been employed successfully produced agglomerated anatase TiO<sub>2</sub> powders which were able to be used directly as feedstock powder for cold spray process. However, only as-synthesized TiO<sub>2</sub> and TiO<sub>2</sub> powders, that calcined at 200°C and 300°C showed the successful deposition of TiO<sub>2</sub> coating on the ceramic tile substrate by the cold spray method. The calcined TiO<sub>2</sub> powders indicated a better crystallinity and thicker coating compared to the as-synthesized powder. A higher calcination temperature of 400°C not only promotes grain growth and the crystallite size of the as-synthesized TiO<sub>2</sub> powders, but also reduces the porosity present in the agglomerated powder by densification of the particles which resulting in unsuccessful of coating deposition. The presence of a certain amount of porosity in the ceramic feedstock powder is crucial in order to build up the coating during deposition.

### 3.5 References

- 1) S.-Q. Fan, G.-J. Yang, C.-J. Li, G.-J. Liu, C.-X. Li, L.-Z. Zhang: *J. Therm. Spray Technol.* 15 (2006) 513–517.
- 2) P.F. Rios, H. Dodiuk and S. Kenig: *Surf. Eng.* 25 (2009) 89–92.
- 3) D. Verhovšek, N. Veronovski, U. Lavrenčič Štangar, M. Kete, K. Žagar and M. Čeh: *Int. J. Photoenergy.* 2012 (2012) 1–10.
- 4) L. Frazer: *Environ Health Perspect.* 109 (4) (2001) 174–177.
- 5) Y. Lu, K. Kobayashi, S. Guan, L. Hao, H. Yoshida, H. Asanuma, and J. Chen: *Mater. Sci. Semicond. Process.* 30 (2015) 128–134.
- 6) B.W. Robinson, C.J. Tighe, R.I. Gruar, A. Mills, I.P. Parkin, A. K. Tabecki, H. L. de Villiers Lovelock and J. A. Darr: *J. Mater. Chem. A.* 3 (2015) 12680–12689.
- 7) M. Yamada, Y. Kandori, K. Sato, & M. Fukumoto: *J. Solid Mech. Mater. Eng.* 3 (2009) 210–216.
- 8) M. Gardon, C. Fernández-Rodríguez, D. Garzón Sousa, J.M. Doña-Rodríguez, S. Dosta, I.G. Cano and J. M. Guilemany : *J. Therm. Spray Technol.* 23 (2014) 1135–1141.
- 9) Z. Yi, C. Guofeng, W. Ma and W. Wei: *Prog. Org. Coatings.* 61 (2008) 321–325.
- 10) M. Yamada, H. Isago, H. Nakano and M. Fukumoto: *J. Therm. Spray Technol.* 19 (2010) 1218–1223.
- 11) M. Gardon and J.M. Guilemany: *J. Therm. Spray Technol.* 23 (2014) 577–595.
- 12) N.T. Salim, M. Yamada, H. Nakano, K. Shima, H. Isago and M. Fukumoto: *Surf. Coatings Technol.* 206 (2011) 366–371.

- 13) J.-O. Kliemann, H. Gutzmann, F. Gärtner, H. Hübner, C. Borchers and T. Klassen: *J. Therm. Spray Technol.* 20 (2010) 292–298.
- 14) G.-J. Yang, C.-J. Li, F. Han, W.-Y. Li and A. Ohmori: *Appl. Surf. Sci.* 254 (2008) 3979–3982.
- 15) S. Ngamta, N. Boonprakob, N. Wetchakun, K. Ounnunkad, S. Phanichphant and B. Inceesungvorn: *Mater. Lett.* 105 (2013) 76–79.
- 16) A. Di Paola, M. Bellardita, L. Palmisano, R. Amadelli and L. Samiolo: *Catal. Letters.* 143 (2013) 844–852.
- 17) J. Huang, X. Guo, B. Wang, L. Li and M. Zhao: *Journal of Spectroscopy* 2015 (2015).
- 18) M.-Q. Wang, J. Yan, H.-P. Cui and S.-G. Du: *Mater. Charact.* 76 (2013) 39–47.
- 19) Z. He, W. Que, J. Chen, Y. He and G. Wang: *J. Phys. Chem. Solids.* 74 (2013) 924–928.
- 20) S. Hu, A. Wang, X. Li and H. Löwe: *J. Phys. Chem. Solids.* 71 (2010) 156–162.
- 21) S. A. Simakov and Y. Tsur: *J. Nanoparticle Res.* 9 (2006) 403–417.
- 22) J.-G. Li and T. Ishigaki: *J. Am. Ceram. Soc.* 88 (2005) 3232–3234.
- 23) S. Sathyamoorthy, G.D. Moggridge and M.J. Hounslow: *AIChE J.* 47 (2001) 2012–2024.
- 24) S. Bakardjieva, J. Šubrt, V. Štengl, M.J. Dianez and M.J. Sayagues: *Appl. Catal. B Environ.* 58 (2005) 193–202.
- 25) S.-Q. Fan, G.-J. Yang, C.-J. Li, G.-J. Liu, C.-X. Li and L.-Z. Zhang: *J. Therm. Spray Technol.* 15 (2006) 513–517.
- 26) M. Yamada, H. Isago, K. Shima, H. Nakano, M. Fukumoto: *Proc. ITSC 2010, Thermal spray: Global Solutions for Future Applications*, (Singapore, 2010), pp. 187-191.
- 27) B. Souvereyns, K. Elen, C. De Dobbelaere, A. Kelchtermans, N. Peys, J. D’Haen, M. Mertens, S. Mullens, H. Van den Rul, V. Meynen, P. Cool, A. Hardy and M. K. Van Bael: *Chem. Eng. J.* 223 (2013) 135–144.

## **4 Cold Sprayed TiO<sub>2</sub> Coating from Nanostructured Ceramic Agglomerated Powders**

### **4.1 Introduction**

In the recent years, attention has been given to nanostructured ceramic powder feedstock used for thermal spray process. The nanoparticle powder was normally spray dried and sintered for agglomeration in order to allow it to be used in regular powder feeder. This is to avoid the fine particles from blocking the hoses and fittings during the powder supply [1-3]. Moreover, fine particles also require high levels of carrier gas flow during the thermal spraying process and the impact during the collision is low due to tiny mass of individual particles [2]. The agglomeration processes not only require the addition of binder to improve the ductility of the powder during the collision [4], but also require additional post treatment process to remove the binder from the agglomerates. Post treatment process usually promotes grain growth of the starting nanostructured powders [4]. However, by controlling process parameters during synthesis, agglomerated form of ceramic powder was directly produced. The agglomeration of particles can be achieved by addition of structure-directing agent (SDA) such as (NH<sub>4</sub>)<sub>2</sub>SO<sub>4</sub> [4–6], cetyltrimethyl-ammonium bromide (CTAB) [7, 8] and urea [9] which acts to provide network to organize the nanoparticles into micron sized structures. Addition of these structure-directing agents during synthesis eliminates the needs of agglomeration process using spray drying method as post treatment.

Besides, phase transformation [4, 10, 11] is also an issue for thermal spray process for some of ceramic materials for coating applications. For thermal spray which involves high

temperature during the process, ceramic materials such as anatase titanium dioxide ( $\text{TiO}_2$ ) powder has possibilities to transform to rutile  $\text{TiO}_2$ . This phase transformation is undesirable and irreversible as it is well known that anatase  $\text{TiO}_2$  has outstanding photocatalytic property compared to rutile  $\text{TiO}_2$ . Thus, preservation of the initial phase of the feedstock materials is very crucial in order to maintain the performance of photocatalysts. One of best solution to overcome this problem is using cold spray process. Cold spray (CS) [1, 4, 10–15] is an emerging coating technique where the spray materials which is in solid state are adhered onto surface of substrate by plastic deformation. This method utilizes high kinetic energy and high particle velocities to form coating on the substrate by particles impact [11, 15] on the substrate at lower temperatures in comparison to other thermal spray methods. During particles impact, bonding occurred due to plastic deformation and coating is formed.

Ceramics is a brittle material. This property makes ceramics difficult to be deformed during the collision using CS. However, coating of  $\text{TiO}_2$  is possible to be produced using CS process [4, 16, 17]. These previous studies suggested that chemical bonding between  $\text{TiO}_2$  particles and substrate or among particles during CS process may lead to coating formation. Salim et al revealed that  $\text{TiO}_2$  coating can be fabricated using cold spray method [4]. Yet, thick coating was produced only using the post- treated powders.

In this paper, nanocrystalline anatase  $\text{TiO}_2$  powders in agglomerated form were obtained by hydrolysis method at  $80^\circ\text{C}$ . In order to produce agglomerated powders of  $\text{TiO}_2$ , ammonium sulfate  $(\text{NH}_4)_2\text{SO}_4$  has been used as structure-directing agent. The influence of  $(\text{NH}_4)_2\text{SO}_4$  addition on surface morphology and crystallinity of the obtained powder was investigated. Moreover, preliminary study on the coating formation on ceramic tiles substrate using the as-synthesized powders was also conducted.

## 4.2 Experimental Procedure

### 4.2.1 Materials

The hydrolysis reaction was performed using 10 wt. % of  $\text{TiOSO}_4$  as the precursor for  $\text{TiO}_2$  and distilled water. During the hydrolysis, 1 mol% of ammonium sulfate  $[(\text{NH}_4)_2\text{SO}_4]$  was added. The white solution was stirred on a hot plate to hold the temperature of the solution at  $\sim 80^\circ\text{C}$  for 8 h. During the reaction, the white solution was transformed to clear solution. Upon completion the synthesis, a white precipitate was formed. The precipitate was washed with distilled water several times and collected by decantation. The precipitate was then dried in an oven to obtain a powder. As a comparison, a reference  $\text{TiO}_2$  powder without the addition of  $(\text{NH}_4)_2\text{SO}_4$  as structure-directing agent was performed with the same procedure. The details procedure for the synthesis process has been illustrated in Fig. 4.1.



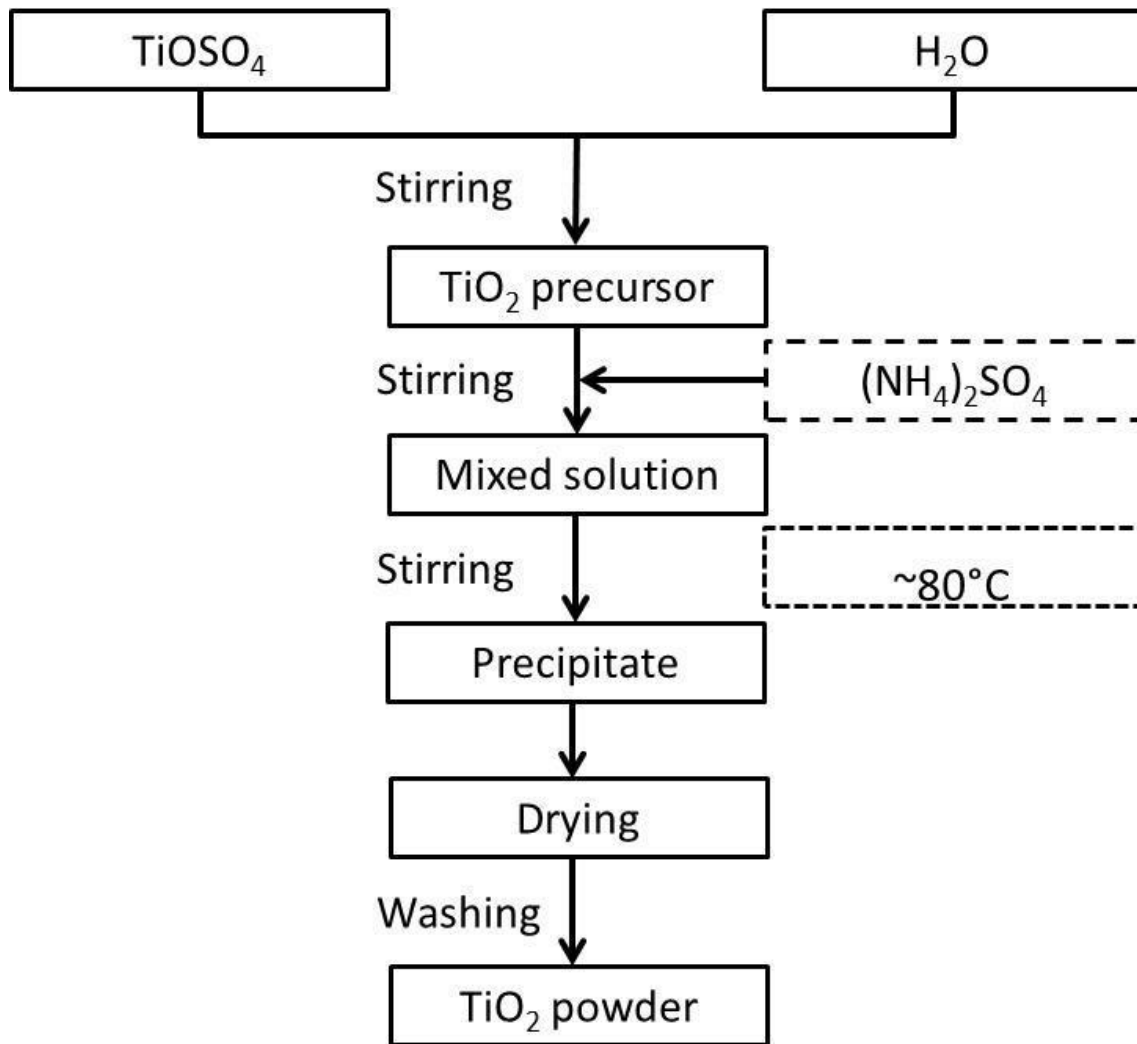


Figure 4.1: Synthesis of TiO<sub>2</sub> powders with different mol% addition of (NH<sub>4</sub>)<sub>2</sub>SO<sub>4</sub> by simple hydrolysis method.

#### 4.2.2 Cold Spray Process

The as-synthesized powders were deposited by cold spray process using CGT KINETIKS 4000 (Cold Gas Technology, Germany) with a suction nozzle which is custom-made in our

laboratory. Nitrogen was used as the process gas. Grit blasted ceramic tiles (INAX ADM-155M) were used as the substrate for spray coatings. Table 4.1 describes the optimum spray condition that was used in this study.

Table 4.1: Cold spray conditions

<b>Gas nature</b>	<b>Nitrogen</b>
<b>Gas pressure, MPa</b>	3.0
<b>Gas Temperature, °C</b>	500
<b>Spray distance, mm</b>	30
<b>Traverse speed, mm/s</b>	20

#### 4.2.3 Characterization of Feedstock Materials and Cold-sprayed TiO<sub>2</sub> Coatings

The morphology of the resulting powders and the obtained fractured cross sections of coating samples were examined using Scanning Electron Microscope (SEM: JSM-6390, JEOL) and Field Emission Scanning Electron Microscope (FESEM: SU8000, Hitachi). Transmission Electron Microscope (TEM: JEM-2100F, JEOL) was used to measure the primary particles size of the as-synthesized TiO<sub>2</sub>. The phase purity and crystallinity of the as-synthesized powders and coatings were characterized by X-Ray Diffraction (XRD: RINT 2500, Rigaku) with Cu-K $\alpha$

radiation ( $\lambda = 1.5406 \text{ \AA}$ ) over the  $2\theta$  range of  $10\text{-}80^\circ$ . Scherrer equation was used to calculate the crystal size of  $\text{TiO}_2$ . The microhardness of coating was measured using a HMV-G Micro Vickers Hardness Tester (Shimadzu) at a load of 245.2 mN for 15s. Surface roughness was measured by LEXT OLS3100/ OLS3000 (Olympus) with a 20X lens. Porosity of the coating samples were measured using Archimedes principle method.

### 4.3 Results & Discussion

#### 4.3.1 Characterization of as-synthesized $\text{TiO}_2$ powders with different mol % addition of $(\text{NH}_4)_2\text{SO}_4$

Prior to this study,  $\text{TiO}_2$  powders were synthesized with different mol % addition of  $(\text{NH}_4)_2\text{SO}_4$  in order to study the effect of addition of  $(\text{NH}_4)_2\text{SO}_4$  on the properties of the obtained powders especially in terms of morphology and agglomeration of the nano-sized particles up to micrometer ranged. Figure 4.2 shows the SEM image illustrating the morphology of the  $\text{TiO}_2$  powders obtained from 0-5 mol%  $(\text{NH}_4)_2\text{SO}_4$  addition during the synthesis process. The results indicated that adding of  $(\text{NH}_4)_2\text{SO}_4$  to the starting precursor has noticeably affected the morphology of particles. Powder that synthesized without the addition of  $(\text{NH}_4)_2\text{SO}_4$  and low molar ratio of  $(\text{NH}_4)_2\text{SO}_4$  having structure with loose/ soft agglomerates compared to the powder that synthesized with high molar ratio which has the characteristic of hard agglomerates as shown in Fig. 4.2. Detailed view on the powder that synthesized with low molar ratio and high molar ratio indicates that the powder comprised of group of nanoparticles. Moreover, it is clearly evident from the SEM image that the  $\text{TiO}_2$  powders that synthesized without the addition of

$(\text{NH}_4)_2\text{SO}_4$  seem highly porous, where big pores were observed indicating that the agglomerates have poor network of crystalline bridges connecting the primary agglomerates. Sathyamoorthy et al. reported that primary agglomerates that formed the secondary and tertiary agglomerates were hold by weak binding force. This type of bonding could be easily broken down to its individual units of smaller particles when exposed to harsh conditions such as stronger attraction forces or changes in surface charges [18].

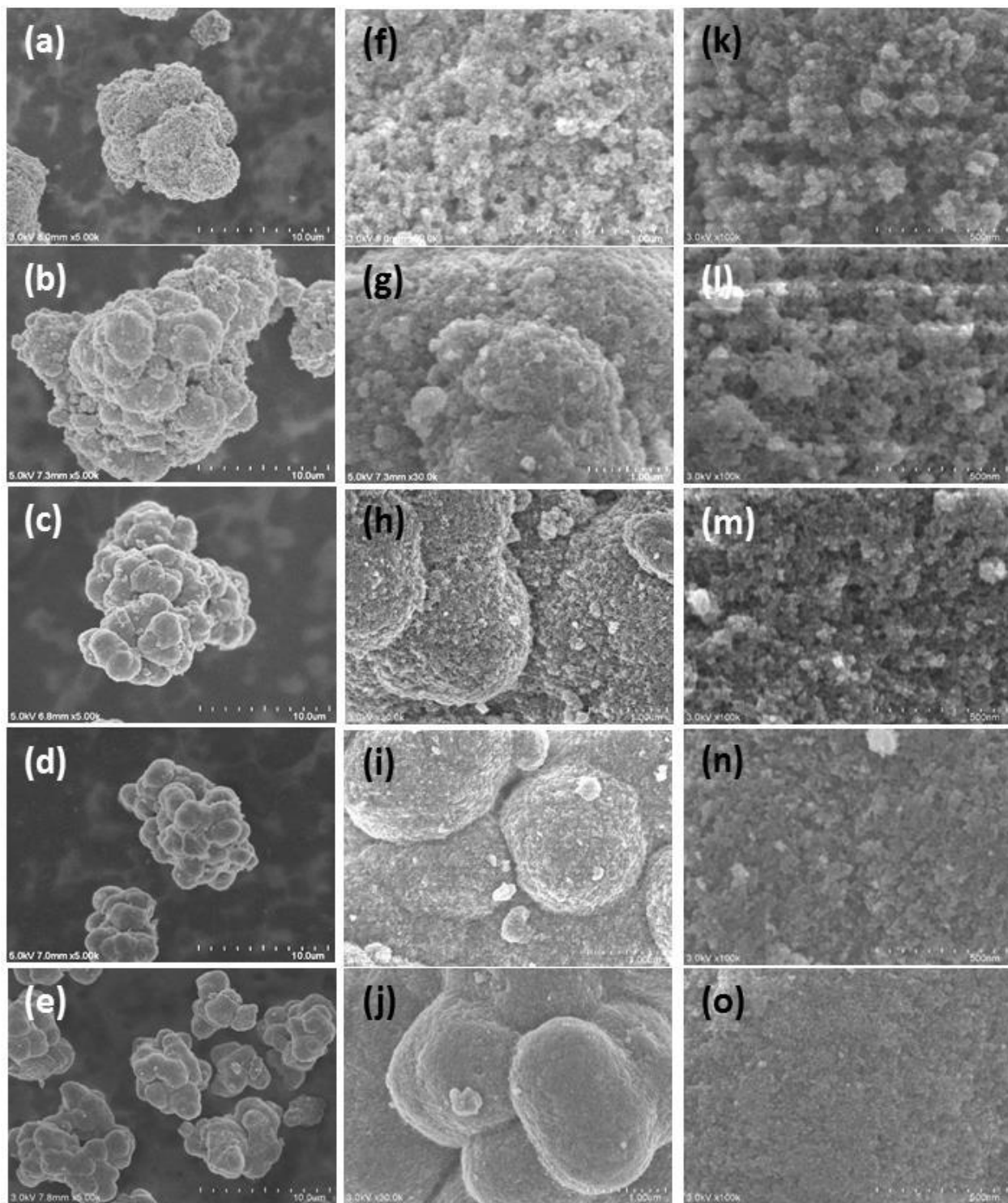


Figure 4.2: SEM images of the  $\text{TiO}_2$  powders synthesized with different mol% addition at different magnifications: (a, f & j) 0, (b, g & l) 0.1, (c, h & m) 0.5, (d, i & n) 1 and (e, j & o) 5.

However, it is noticeable that with increasing the addition of  $(\text{NH}_4)_2\text{SO}_4$  in the starting precursor up to 5 mol%, the diameter of the tertiary particles which represent the size of the agglomerates was slightly decreased but the secondary and primary size was increased. The decrease in the diameter of the agglomerated powder can be described as follow.  $(\text{NH}_4)_2\text{SO}_4$  which has been added in the precursor during the synthesis is also the source of  $\text{SO}_4^{2-}$  ions. These  $\text{SO}_4^{2-}$  ions together with  $\text{NH}_4^+$  ions has improved the precipitation reaction during the synthesis which has promoted the growth of  $\text{TiO}_2$  crystals. The average crystallite sized was calculated by applying the Scherrer equation to the full-width at half-maximum of the (101) crystal plane of anatase  $\text{TiO}_2$  (Table 4.2). From the results obtained it is clear that the crystallite size of the  $\text{TiO}_2$  with the addition of  $(\text{NH}_4)_2\text{SO}_4$  was increased with an increasing of molar ratio of SDA. This finding suggests that incorporation of sulfur ion from the initial precursor;  $(\text{NH}_4)_2\text{SO}_4$  which act as template for microstructure organization leads to promote crystal growth of the anatase  $\text{TiO}_2$  during the hydrolysis process.  $\text{TiO}_2$  nanoparticles with bigger crystallite size are more stable compared to smaller particles. Therefore the van der Waals attraction between the adjacent big particles to form agglomerate is less. This will lead to formation of bigger size of secondary particles. Moreover, detailed view on the morphology of the particles using SEM shows that powder that synthesized with higher mol % experienced densification of nanostructures and tightly agglomerated particles which also refer as hard agglomerates. This densification will facilitate elimination of porosity which is one of important criteria for feedstock powder should have in order to build up the coating during deposition using cold spray. The existence of porosity at nano level will make the feedstock powder as soft agglomerates which can fracture easily during the impact and adhered on the substrate and rebound again due to tamping effect.

Table 4.2: The correlation between  $(\text{NH}_4)_2\text{SO}_4$  addition during the synthesis and the crystallite size and particle size.

$(\text{NH}_4)_2\text{SO}_4$ addition <sup>a</sup> (mol%)	Crystallite size <sup>b</sup> nm	2° particle <sup>c</sup> $\mu\text{m}$	3° particle <sup>c</sup> $\mu\text{m}$
0	11.09	-	10-25
0.1	11.09	-	10-25
0.5	10.37	~1.5	10-25
1	12.23	~1.9	10-25
5	17.02	~2.3	5-10

<sup>a</sup>Initial mol% addition used in the hydrolysis process

<sup>b</sup>Measured by Scherrer equation

<sup>c</sup>Measured by SEM

Preliminary study on coating deposition using the synthesized  $\text{TiO}_2$  powders with different mol% of  $(\text{NH}_4)_2\text{SO}_4$  were conducted using cold spray process on ceramic tiles substrate. From the results obtained, the powders that synthesized without the addition of  $(\text{NH}_4)_2\text{SO}_4$  and low mol% can be deposited on the substrate. However, feedstock powders with 5 mol % of  $(\text{NH}_4)_2\text{SO}_4$  was failed to be deposited by cold spray process. This made it possible to assume that the feedstock materials that has less porosity and higher densification which shown by SEM image in Fig. 4.2-o, has strong network bonding between the particles. The results could be interpreted as follows: The strong bonding made the particles resistant to fracture upon the

impact onto the substrate, in turns no deposition was formed. Since no fracture was occurred during the impact of the particles, the particles were collided as big and hard particles where the kinetic energy of the particles was exceeded the adhesion energy that needed during the bonding between the particle-to-substrate. It is believed that fracture of particles are very difficult to occur when the feedstock materials has less porosity and strong binding force holding the agglomerates particles. As the impact particles are larger and harder, resulting to a greater velocity which cause the particles to rebound rather than deformed or fragmented during the deposition.

Therefore, in this study,  $\text{TiO}_2$  powders which was synthesized without the addition of  $(\text{NH}_4)_2\text{SO}_4$  and  $\text{TiO}_2$  powders which synthesized with 1 mol%  $(\text{NH}_4)_2\text{SO}_4$  addition were used to study for further clarification to be used as feedstock powders to prepare cold sprayed  $\text{TiO}_2$  coatings.

#### **4.3.2 Characterization of as-synthesized $\text{TiO}_2$ powders used for cold spray process**

The crystallographic characteristics of as-synthesized  $\text{TiO}_2$  were examined using X-ray diffraction as shown in Fig. 4.3. Five obvious peaks of anatase  $\text{TiO}_2$  were observed at  $25.197^\circ$ ,  $38.067^\circ$ ,  $47.735^\circ$ ,  $54.372^\circ$  and  $62.622^\circ$  corresponded to the (101), (004), (200), (105) and (204) planes for  $\text{TiO}_2$  with 1 mol%  $(\text{NH}_4)_2\text{SO}_4$  addition. Identification of phases in the prepared powders was achieved by comparing the obtained XRD patterns with PDF Card No. 21-1272 for anatase  $\text{TiO}_2$ . The broad diffraction peaks of XRD patterns of these powders reveal that as-prepared  $\text{TiO}_2$  powders contain of nano crystalline anatase  $\text{TiO}_2$ . This XRD results indicate that



anatase TiO<sub>2</sub> already can be obtained without further post treatment process. Moreover, only slight difference in the peak broadening can be observed upon (NH<sub>4</sub>)<sub>2</sub>SO<sub>4</sub> addition. Besides, there is also no existence of sulfur and rutile peak can be found in the obtained XRD pattern. No diffraction lines of sulfur was detected in the XRD patterns might due to only small addition of the elements was added during the reaction and all sulfur is incorporated into the TiO<sub>2</sub> structure [19]. The mean crystallite size was calculated from the (101) plane by Scherrer equation were 11.09 nm and 12.23 nm for TiO<sub>2</sub> without addition and TiO<sub>2</sub> with the addition of (NH<sub>4</sub>)<sub>2</sub>SO<sub>4</sub>, respectively (Table 4.2). These fine particles contribute to high surface area and energy which lead to promotion of agglomerates due to van der Waals attraction [20]. Furthermore, this result showed that addition of (NH<sub>4</sub>)<sub>2</sub>SO<sub>4</sub> in the lower molar percent only slightly changed the crystallite size. Moreover, there is no significant different in term of lattice parameters between the powder without the addition and addition of (NH<sub>4</sub>)<sub>2</sub>SO<sub>4</sub> as shown in Table 4.3. Lattice strain,  $\epsilon$  was calculated based on the following equation (1).

$$B_s = 4 \times \epsilon \times \tan\theta \quad (1)$$

Where:

$$B = B_s + B_g + B_i$$

B= experimentally decided FWHM value

B<sub>s</sub>= Strain broadening

B<sub>g</sub>= grain size ( $D = 0.9 \times \lambda / (B_g \sin\theta)$ )

B<sub>i</sub>= initial broadening from standard sample; CaCO<sub>3</sub>

The results revealed that a slight increase of lattice strain,  $\epsilon$  for TiO<sub>2</sub> powders which synthesized with addition of (NH<sub>4</sub>)<sub>2</sub>SO<sub>4</sub> shows that incorporation of S<sup>6+</sup> ion into TiO<sub>2</sub> lattice [21]. Chemical composition analysis by energy-dispersive X-ray spectroscopy (EDS) shows that

the TiO<sub>2</sub> powders synthesized in this study is mainly composed of titanium (Ti) and oxygen (O) with a small amount of sulfur (S) element (Table 4.4). Besides, EDS mappings as illustrated in Fig. 4.4 concluded that the sulfur element was homogeneously distributed on the surface of TiO<sub>2</sub>. Figure 4.5 shows the XPS spectra of the S 2*p* region of the TiO<sub>2</sub> powders. The sulfur present in these samples is all in the state of S<sup>6+</sup> which located at around 169 eV and can be assigned to the SO<sub>4</sub><sup>2-</sup> species in the titania lattice [21-23]. Moreover, it should be noted that no peaks are found around 160-161 eV, which corresponds to the sulfur atom in the state of S<sup>2-</sup> [21, 22]. This result suggested that no Ti-S bond was formed and oxygen was not replaced by sulfur in anatase TiO<sub>2</sub>. This might due to low synthesis temperature which below the boiling point of sulfur; which is at 445°C [21].

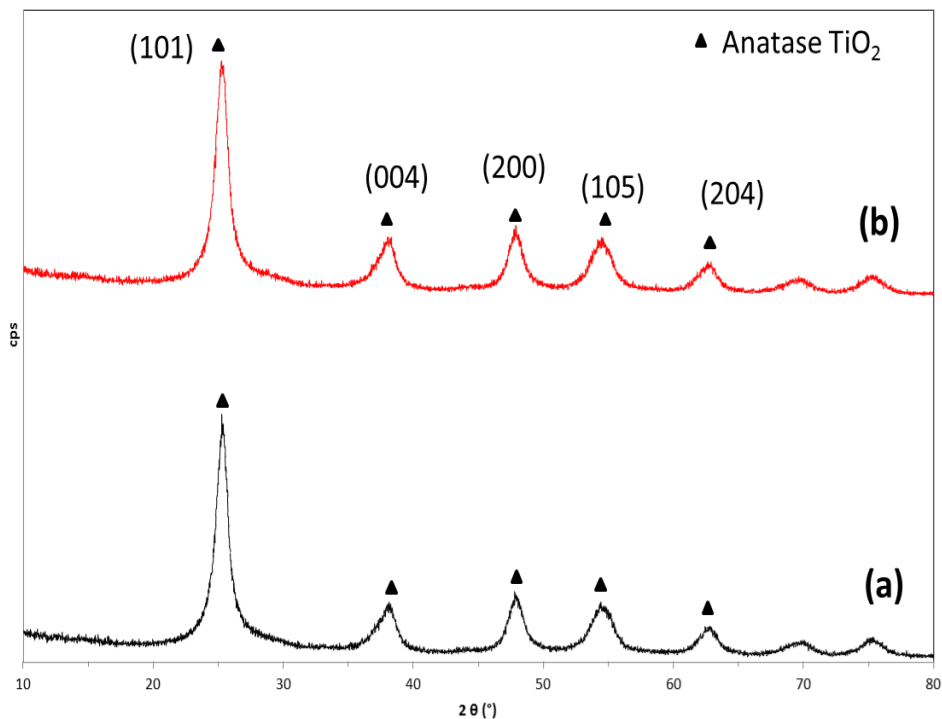


Figure 4.3: X-ray diffraction patterns of as-synthesized TiO<sub>2</sub>: (a) without addition of (NH<sub>4</sub>)<sub>2</sub>SO<sub>4</sub> and (b) with 1 mol% addition of (NH<sub>4</sub>)<sub>2</sub>SO<sub>4</sub>.

Table 4.3: Lattice strain, primary particle size and lattice parameters of as-synthesized TiO<sub>2</sub> powders.

Sample	B	B <sub>s</sub>	B <sub>g</sub>	B <sub>i</sub>	ε	Primary particle (nm)	Lattice parameters in Å
TiO <sub>2</sub>	0.727	0.426	0.2113	0.09	0.475	3	a=b= 3.7937 c=9.4571
TiO <sub>2</sub> -1 mol% (NH <sub>4</sub> ) <sub>2</sub> SO <sub>4</sub>	0.795	0.578	0.1268	0.09	0.645	5	a=b= 3.7932 c=9.4698

Table 4.4: Chemical composition analysis by EDS for as-synthesized TiO<sub>2</sub> powders synthesized by hydrolysis method.

Element	Composition weight %	
	TiO <sub>2</sub>	TiO <sub>2</sub> -1 mol% (NH <sub>4</sub> ) <sub>2</sub> SO <sub>4</sub>
Ti	47.64	64.15
O	48.86	32.18
S	3.5	3.67
Total	100	100

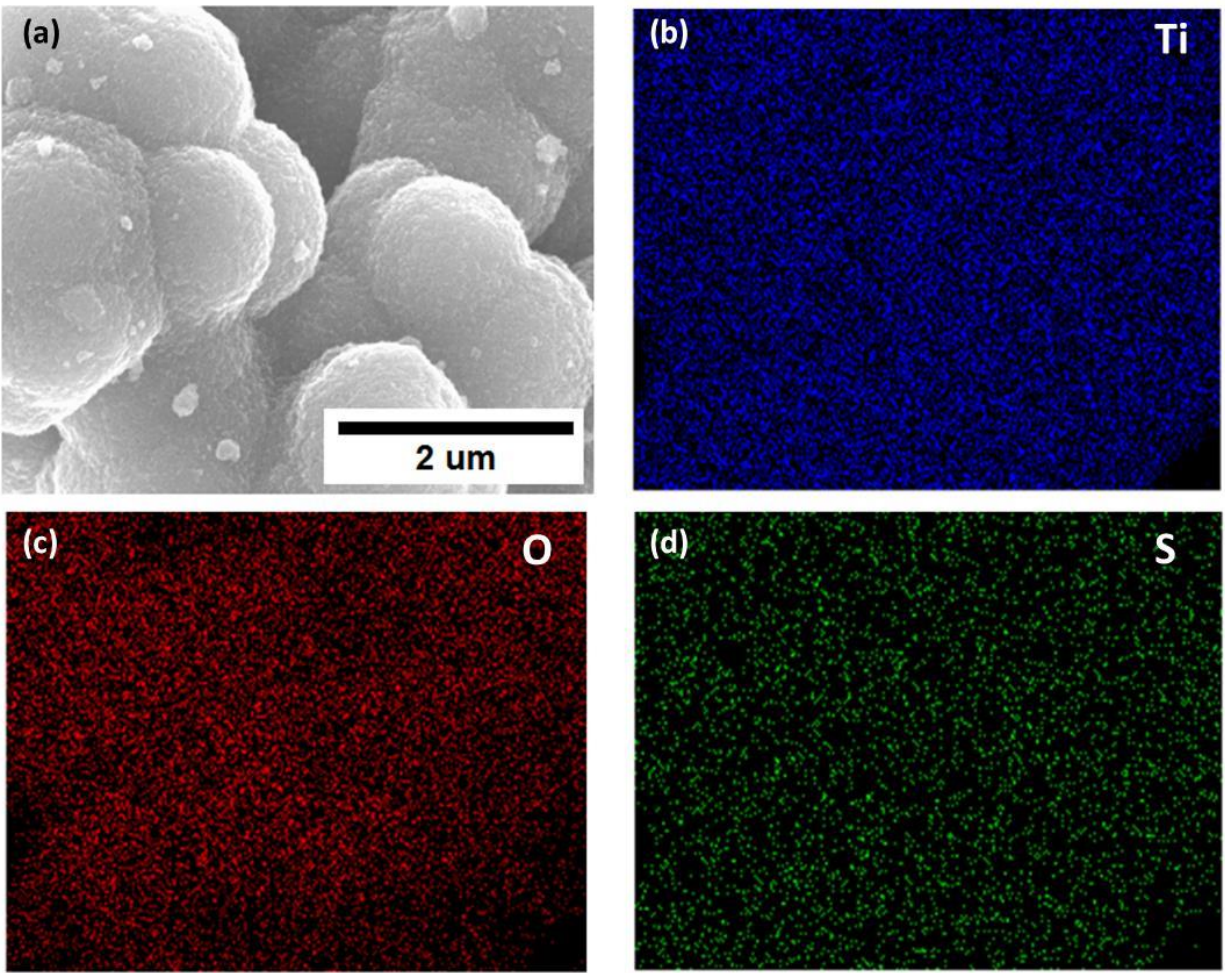


Figure 4.4: SEM image and EDX elemental mapping of Ti, O and S in  $\text{TiO}_2$  powders synthesized with 1 mol% addition of  $(\text{NH}_4)_2\text{SO}_4$ .

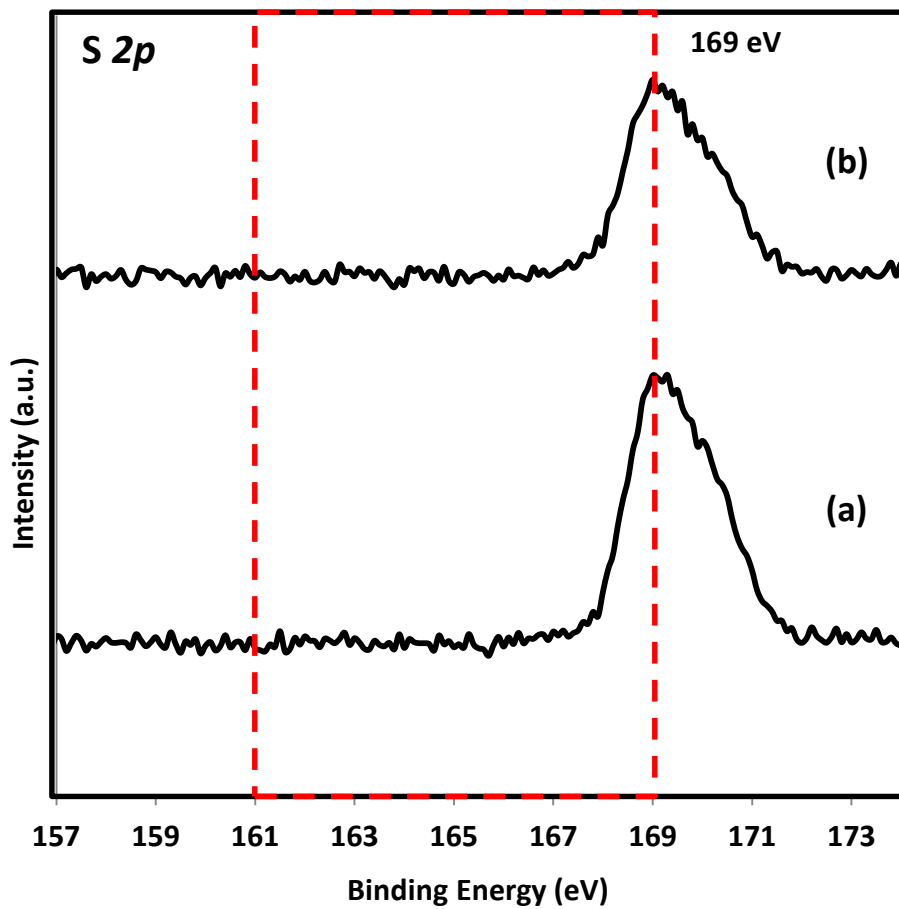


Figure 4.5: XPS spectra of the S 2p region for the as-synthesized TiO<sub>2</sub> powders: (a) without addition of (NH<sub>4</sub>)<sub>2</sub>SO<sub>4</sub> and (b) with 1 mol% addition of (NH<sub>4</sub>)<sub>2</sub>SO<sub>4</sub>.

SEM images show significant different in terms of powder morphology for the powders synthesized with or without the addition of  $(\text{NH}_4)_2\text{SO}_4$ . The morphology of the synthesized  $\text{TiO}_2$  powders was first observed by SEM at low magnification (Fig. 4.6- a & b) which indicates that both types of  $\text{TiO}_2$  powders were agglomerated to a structure of 10-30  $\mu\text{m}$ .  $\text{TiO}_2$  powders that synthesized without the addition of  $(\text{NH}_4)_2\text{SO}_4$  composed of giant particle with loose agglomeration. When  $(\text{NH}_4)_2\text{SO}_4$  was added in the precursor solution during the synthesis, more spherical profile with more pronounce of small agglomerates (secondary particles,  $2^\circ$ ) inside larger agglomerates (tertiary,  $3^\circ$ ) was obtained and more visible in the 1% mol addition of  $(\text{NH}_4)_2\text{SO}_4$ . The results indicate that addition of  $(\text{NH}_4)_2\text{SO}_4$  during the synthesis significantly promote agglomeration of  $\text{TiO}_2$  powders which shown by SEM images. The addition of  $(\text{NH}_4)_2\text{SO}_4$  in this process not only act as structure-directing agent but also improved the densification of the synthesized powders. This can be seen at high magnification image using SEM. The image (Fig. 4.6-d) depicts that  $\text{TiO}_2$  with the addition of  $(\text{NH}_4)_2\text{SO}_4$  compose of denser packing of  $2^\circ$  particles with low number of porosity compared to the  $\text{TiO}_2$  without the addition of  $(\text{NH}_4)_2\text{SO}_4$ . This close packing structure together with minimize number of porosity is an important factor to build-up the coating during the cold spray deposition. Moreover, at higher magnifications using TEM observations, small subunits; primary ( $1^\circ$ ) particles forming the  $2^\circ$  particles can be observed.

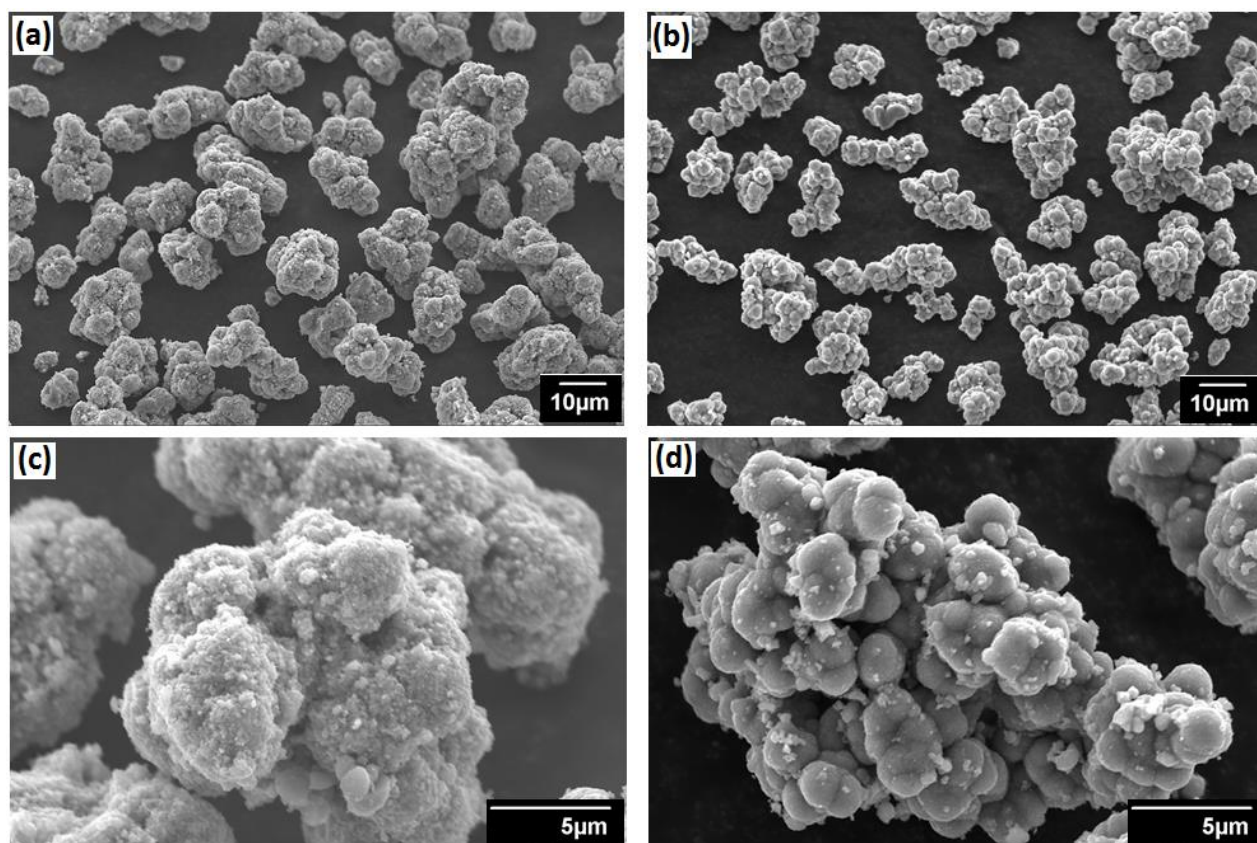


Figure 4.6: SEM micrograph of as-synthesized  $\text{TiO}_2$ : (a & c) without addition of  $(\text{NH}_4)_2\text{SO}_4$  and (b & d) with addition of  $(\text{NH}_4)_2\text{SO}_4$ .

Figure 4.7 shows the HRTEM image of both synthesized powders. The micrographs reveal that agglomerated  $\text{TiO}_2$  powders that synthesized using hydrolysis method with the addition of  $(\text{NH}_4)_2\text{SO}_4$  were formed from spherical particle with average size of 5 nm. Similar result was observed for sample without the addition of  $(\text{NH}_4)_2\text{SO}_4$ . However, the average sizes of  $1^\circ$  particles were reduced to 3 nm. This occurs as addition of  $(\text{NH}_4)_2\text{SO}_4$  has accelerated the precipitation of the precursor during the hydrolysis. Therefore, the precursor solution for  $\text{TiO}_2$  powders without the addition of  $(\text{NH}_4)_2\text{SO}_4$  has slower rate of hydrolysis compared to the

powder with the addition of  $(\text{NH}_4)_2\text{SO}_4$ . It is well known that slow hydrolysis rate will lead to crystalline nanoparticles formation [9]. However, the measured crystallite size were not in good agreement with the calculated from the (101) reflection by the Scherrer equation. This might occur as the diffraction peak broadening of XRD pattern uses in the Scherrer equation neglect the strains that may have in the examine  $\text{TiO}_2$  powders [4]. Therefore, the measured  $1^\circ$  particle size using TEM was considered more accurate compared to the calculated one using Scherrer equation.

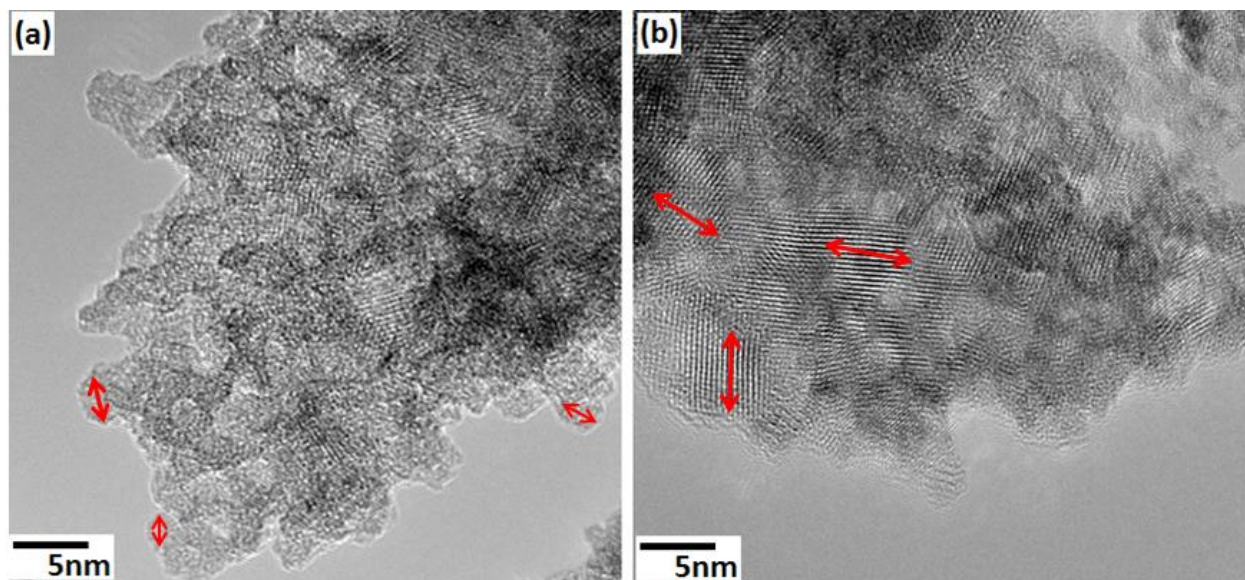
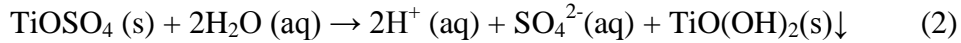


Figure 4.7: High-resolution TEM pictures of crystalline grains for the as-synthesized  $\text{TiO}_2$ : (a) without addition of  $(\text{NH}_4)_2\text{SO}_4$  and (b) with addition of  $(\text{NH}_4)_2\text{SO}_4$ . The red arrows show some of the single size of  $1^\circ$  nano-particles.



Furthermore, the result shows that dissolving  $(\text{NH}_4)_2\text{SO}_4$  solution into the starting precursor has induced rapid precipitation. This can be observed during the experiment where the transformation from white solution to clear solution of starting precursor with the addition of  $(\text{NH}_4)_2\text{SO}_4$  occurred faster than the solution without the addition of  $(\text{NH}_4)_2\text{SO}_4$ . This argument was confirmed by DTA curve in Fig. 4.8. The DTA results show that the  $\text{TiO}_2$  powder with  $(\text{NH}_4)_2\text{SO}_4$  addition experienced rapid super saturation and precipitation which started to occur at  $\sim 56.6^\circ\text{C}$ . Meanwhile, for the powder without the addition of  $(\text{NH}_4)_2\text{SO}_4$ , the precipitation occurred at  $\sim 72^\circ\text{C}$ . This result indicates that  $(\text{NH}_4)_2\text{SO}_4$  has induced instantaneous precipitation during the reaction. This reaction referred to decomposition of  $\text{TiOSO}_4$  during the hydrolysis to form white precipitate  $\text{TiO}(\text{OH})_2$  as shown in following equation 2 [20]:



However,  $\text{TiO}(\text{OH})_2$  that produced upon the hydrolysis mostly were amorphous. Drying process has been conducted to improve the crystallinity of the obtained precipitate. This thermal treatment contribute to loose of water in the  $\text{TiO}(\text{OH})_2$  precipitate and anatase  $\text{TiO}_2$  was produced as shown in equation 3 [20].



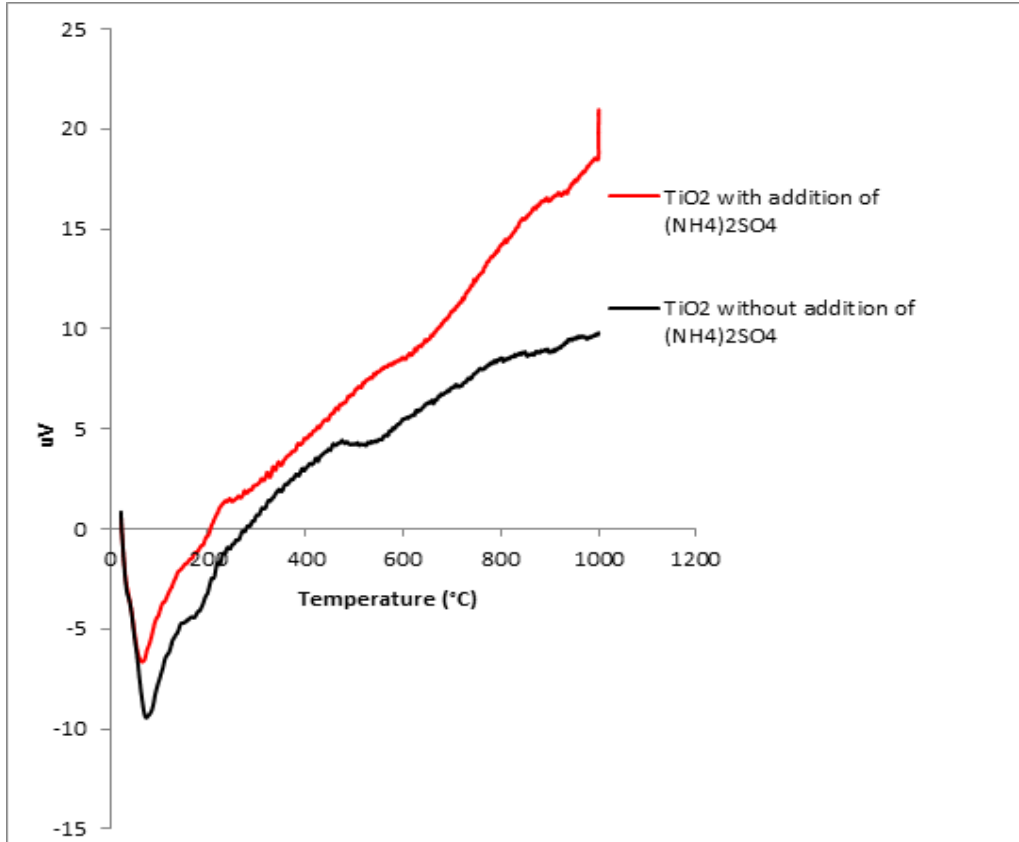


Figure 4.8: DTA curved of as-synthesized TiO<sub>2</sub> via hydrolysis method.

#### 4.3.3 Characterization of TiO<sub>2</sub> coatings prepared by cold spray method

Figure 4.9 (a) and (b) shows the images of coating cross section microstructures sprayed by cold spray using different types of TiO<sub>2</sub> powders on ceramic tiles substrates. The results indicate that the powder with the addition of (NH<sub>4</sub>)<sub>2</sub>SO<sub>4</sub> can building-up the coating about ~140μm (Fig. 4.9-b). Meanwhile, for the powder without the addition of (NH<sub>4</sub>)<sub>2</sub>SO<sub>4</sub>, a thinner coating of about 50 μm was formed using the same cold spray parameters. Moreover, this result shows that the thickness of TiO<sub>2</sub> coating in this study is comparable to the coating thickness that

was deposited using hydrothermal treated TiO<sub>2</sub> powder reported by Salim [4]. This study suggests that the as-synthesized TiO<sub>2</sub> powder with addition of (NH<sub>4</sub>)<sub>2</sub>SO<sub>4</sub> is not only free from the addition of polymeric binder but also do not require any post treatment process prior to coating process.

XRD patterns of anatase TiO<sub>2</sub> coatings compared with the feedstock powders for both type of TiO<sub>2</sub> are shown in Fig. 4.10 (a) and (b). The present results disclosed that anatase phase was preserved for cold-sprayed coating using both type of TiO<sub>2</sub> powders that were synthesized in this study. This result shows that cold spray is a coating method that able to maintain the original crystalline structure of the initial feedstock materials.

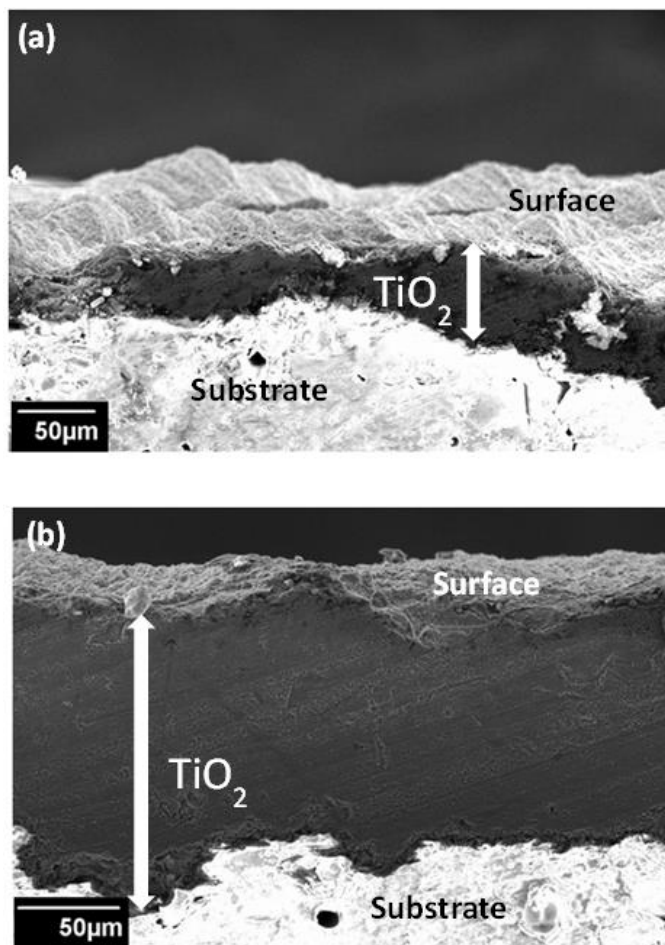


Figure 4.9: Cross-sectional view of  $\text{TiO}_2$  coating deposited on ceramic tiles by cold spray process, respectively: (a) without addition of  $(\text{NH}_4)_2\text{SO}_4$  and (b) with addition of  $(\text{NH}_4)_2\text{SO}_4$ .

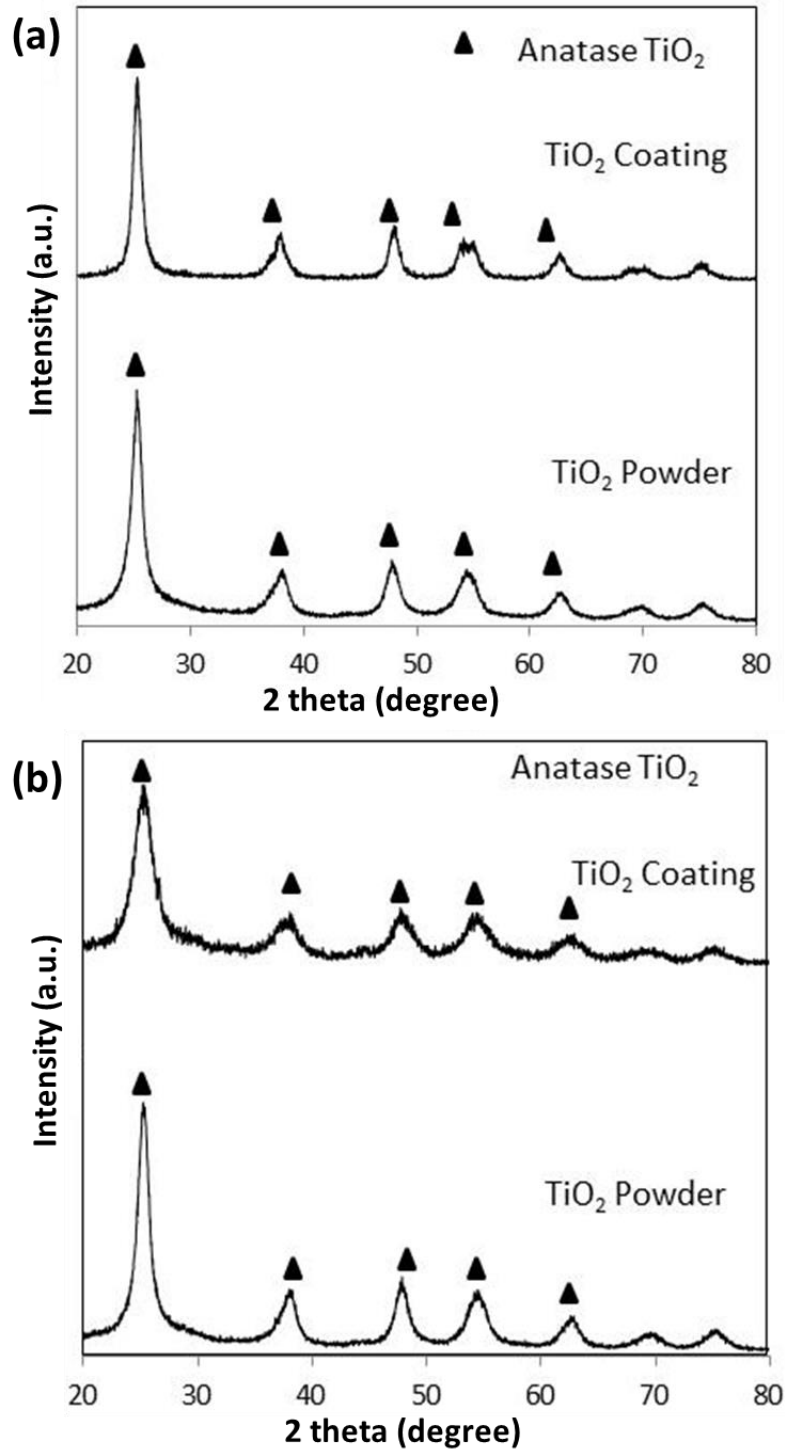


Figure 4.10: XRD patterns of powder and coating using different type of TiO<sub>2</sub> powder, respectively: (a) without addition of (NH<sub>4</sub>)<sub>2</sub>SO<sub>4</sub> and (b) with addition of (NH<sub>4</sub>)<sub>2</sub>SO<sub>4</sub>.

The TiO<sub>2</sub> coating formation using cold spray is explained as below. When high kinetic energy and pressure was supplied during the process, agglomerated TiO<sub>2</sub> which has some degree of porosity was accelerated by supersonic gas stream and collision occurred. The collision shattered the agglomerated TiO<sub>2</sub> (3° and 2° particles) into smaller particles. Porosity which contain in the structure initiated the particles to break down during the collision. However, for the TiO<sub>2</sub> powder with the addition of (NH<sub>4</sub>)<sub>2</sub>SO<sub>4</sub>, breaking of particles were more difficult in comparison with the loose packed TiO<sub>2</sub> which was synthesized without the addition of (NH<sub>4</sub>)<sub>2</sub>SO<sub>4</sub>. This is due to the tightly agglomerated particles resulting in less number of porosity. Thus, minimum possibilities of breakdown of particles to smaller particles led to collision of bigger agglomerated particles which has higher momentum during the impact, as shown in Fig. 4.11 (b). This impact promoted better adhesion between agglomerated TiO<sub>2</sub> particles with the substrate. Then, the coating thickness was increased by continuous stacking of agglomerates TiO<sub>2</sub> which composed of nanoparticles. The adhesion between particles-to-particles will be easier on the previously-deposited particles. Fan et al. [24] suggested that the particle-to-particle bonding was due to tamping effect which will compact the coating through slipping of the nanoparticles in the coating under high pressure. The slipping or sliding of particles over other particles will be much easier to occur for ceramic materials that composed of nanoparticles [25]. This mechanism is responsible for the deposition of dense TiO<sub>2</sub> coating that obtained in this study as the 1° particles of this feedstock materials were nanoparticles.

However, in the case of TiO<sub>2</sub> powders that was synthesized without the addition of (NH<sub>4</sub>)<sub>2</sub>SO<sub>4</sub> which have loose agglomerated particles, the particles were easily shattered to smaller single particle when high kinetic energy was applied (Fig. 4.11-a). Then, the particle tends to collide as individual particle more than as agglomerated particles. The impact of single

particle is weak and exhibit low inertial levels to penetrate the stagnation layer on the substrate [2]. This explains why the coating thickness of this  $\text{TiO}_2$  powders was just about  $50\mu\text{m}$ .

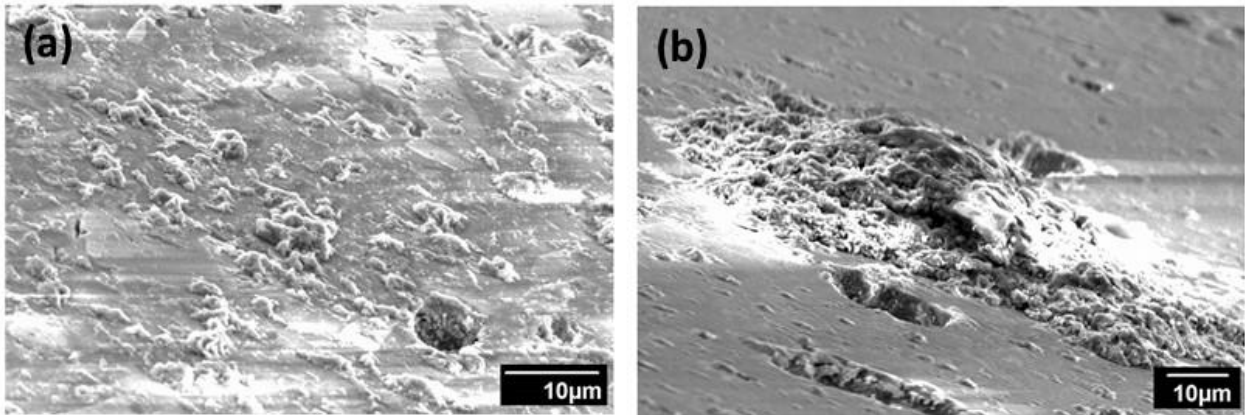


Figure 4.11: SEM images of single impact morphologies of  $\text{TiO}_2$  powders on substrate using  $\text{TiO}_2$  powders synthesized (a) without addition of  $(\text{NH}_4)_2\text{SO}_4$  and (b) with addition of  $(\text{NH}_4)_2\text{SO}_4$ .

The results obtained in this study also reveals that by adding  $(\text{NH}_4)_2\text{SO}_4$  during the synthesis not only agglomerates the nanoparticles into micro-sized structure, but also promotes mobility of dislocation [3] to occur when high pressure and temperature was applied during the cold spray process. When dislocations were sufficiently mobile, plastic deformation of  $\text{TiO}_2$  occurred and  $\text{TiO}_2$  powder was deformed on the substrate. Deformation of the powder was expected to occur due to the nature of hard ceramic tile which is difficult to be deformed.  $\text{TiO}_2$  powders that have dislocation in the crystal structure allow deformation to occur at much lower stress in comparison to a crystal that was produced in the  $\text{TiO}_2$  powder synthesized without the addition of  $(\text{NH}_4)_2\text{SO}_4$ . Furthermore, since there was no and/or very little dislocation introduced

during the synthesis for this type of TiO<sub>2</sub> powder, deformations for the powder particles were difficult to be induced. During the cold spray, higher stress is required for deposition of this type of TiO<sub>2</sub> powder. Further study on the detail dislocation at nanoparticle level using TEM should be conducted to confirm the deformation of single crystals.

The finding of this study also shows that the existence of nanoporosity [4] in the feedstock powder is one of important criteria for deposition of ceramic materials for cold spray process. Therefore, the sizes and amount of the pores need to be considered. Figure 4.12 (a) and (b) depict the SEM images of TiO<sub>2</sub> powders. Larger pores which were pointed out by arrows can be seen clearly exist in the TiO<sub>2</sub> powder synthesized without the addition of (NH<sub>4</sub>)<sub>2</sub>SO<sub>4</sub>. Pores usually are formed due to poorer particle packing in the powder [26]. This poor packing leading to loose tightly bonded between the 3° and 2° particles. As the number of pores increased, the porosity of the materials also increased. Thus it will reduce the density of the materials. Particles that have small density have less tamping effect acts on compared to powders that has less porosity [27]. This can be proved by SEM image of cross sectional area and surface coating as shown in Fig. 4.13. The image reveals that coating that was produced using powder synthesized without the addition of (NH<sub>4</sub>)<sub>2</sub>SO<sub>4</sub> contains agglomerated particles with more porosity compared to the coating that was made from TiO<sub>2</sub> powder with addition of (NH<sub>4</sub>)<sub>2</sub>SO<sub>4</sub>. The result of porosity, hardness and surface roughness of the cold sprayed TiO<sub>2</sub> coating is presented in Table 4.5. Porosity measurements showed the average porosity of 45.1 and 31.0 % for TiO<sub>2</sub> without addition of (NH<sub>4</sub>)<sub>2</sub>SO<sub>4</sub> and with addition of (NH<sub>4</sub>)<sub>2</sub>SO<sub>4</sub>, respectively. This study reveals that characteristics of the original powder influenced the properties of the obtained coating. Moreover, Fig. 4.13 (a) & (b) which show the detail microstructure of the coatings also proved that cold spray method conserved the initial features of 2° particles of the agglomerated TiO<sub>2</sub>, which are



comparable to the starting feedstock powder. Fracture of 3° particles can be confirmed during the CS process as absence of particles with similar size of feedstock powder as shown in the cross-sectional area and also on the surface of the coating for both types of powder.

Moreover, details observation of the cross-sectional views and surface of cold sprayed TiO<sub>2</sub> coating which synthesized with addition of (NH<sub>4</sub>)<sub>2</sub>SO<sub>4</sub> have been conducted at high magnification using SEM (Fig. 4.14-d and 4.15-d, respectively). The SEM images show that both views of the coatings composed of small TiO<sub>2</sub> particles in the size of <20 nm can be distinguished. The cross-sectional views of the coatings shows that the successful impact particles were compactly attached together (Fig. 4.14- b &c). These structures look like ceramic sintering phenomena has occurred during the deposition of the TiO<sub>2</sub> powders by cold spray process. However, by considering the temperature used in this process and also the melting temperature of the TiO<sub>2</sub> powders, sintering phenomena is impossible can occur during the deposition. The densified parts also shows limited amount of porosity presence in the coating. Densification of the coating parts was attributed to tamping effect when the previously coated particles receiving multiple impact of particles during the process. This led to reduction of porosity in the TiO<sub>2</sub> coating resulting from the reduction of pores in the successful deposited particles. Moreover, multiple impacts from incoming particle on the 1<sup>st</sup> layer deposited on the substrates compact the previous layer which in turns, improve the adhesion of the coating. In addition, compared to the 2° particles of the feedstock powders as shown in Fig. 4.10 (a), changes in morphology and grain size can be observed. As notice from the coatings image as shown in Fig. 4.14 (b), the size and shape of the sphere shape of 2° particles were no longer spherical upon the impact. This is likely attributed to plastic deformation where nanostructured

TiO<sub>2</sub> powders receiving enough local compact pressure and high strain rate of impacting particles [3].

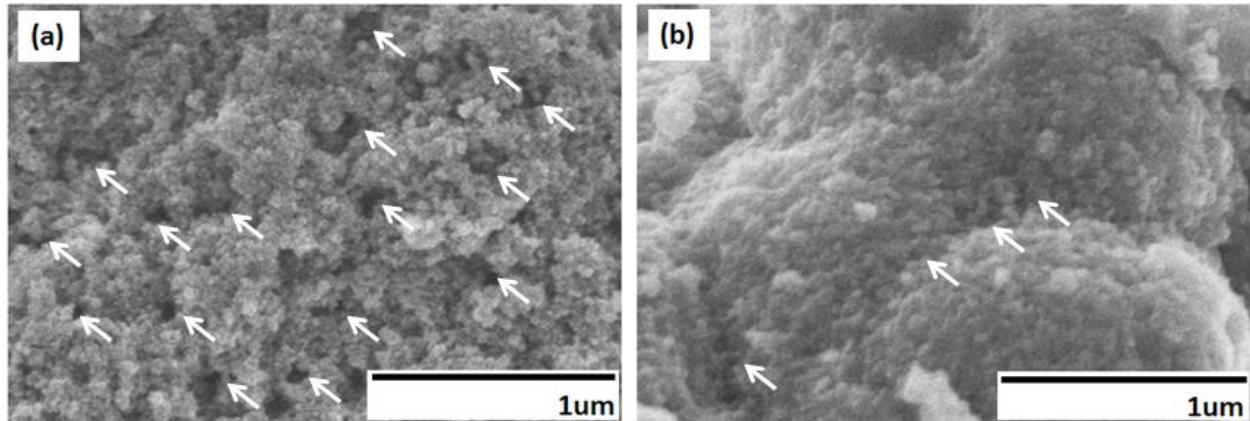


Figure 4.12: Details of SEM images of existing porosity of as-synthesized TiO<sub>2</sub> with arrows show some of the existing porosity in the obtained TiO<sub>2</sub> powder; (a) TiO<sub>2</sub> powders without addition of (NH<sub>4</sub>)<sub>2</sub>SO<sub>4</sub> and (b) with addition of (NH<sub>4</sub>)<sub>2</sub>SO<sub>4</sub>, respectively.

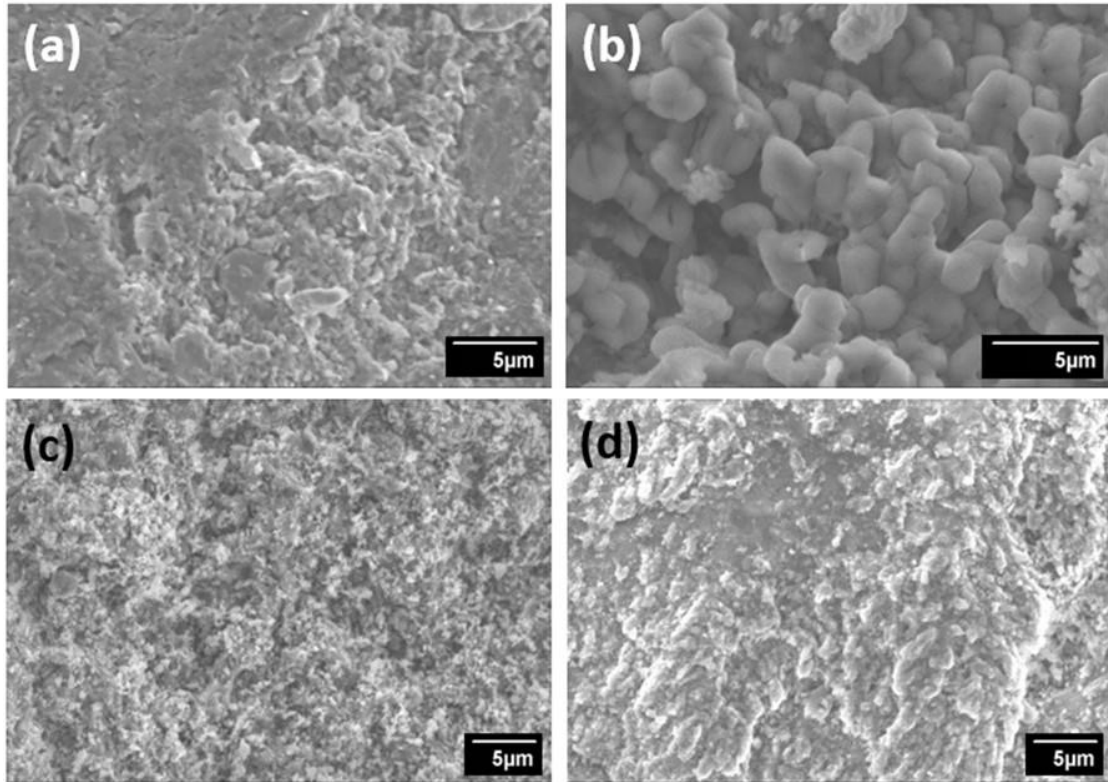


Figure 4.13: SEM images of cross-section of coating and surface of coating, respectively: (a) & (c)  $\text{TiO}_2$  without addition of  $(\text{NH}_4)_2\text{SO}_4$  and (b) & (d)  $\text{TiO}_2$  with addition of  $(\text{NH}_4)_2\text{SO}_4$ .

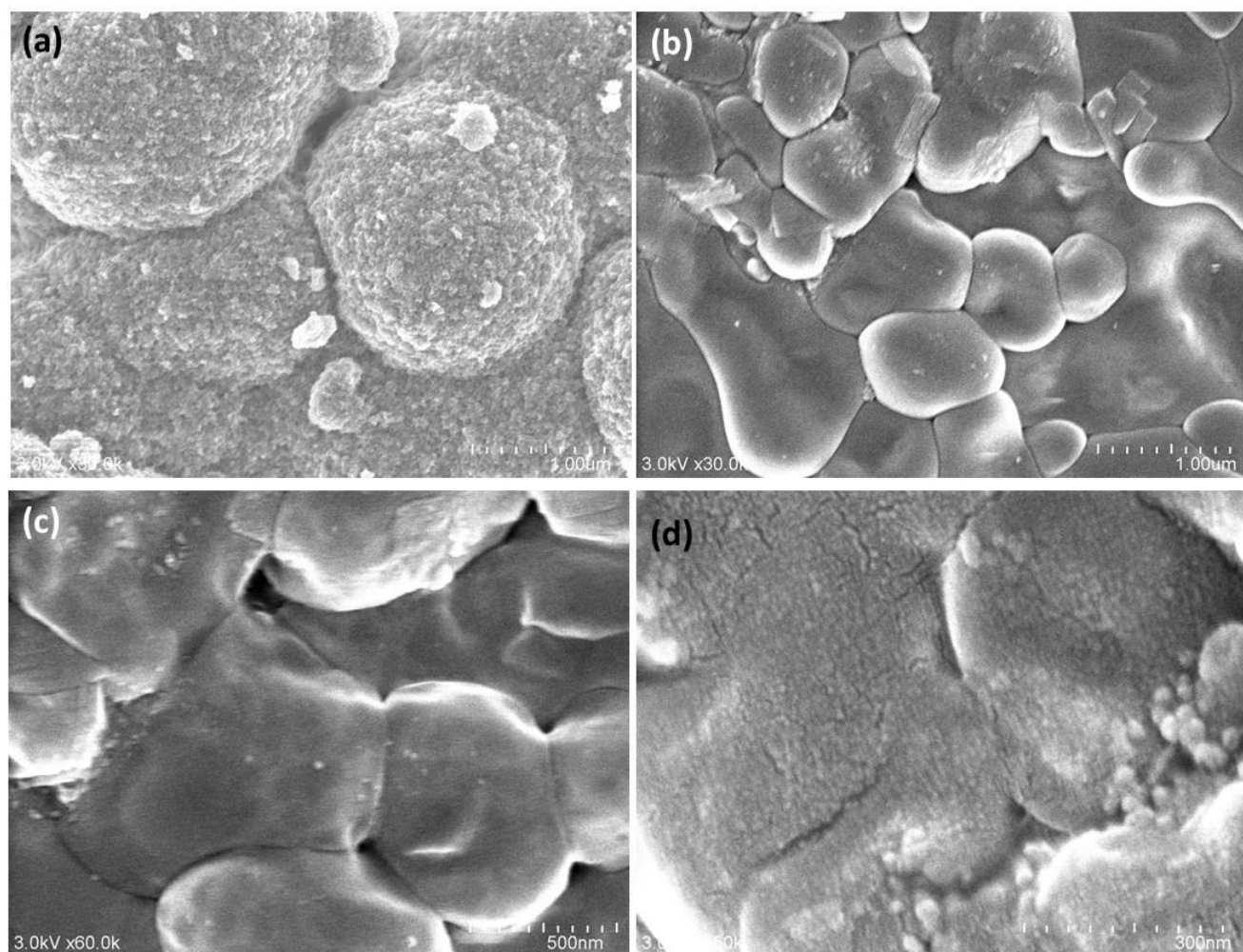


Figure 4.14: High magnification SEM micrographs of (a) TiO<sub>2</sub> feedstock powders synthesized with (NH<sub>4</sub>)<sub>2</sub>SO<sub>4</sub> addition and (b-d) cross-sectional views of TiO<sub>2</sub> coating prepared by cold spray process at different magnifications.

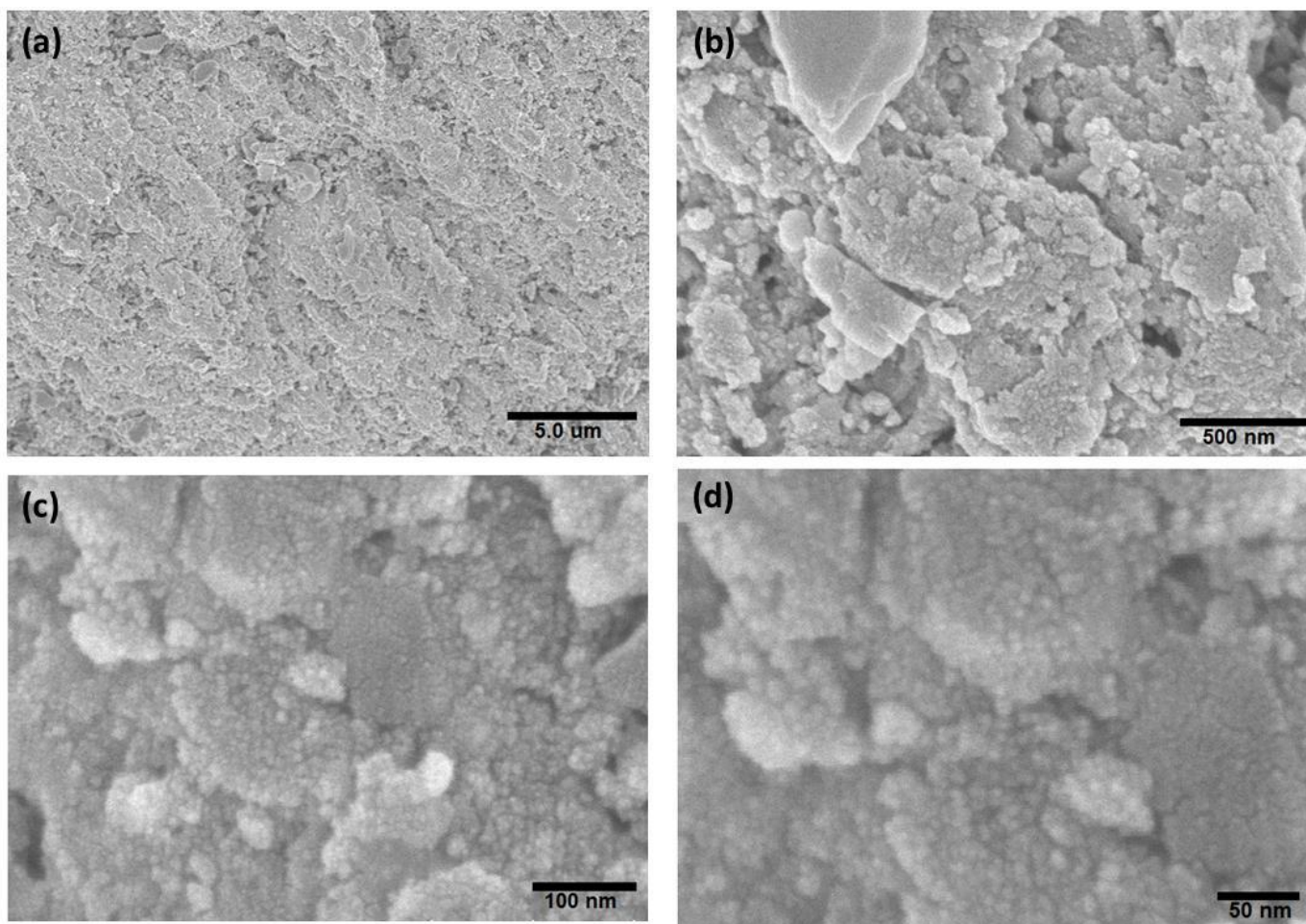


Figure 4.15: SEM micrographs of surface topography of TiO<sub>2</sub> coating prepared by cold spray process at different magnification using TiO<sub>2</sub> feedstock powders synthesized with (NH<sub>4</sub>)<sub>2</sub>SO<sub>4</sub> addition; (a) 5000 X, (b) 50 000 X, (c) 200 000 X and (d) 300 000 X.

Table 4.5: Properties of TiO<sub>2</sub> coating prepared by cold spray process.

<b>Sample</b>	<b>Thickness (<math>\mu\text{m}</math>)</b>	<b>Roughness (<math>\mu\text{m}</math>)</b>	<b>Hardness (Hv)</b>	<b>Porosity (%)</b>
<b>TiO<sub>2</sub></b>	~50	$5.0 \pm 0.8$	$58.0 \pm 13.4$	45.1
<b>TiO<sub>2</sub> -(NH<sub>4</sub>)<sub>2</sub>SO<sub>2</sub></b>	~150	$4.9 \pm 0.6$	$71.9 \pm 11.2$	31.0

Porosity that was formed in the coating also affects the microhardness measurement. Lower microhardness was measured for both types of coatings compared to bulk TiO<sub>2</sub>. The average hardness values were  $58.0 \pm 13.4$  and  $71.9 \pm 11.2$  HV for TiO<sub>2</sub> coatings that were built up from TiO<sub>2</sub> powder without addition of (NH<sub>4</sub>)<sub>2</sub>SO<sub>4</sub> and with addition of (NH<sub>4</sub>)<sub>2</sub>SO<sub>4</sub>, respectively. Low microhardness of the coating was not surprising as the coating was made from solid state reaction. The initial powders were preserved and no melting of particles occurred in the process as the process temperature was below the melting temperature of TiO<sub>2</sub>. Moreover, necking among the particles was expected to occur during cold spraying [17]. Due to the porous structure of the feedstock powders, pores could be formed from the fragmentation of particles upon impact. However, since TiO<sub>2</sub> powder with addition of (NH<sub>4</sub>)<sub>2</sub>SO<sub>4</sub> has less porosity in the powder and produce denser coating, increase of hardness value was expected. This was due to good inter-particle contact in the coating as shown in Fig. 4.13 (b) and (d). Well bonded particles in the coating also produced finer surface roughness. Surface roughness of TiO<sub>2</sub> coating was found decreased with coating that was made from TiO<sub>2</sub> powder with addition of (NH<sub>4</sub>)<sub>2</sub>SO<sub>4</sub>. The surface roughness was  $4.9 \pm 0.6$   $\mu\text{m}$  compared to  $5.0 \pm 0.8$   $\mu\text{m}$  for TiO<sub>2</sub> powder without addition

of  $(\text{NH}_4)_2\text{SO}_4$ . This preliminary result showed that addition of  $(\text{NH}_4)_2\text{SO}_4$  during powder synthesis provides denser microstructure of agglomerated  $\text{TiO}_2$  powders which lead to better properties of cold sprayed  $\text{TiO}_2$  coating.

#### **4.4 Conclusions**

This study shows that addition of  $(\text{NH}_4)_2\text{SO}_4$  has altered the morphology of the as synthesized powders during the hydrolysis. The acidic environment in the precursor will lead to formation of anatase  $\text{TiO}_2$  with small crystal grain which has improved thermal stability of the obtained powder. The addition of  $(\text{NH}_4)_2\text{SO}_4$  also has accelerated the precipitation of the precursor during the hydrolysis. The results also indicate that the addition of  $(\text{NH}_4)_2\text{SO}_4$  significantly promotes agglomeration of  $\text{TiO}_2$  powders and also denser packing of  $\text{TiO}_2$  particles. The synthesis method used in this study also shows that organizing of nanoparticles into micron sized structures was achieved directly just after the synthesis. These agglomerated particles which are consisted of nanoparticles  $\text{TiO}_2$  and some amount of porosity can be used as feedstock materials for cold spray process. Moreover, addition of  $(\text{NH}_4)_2\text{SO}_4$  has induced plastic deformation to occur when the  $\text{TiO}_2$  powder was cold sprayed using adequate pressure and temperature. These criteria are crucial to build up the coating during the deposition. The coating deposition occurred due to tamping effect through slipping of nanoparticles due to high impact during the particle collision. The results show that hydrolysis synthesis with  $(\text{NH}_4)_2\text{SO}_4$  addition is a convenient way to prepare  $\text{TiO}_2$  for CS application.

## 4.5 References

- 1) M. Gardon, J.M. Guilemany: *J. Therm. Spray Technol.* 23 (2014) 577–595.
- 2) R.S. Lima, B.R. Marple: *J. Therm. Spray Technol.* 16 (2007) 40–63.
- 3) Y. Liu, J. Huang, H. Li: *J. Therm. Spray Technol.* 23 (2014) 1149–1156.
- 4) N.T. Salim, M. Yamada, H. Nakano, K. Shima, H. Isago, M. Fukumoto: *Surf. Coat. Technol.* 206 (2011) 366–371.
- 5) X. Jiang, F. Du, C. Guo, Q. Yang, X. Zheng: *J. Zhejiang Univ. Sci. A.* 10 (2009) 1651–1659.
- 6) J.-G. Li, T. Ishigaki: *J. Am. Ceram. Soc.* 88 (2005) 3232–3234.
- 7) H. Wang, J.-J. Miao, J.-M. Zhu, H.-M. Ma, J.-J. Zhu, H.-Y.: *Langmuir.* 20 (2004) 11738–47.
- 8) S. Ghosh, D. Majumder, A. Sen, S. Roy: *Mater. Lett.* 130 (2014) 215–217.
- 9) J. Šubrt, V. Štengl, S. Bakardjieva, L. Szatmary: *Powder Technol.* 169 (2006) 33–40.
- 10) M. Yamada, H. Isago, H. Nakano, M. Fukumoto: *J. Therm. Spray Technol.* 19 (2010) 1218–1223.
- 11) N. Bala, H. Singh, J. Karthikeyan, S. Prakash: *Surface Engineering* 30(6) (2014) 414-421.
- 12) F. Wang, B. Qi, Q. Wang, W. Cui: *International Journal of Hydrogen Energy* 39 (2014) 13852-13858.
- 13) Z. Sayyar, A. A. Babaluo, J.R. Shahrouzi: *Applied Surface Science* 335 (2015) 1–10
- 14) M. Gardon, A. Concustell, S. Dosta, N. Cinca, I.G. Cano, J. M. Guilemany: *Materials Science and Engineering C* 45 (2014) 117-121.
- 15) H. Koivuluoto, P. Vuoristo: *Surface Engineering* 30(6) (2014) 451-454.



- 16) M. Yamada, Y. Kandori, K. Sato, M. Fukumoto: *J. Solid Mech. Mater. Eng.* 3 (2009) 210–216.
- 17) M. Gardon, C. Fernández-Rodríguez, D. Garzón Sousa, J.M. Doña-Rodríguez, S. Dosta, I.G. Cano, et al.: *J. Therm. Spray Technol.* 23 (2014) 1135–1141.
- 18) S. Sathyamoorthy, G. D. Moggridge and M. J. Hounslow: *AIChE J.* 47 (2001) 2012-2024.
- 19) L. Szatmárya, S. Bakardjievaa, J. S̆ubrt, P. Bezdic̆kaa, J. Jirkovsky', Z. Bastl, V. Brezováč, M. Korenko: *Catalysis Today* 161 (2011) 23–28
- 20) S. A. Simakov, Y. Tsur: *J. Nanoparticle Res.* 9 (2006) 403–417.
- 21) S.-Q. Fan, G.-J. Yang, C.-J. Li, G.-J. Liu, C.-X. Li, L.-Z. Zhang: *J. Therm. Spray Technol.* 15 (2006) 513–517.
- 22) L.G. Devi, R. Kavitha: *Materials Chemistry and Physics* 143 (2014) 1300-1308.
- 23) W. Ho, J. C. Yu, S. Lee: *Journal of Solid State Chemistry* 179 (2006) 1171-1176.
- 24) P. Periyat, D. E. McCormack, S. J. Hinder, S. C. Pillai: *J. Phys. Chem. C* 113 (2009) 3246-3253.
- 25) L. Pawlowski: *Surf. Coatings Technol.* 202 (2008) 4318–4328.
- 26) Rice, Roy W. *Porosity of Ceramics*; Marcel Dekker. Inc.: New York, 1998; 13 pp.
- 27) Chang-jiu, LI. ; Wen-ya, LI: *Transactions of Nonferrous Metals Society of China* 14 (2004) 49-54.

## **5 Effect of Substrate Material on Cold-Sprayed Titanium Dioxide Coating**

### **5.1 Introduction**

Titanium dioxide ( $\text{TiO}_2$ ) coating has attracted great interest in variety of applications such as photocatalysis, biomedical coating and solar cells [1]. For a photocatalyst application, anatase phase works more efficiently than rutile phase. The coating of  $\text{TiO}_2$ , especially for thick and large surfaces, can be accomplished with a thermal spray process that uses minimum time and is more cost effective [2]. In a conventional thermal spray method, such as high-velocity oxy-fuel (HVOF) and atmospheric plasma spray (APS), high processing gas temperatures are required to deposit the feedstock materials in molten and semi-molten conditions onto the prepared surface for fabrication of the coating. The temperatures required to melt the particles contributes to the transformation of the metastable of anatase phase to stable phase of rutile [1, 3, and 4]. Furthermore, this phase transformation is irreversible. On the other hand, the performance of ceramic material, which is used for photocatalyst applications, depends mainly on its crystal structure, surface area, crystallinity and textural properties. Therefore, it is very important to consider a coating process that can maintain the properties of the initial feedstock materials.

The cold spray (CS) method has shown great advantages compared to other thermal spray methods in this regard as it operates below the transformation temperature of the feedstock powder and the exposure time to the hot gas stream is very short [5]. This coating technique utilizes kinetic energy for powder deposition; instead of thermal energy, to form the coating. Therefore, phase transformation from the anatase phase to an unfavorable rutile phase can be

avoided. Generally, plastic deformation is essential for cold spray coating. Cold spray deposition using ceramic powders as feedstock materials have been considered challenging due to the brittle nature possessed by ceramic materials, which are resistant to plastic deformation. However, in certain conditions, it is possible to deposit ceramic materials onto the substrates by a cold spray process [6, 7].

Of the several factors contributing to successful ceramic coating formation during the cold spray process, feedstock powder, in particular, stands out as shown by several studies that have been conducted [3,8,9]. Plastic deformation, which is required for powder deposition using cold spray method, can occur in ceramic material when the feedstock materials are in nanosized particles [10]. The used of nanoparticle powder for cold spray can promote ductility [11] in the powder by having a better capacity for the sliding of small grains over each other and it is believed to be a factor that help build up the coating when using ceramic as feedstock material. Preservation of the original nanostructure in the prepared coating using the nanostructure of feedstock powders can also be achieved using cold spray method. For a cold spray process, the feedstock powder should be in the microsized range as to avoid the powder clogging inside the feeding system that transports the particles from the powder feeder to the nozzle [1,12] and also to overcome the bow shock layer during the coating process [13,14]. Moreover, due to a safety and environmental regulations issue, the handling of fine particles during spraying requires more safety precautions than with the handling of coarser particles [1, 11]. Usually nanosized powders were agglomerated up to submicron sized by means of a spray drying process. For example, a cold-sprayed TiO<sub>2</sub> coating using agglomerated TiO<sub>2</sub> powder, where a binder was used during the agglomeration process, was formed under high transient impact pressure [15]. In this case, deformation occurred due to the ductility that was provided by the binder.

The penetration of particle collisions on the substrate and the deformation of the powder particle and the substrate using a cold spray process also depends on the properties of the feedstock particles and the substrate materials [16]. J.-O Kliemann et al [5] has reported on the study of dense TiO<sub>2</sub> particles with nanosized crystallites and their impact on different metal surfaces. They concluded that deposition efficiency was determined by spray temperature, feedstock powder characteristics as well as the properties of the substrate. They also reported that a single particle impact gave different bonding mechanisms for soft and hard substrate. Lee et al [6] revealed that craters that were produced by an Al-Al<sub>2</sub>O<sub>3</sub> cold sprayed coating with a different shape and size of Al<sub>2</sub>O<sub>3</sub> on Al and Si substrate was affected by the starting characteristics of the initial Al<sub>2</sub>O<sub>3</sub> particles. It was found that the depth of the craters that attack the Si substrate were larger when the size of the starting Al<sub>2</sub>O<sub>3</sub> was bigger. They also summarized that a cold spray coating can be formed even on hard substrate when the composition, size and shape of the impact particles have been considered. Besides this, the hardness and chemical composition of the substrate is also important for chemical bonding between nanostructured TiO<sub>2</sub> particles and substrate or among particles when the powders are coated by a cold spray process [2]. M. Gardon et al [2] demonstrated that cold sprayed nano-anatase coatings were deposited onto steel which was coated with titanium sub-oxide layers. The result of the study revealed that a hard and rough surface provided by the titanium sub-oxide on the substrate facilitated the deposition of anatase particles by chemical bonding. However, despite the suggested bonding of ceramic particles in cold gas spraying by these previous studies, the bonding mechanism on how the ceramic coating was formed on the substrate is still unclear.

In this study, the single particle impact of agglomerated TiO<sub>2</sub> powder that was synthesized by a simple hydrolysis method via the cold spray process on ceramic tile, copper and

aluminum substrate was investigated. The influence of hardness and surface roughness of the substrates were also discussed. Powder depositions by cold spray on various substrates also have been undertaken using agglomerated  $\text{TiO}_2$  powders. Moreover, the present study includes a proposed deposition mechanism of ceramic coating with respect to the properties of the substrates.

## **5.2 Experimental Procedure**

### **5.2.1 Synthesis of Agglomerated $\text{TiO}_2$ Powders**

A simple hydrolysis process was carried out using titalyl sulfate ( $\text{TiOSO}_4 \cdot n\text{H}_2\text{O}$ , Chameleon Reagent, Japan) and distilled water. Typically,  $\text{TiOSO}_4$  was dissolved in distilled water in a weight percentage of 10:90. The solution was stirred at high speed, then 1 mol% of ammonium sulfate  $[(\text{NH}_4)_2\text{SO}_4]$  was added to the solution. The temperature of the solution was kept at  $\sim 80^\circ\text{C}$  to complete the hydrolyzation and nucleation process for about 8 h until white precipitates formed. The precipitates of titanium hydroxide/ hydrous titanium oxide ( $\text{TiO}_2 \cdot n\text{H}_2\text{O}$ ) were then collected via decantation and washed several times with distilled water before they were dried in an oven at  $120^\circ\text{C}$ .

### **5.2.2 $\text{TiO}_2$ Coating Preparation by Cold Spray Process**

A CGT Kinetiks 4000 cold-spray system (Cold Gas Technology, Ampfing, Germany) with a custom made suction nozzle was used to perform the wipe test and coating using as-synthesized  $\text{TiO}_2$  powder onto the ceramic tile (INAX ADM-155M), aluminum and copper

substrates. The wipe test was conducted to study the deformation behavior of a single particle on various types of substrate. Prior to deposition, all substrates were ground and polished until a mirror finish surface was obtained. The process gas temperature and pressure used were 500°C and 3 MPa, respectively. Nitrogen was used as the process gas in this experiment. The distance between the exit of the nozzle and the substrate was fixed at 30 mm. The traverse speed of the process was 1000 mm/s. The coating was also deposited on ceramic tile, aluminum and copper substrates. Prior to spraying, the substrates were rinsed with acetone. The parameters for coating deposition were similar to the wipe test. However, the traverse speed was altered from 1000 mm/s to 20 mm/s. The spray parameters are shown in Table 5.1.

Table 5.1: Cold spray conditions.

<b>Type of experiment</b>	<b>Wipe test</b>	<b>Powder deposition</b>
<b>Gas</b>	N <sub>2</sub>	N <sub>2</sub>
<b>Gas pressure [MPa]</b>	3	3
<b>Gas temperature [°C]</b>	500	500
<b>Substrate</b>	1. Ceramic tile 2. Copper 3. Aluminum	1. Ceramic tile 2. Copper 3. Aluminum
<b>Surface condition</b>	Mirror polished surface	Blasted surface
<b>Traverse speed [mm/s]</b>	1000	20
<b>Nozzle-substrate distance [mm]</b>	30	30

### 5.2.3 Characterization of TiO<sub>2</sub> Powders and TiO<sub>2</sub> Coating

The XRD patterns were obtained using a Rigaku RINT 2500 with Cu-K $\alpha$  radiation ( $\lambda = 1.5406 \text{ \AA}$ ) over the  $2\theta$  range of 20-80°. The morphology of the resulting powders, single particle impact morphology on each substrate and the obtained fractured cross sections of the coating samples were examined using a Scanning Electron Microscope (SEM: JSM-6390, JEOL) and a Field Emission Scanning Electron Microscope (FESEM: SU8000, Hitachi). A Transmission Electron Microscope (TEM: JEM-2100F, JEOL) was used to measure the primary particle size of the as-synthesized TiO<sub>2</sub>. The agglomerate size of the initial feedstock powder was measured using Nano Particle Size Analyzer SALD-7100 (Shimadzu). The microhardness of substrates was measured using a HMV-G Micro Vickers Hardness Tester (Shimadzu). Surface roughness was measured by LEXT OLS3100/ OLS3000 (Olympus) with a 20X lens.

## 5.3 Results & Discussion

Figure 5.1 (a) and (b) shows the morphology of the synthesized TiO<sub>2</sub> powders at low and higher magnification which depicts agglomerated particles with uniform distribution ranging between 5-20  $\mu\text{m}$ . The image in Fig. 5.1 (c) reveals that hydrolysis synthesis with addition of (NH<sub>4</sub>)<sub>2</sub>SO<sub>4</sub> produced agglomerates of primary and secondary particles which formed the tertiary powder particles. The powder contained porosity that produced by decomposition of certain ammonium ion during the drying process and may also resulted from the necks that were connecting the agglomerate particles. The TEM image revealed that the formed spheres were

made up from naturally agglomerated nanoparticles as shown in Fig. 5.1 (d). The nanoparticles have diameter of about 5 nm. Moreover, Fig. 5.2 shows that the average particle size of the agglomerated TiO<sub>2</sub> powders was about 12 μm ( $D_{10} = 7.35 \mu\text{m}$ ,  $D_{50} = 11.97 \mu\text{m}$ , and  $D_{90} = 20.15 \mu\text{m}$ ). The formation of the agglomerated particles in micrometer range which composed of fine particles allowed this TiO<sub>2</sub> powder to be used directly after the synthesis process as feedstock materials for CS. Since fine particles especially in nanometer size are not suitable for CS using regular powder feeder, usually fine ceramic powders were spray-dried and/ or sintered prior the coating process [12]. Therefore, the synthesis method that has been used to produce the feedstock powder in this work can be an alternative solution to produce nanoparticles that agglomerating to submicron particles for cold spray coating.



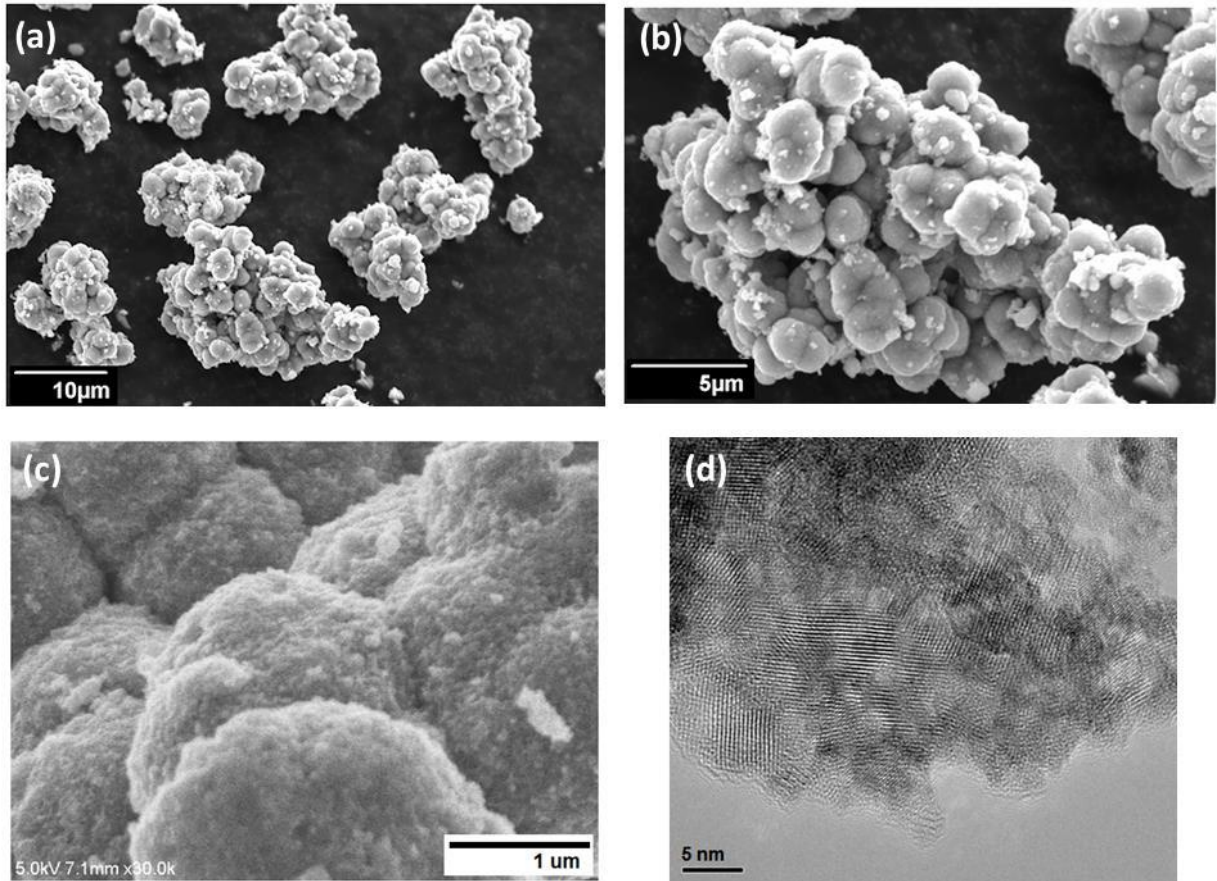


Figure 5.1: Characteristics of the starting  $\text{TiO}_2$  powder for cold spray process: (a) and (b) are SEM images at low magnification, (c) FESEM image at higher magnification and (d) TEM image of the starting  $\text{TiO}_2$  powder.

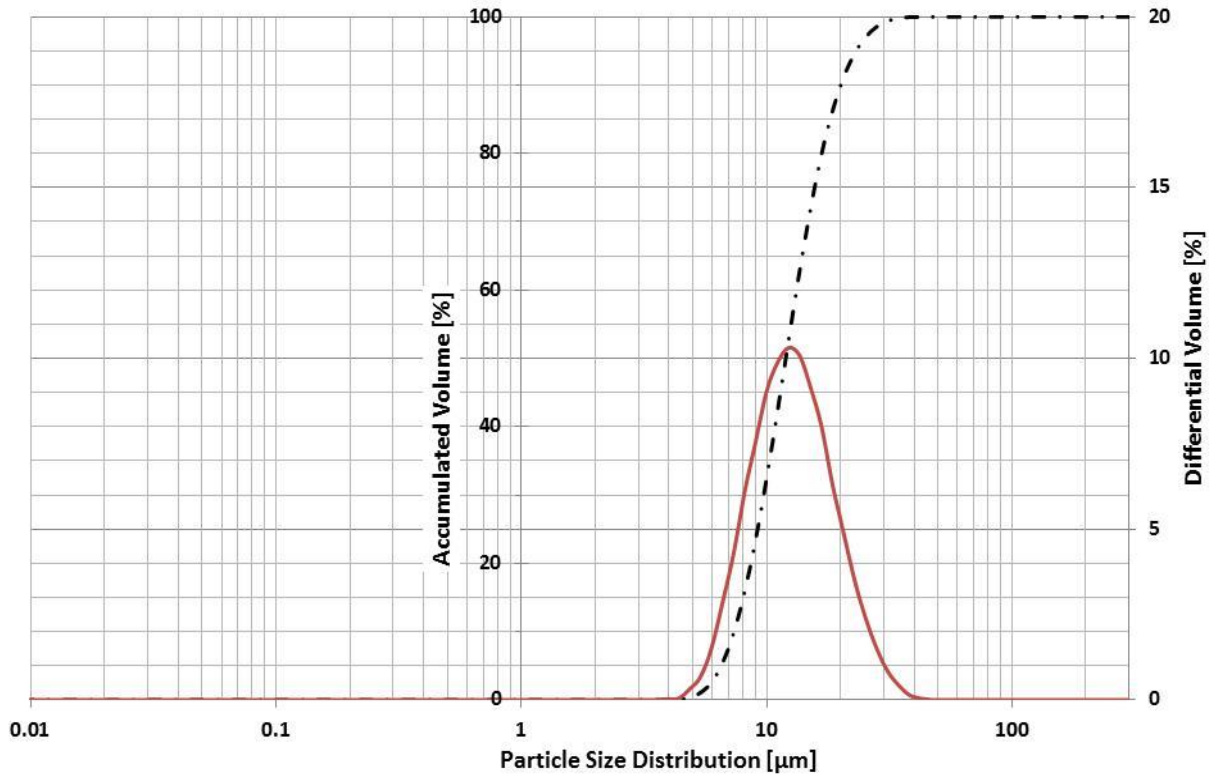


Figure 5.2: Particle size distribution profile of starting agglomerated  $\text{TiO}_2$  powders synthesized via simple hydrolysis method.

Single particle impact morphology, which is also known as the wipe test, was conducted to study the bonding mechanism of  $\text{TiO}_2$  powders on different types of substrates. Figure 5.3 shows the single impact morphologies of  $\text{TiO}_2$  powder that was synthesized by hydrolysis with addition of  $(\text{NH}_4)_2\text{SO}_4$  on ceramic tile, aluminum and copper substrates using similar spraying conditions. The results obtained revealed that different substrates led to different particle deposition behaviors. For hard ceramic tile substrate (Fig. 5.3-a), the  $\text{TiO}_2$  particles were found strongly deformed after collision while the surface of the ceramic tile remained unchanged.

Moreover, the splat diameters were similar or smaller than the initial diameter of the feedstock powder. However, in the case of copper and aluminum substrate (Fig. 5.3-c & e), the splat diameters were mostly smaller than the feedstock powder and the substrates were found deformed by particle collision. These results showed that only a small part of the  $\text{TiO}_2$  particles managed to deform and adhere on the substrates when impacting on soft substrates. This was shown by the many craters observed on the surface of the substrates.

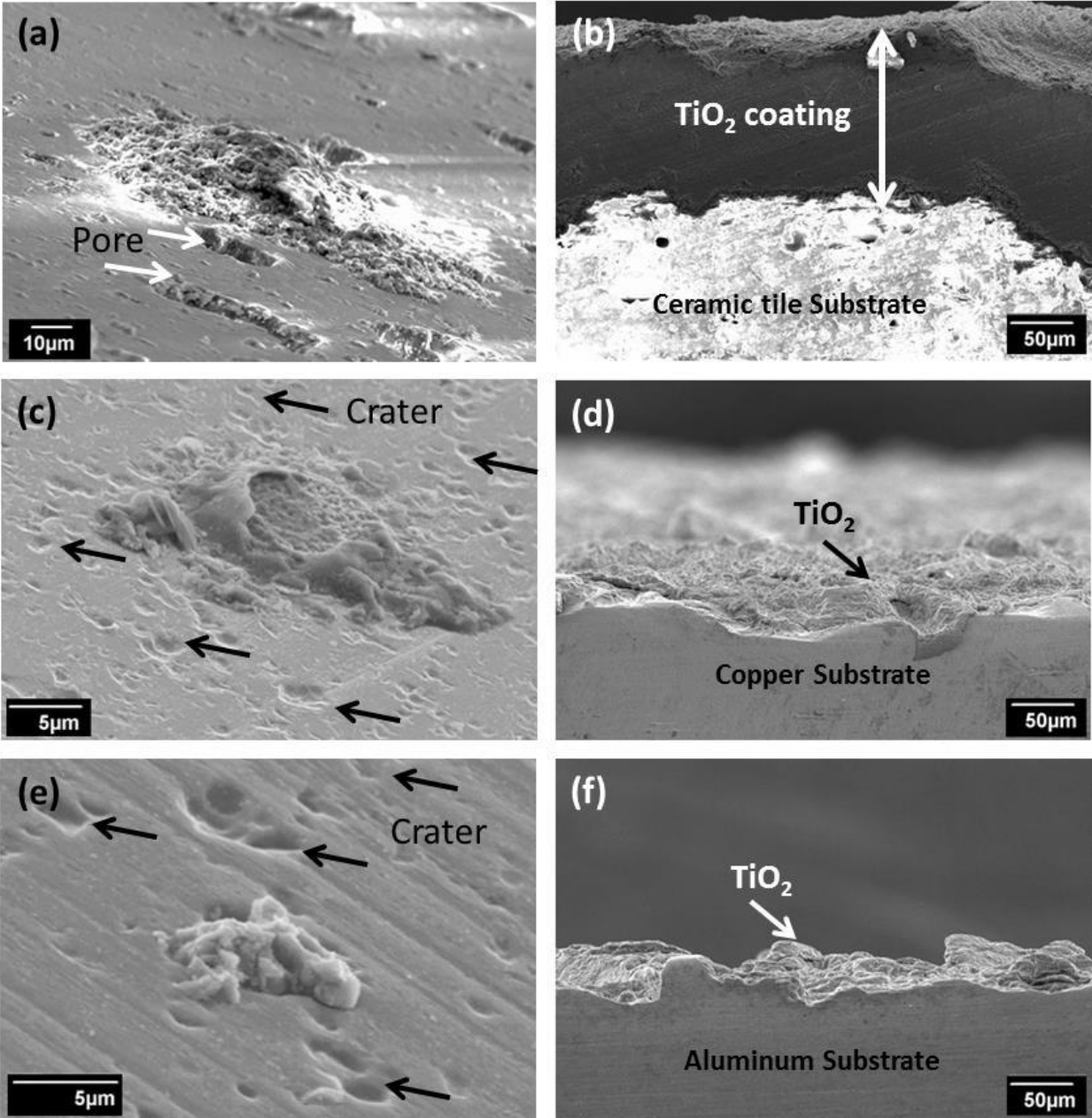


Figure 5.3: Single impact morphologies of TiO<sub>2</sub> particles and cross-sectional view of TiO<sub>2</sub> coating on different types of substrates: (a & b) ceramic tile, (c & d) copper and (e & f) aluminum, respectively. Pores and craters on the surface of substrates for single impact morphologies are indicated by white and black arrows, respectively.

To understand the reason why TiO<sub>2</sub> deposited differently on different types of substrates, the hardness of each substrate used in this experiment was measured using a Micro Vickers Hardness Tester. The hardness of ceramic tile, copper and aluminum were 551.7 HV, 105.3 HV and 28.8 HV respectively. Previous study undertaken by Trompeter et al [17] demonstrated that for solid particles impacting on a substrate, the substrate hardness played a significant role in the as-produced solid particles. The collision of TiO<sub>2</sub> particle on hard ceramic tile was suspected to experience sufficient impact energy which completely converted into the plastic deformation of the particles within a shorter time compared to softer substrates [18]. Moreover, the TiO<sub>2</sub> particles suffered heavy deformation when impacting onto the hard ceramic tile. It is expected that the TiO<sub>2</sub> particles used in this study have lower hardness and are softer when compared to the ceramic tile substrate due to the porous structure of the synthesized TiO<sub>2</sub> powders. Therefore, the agglomerated TiO<sub>2</sub> deformed when impacting onto a harder substrate such as ceramic tile.

Conversely, for soft substrates such as aluminum and copper, the TiO<sub>2</sub> particles were impacting the surface with minimal deformation, and the particles rebounded after the impact, leaving craters on the surface of the substrate. K.-R. Ernst et al [18] also mentioned that for soft substrate, impact energy that was generated during the spraying process was also used for deformation of the substrate. Furthermore, the results in this study revealed that the morphology of the single impacted particle on the copper substrate and aluminum substrate were also dissimilar. The size of the TiO<sub>2</sub> particle that adhered on the copper substrate was relatively bigger than the particle that was observed on the aluminum substrate and the depth of the resulting craters was significantly different. Since aluminum has lower hardness in comparison with copper, the depth of the craters were deeper and experienced heavy damage, as seen in the

observed SEM image in Fig. 5.3 (e). However, Fig. 5.3 (c) shows that the impacting particles on copper substrate are only fragments of the TiO<sub>2</sub> particle at the edges of the impact area but with only a small amount of TiO<sub>2</sub> adhered at the center of the impact area.

In addition to the substrate hardness, the surface roughness of the substrate also plays an important role. The surface roughness was  $6.7 \pm 0.4 \mu\text{m}$ ,  $2.6 \pm 0.1 \mu\text{m}$  and  $1.3 \pm 0.2 \mu\text{m}$  for ceramic tile, copper and aluminum substrate respectively. From the SEM observation as shown in Fig. 5.3, the substrates were found to have different characteristics even after being polished to a mirror finish surface condition before the wipe test was conducted. Copper and aluminum substrates have a smooth surface after the polishing process. Meanwhile for ceramic tile substrate, pores which originally existed in the ceramic tile were still being observed on its polished surface. The rough surface due to presence of pores may ease particle adherence on the surface of the substrate. This also explains why a thick coating of approximately  $140 \mu\text{m}$  was successfully deposited on ceramic tile (Fig. 5.3-b) whereas only particle embedment was observed on the surface of copper (Fig. 5.3-d) and aluminum (Fig. 5.3-f) substrate. The results of this study suggested that the increase of surface roughness leads to an increase in the particle-to-surface interface contact area, consequently increasing the chemical bonding between the particles and substrate [2, 18]. In contrast to the findings of a previous study [17], harder substrate shows a better TiO<sub>2</sub> deposition than the softer substrate. These results showed that the deposition mechanism of cold-sprayed ceramic particles also depends on the characteristics of the starting powder such as the powder synthesis process, crystallinity, agglomeration, particle size, density and shape. Based on this finding, Fig. 5.4 illustrates the schematic diagram of the possible mechanism for TiO<sub>2</sub> deposition onto soft and hard substrates.

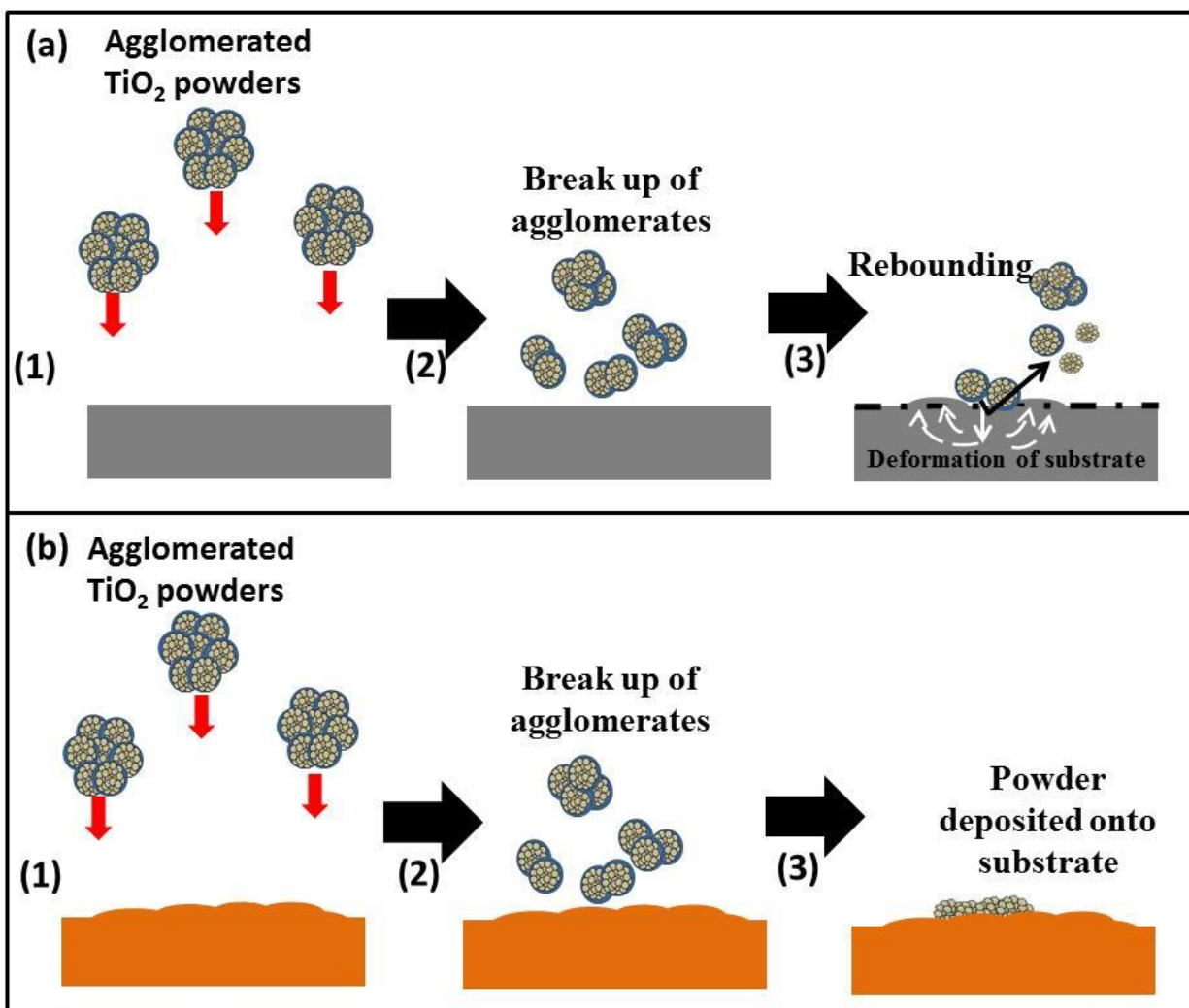


Figure 5.4: Schematic diagram of possible deposition mechanism of agglomerated  $\text{TiO}_2$  on different substrate: (a) soft substrate; copper and aluminum and (b) hard ceramic tile substrate.

As no defined coating was observed on the copper and aluminum substrates, XRD measurement was conducted only on the coating that was obtained on ceramic tile substrate. Figure 5.5 shows the XRD patterns of the as-synthesized  $\text{TiO}_2$  and coatings deposited by cold

spray on ceramic tile substrate. The results revealed that the phase composition of both as-synthesized powder and coating was only the anatase phase, which is more effective than the rutile phase as a photocatalyst. This result also indicates that the newly formed phase was absent suggesting that no phase transformation occurred during the cold spray process. Since the process temperature used in this experiment was only 500°C, which is below the melting temperature of TiO<sub>2</sub>, and also below the phase transformation temperature which occurs above 900°C [3,19], it is not surprising that the crystalline structure of the starting powder can be preserved in the as-deposited coating. However, grain refining was expected to occur in the prepared coating as shown by a broadened XRD peak for the coating as compared to the starting powder.

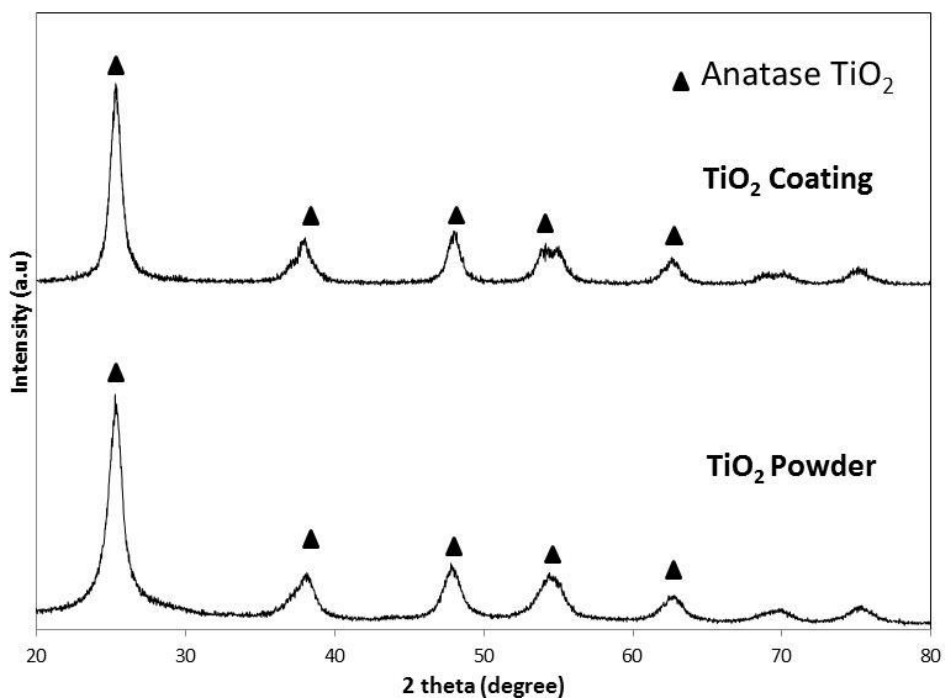


Figure 5.5: XRD pattern of as-synthesized TiO<sub>2</sub> and the coating deposited on ceramic tile substrate by cold spray process.



Grain refinement in the coating was also observed on its cross-sectional view at higher magnification as shown in Fig. 5.6. The SEM image shows that the coating was composed of the breaking up of agglomerated TiO<sub>2</sub> particles which can be proved by the absence of particles that have a similar size to the tertiary particles in the feedstock powder. Moreover, the initial secondary particles of the agglomerated TiO<sub>2</sub> have the size of ~0.5-2.0 μm (Fig. 5.1-c). However, the size of certain TiO<sub>2</sub> grains, as shown in region-(b) of Fig. 5.6, in the coating is smaller when compared to the starting feedstock particles. The breaking up of TiO<sub>2</sub> particles is attributed to the coating formation due to the fragmentation of agglomerated particles when impacting onto the substrate. Plastic deformation in ceramic materials was suspected to occur during this process as the high kinetic energy present during the cold spray process induced dislocations in the fragmented ceramic particles, which contain nanoparticles, due to multiple collisions during particle impact [7].

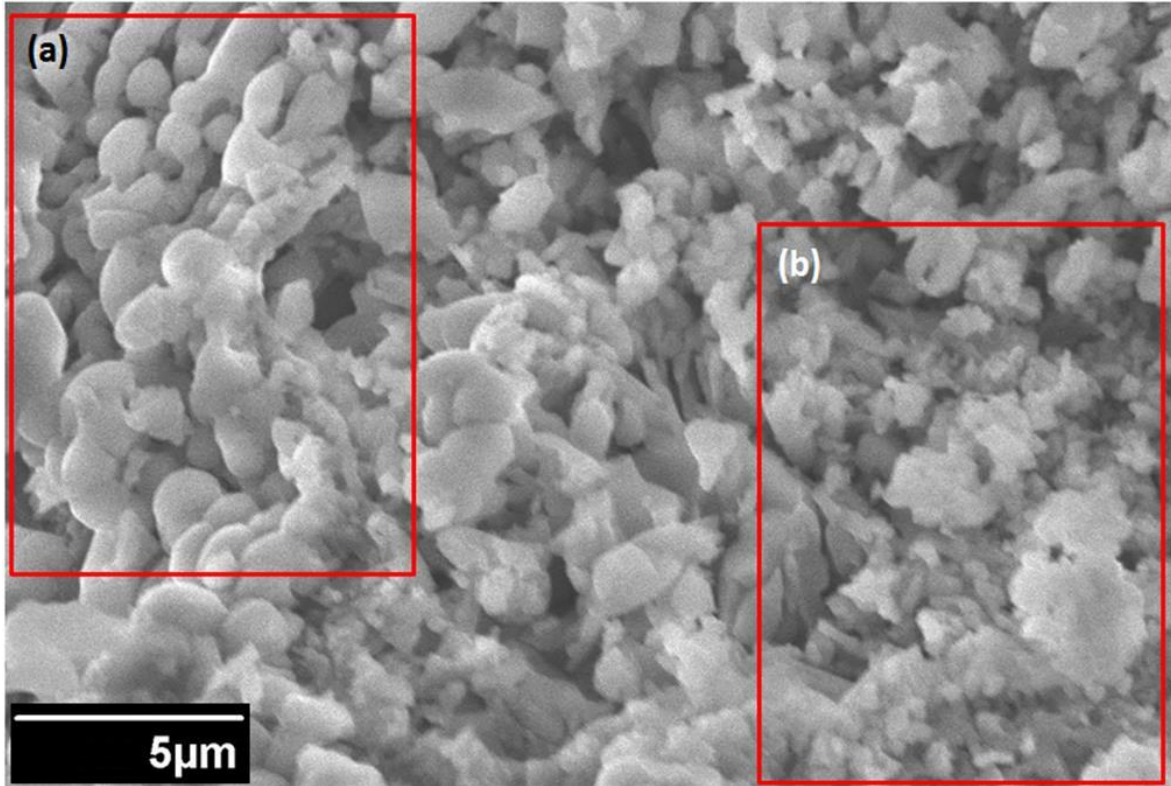


Figure 5.6: Fractured cross-section of  $\text{TiO}_2$  coating on ceramic tile substrate at high magnification. The inset in (a) and (b) are the evidence of presence of different size of fractured  $\text{TiO}_2$  particles after cold-sprayed coating.

## 5.4 Conclusions

In this study, single particle impact and powder deposition on different type of substrates was conducted by cold spray process. Agglomerated TiO<sub>2</sub> powders synthesized by simple hydrolysis method were used as feedstock materials. The results obtained in this study are summarized as the following:

1. Crater formation on the surface of the substrate depends on the properties of the substrates.
2. For hard substrate such as ceramic tile, the substrate surface was not deformed when the TiO<sub>2</sub> particles were impacting on its surface. The TiO<sub>2</sub> particles which have lower hardness than ceramic tile were deformed and successfully deposited on the substrate. Therefore, in order to make TiO<sub>2</sub> coating, the feedstock powders should have lower hardness than the substrate material.
3. For softer substrate such as copper and aluminum, rather than deforming on the substrate, the TiO<sub>2</sub> particles were rebounded and left craters on the surface of the substrate. The depth of the craters also depends on the hardness of the substrate.
4. Roughness of the substrates also contributes to the formation of TiO<sub>2</sub> coating on the substrate. Increased in surface roughness may ease the particles to adhere on the substrate.
5. No phase transformation occurred during and after the cold spray deposition as the TiO<sub>2</sub> coating on ceramic tile maintained the crystal structure of anatase phase.

## 5.5 References

- 1) M. Gardon and J.M. Guilemany: *J. Therm. Spray Technol.*, 23 (2014) 577-595.
- 2) M. Gardon, C. Fernández-Rodríguez, D. Garzón Sousa, J.M. Doña-Rodríguez, S. Dosta, I.G. Cano and J.M. Guilemany: *J. Therm. Spray Technol.*, 23 (2014) 1135-1141.
- 3) N.T. Salim, M. Yamada, H. Nakano, K. Shima, H. Isago and M. Fukumoto: *Surf. Coatings Technol.*, 206 (2011) 366-371.
- 4) M. Yamada, Y. Kandori, K. Sato and M. Fukumoto: *J. Solid Mech. Mater. Eng.*, 3 (2009) 210-216.
- 5) J.-O. Kliemann, H. Gutzmann, F. Gärtner, H. Hübner, C. Borchers and T. Klassen: *J. Therm. Spray Technol.*, 20 (2010) 292-298.
- 6) H.Y. Lee, S.H. Jung, S.Y. Lee, Y.H. You and K.H. Ko: *Appl. Surf. Sci.*, 252 (2005) 1891-1898.
- 7) Y. Liu, J. Huang and H. Li: *J. Therm. Spray Technol.*, 23 (2014) 1149-1156.
- 8) A. R. Toibah, M. Sato, M. Yamada and M. Fukumoto: *Mater. Manuf. Process.* 31 (2016) 1527-1534.
- 9) M. Yamada, H. Isago, K. Shima, H. Nakano and M. Fukumoto, *Proc. ITSC 2010, Thermal Spray: Global Solutions for Future Applications*, May 3-5, Singapore, (2010), pp. 187-191.
- 10) H. Park, J. Kwon, I. Lee and C. Lee: *Scr. Mater.*, 100 (2015) 44-47.
- 11) L. Pawlowski: *Surf. Coatings Technol.*, 202 (2008) 4318-4328.
- 12) R.S. Lima and B.R. Marple: *J. Therm. Spray Technol.*, 16 (2007) 40-63.
- 13) S. Ravanbakhsh, H. Assadi, H. Nekoomanesh, A. Hassanzadeh and E. Taheri-Nassaj, *Thermal Spray 2011: Proceedings of the International Thermal Spray Conference*,

- September 27-29, Hamburg, Germany (2011), pp. 303 - 307.
- 14) M. Yamada, M. E. Dickinson, K. Shima, N. Tjitra Salim, H. Nakano and M. Fukumoto, Thermal Spray 2011: Proceedings of the International Thermal Spray Conference, September 27-29, Hamburg, Germany (2011), pp. 308-313.
  - 15) G. J. Yang, C. J. Li, F. Han, W. Y. Li and A. Ohmori: Appl. Surf. Sci., 254 (2008) 3979-3982.
  - 16) J. Vlcek, L. Gimeno, H. Huber and E. Lugscheider: J. Therm. Spray Technol., 14 (2005) 125-133.
  - 17) W. Trompetter, M. Hyland, D. McGrouther, P. Munroe and A. Markwitz: J. Therm. Spray Technol., 15 (2006) 663-669.
  - 18) K.-R. Ernst, J. Braeutigam, F. Gaertner and T. Klassen: J. Therm. Spray Technol., 22 (2012) 422-432.
  - 19) M. Yamada, H. Isago, H. Nakano and M. Fukumoto: J. Therm. Spray Technol., 19 (2010) 1218-1223.

## 6 General Conclusions & Recommendations for Future Work

### 6.1 General Conclusions

The main interest of this study is to fabricate  $\text{TiO}_2$  coating for photocatalytic applications by maintaining the properties of the initial feedstock materials. Nanostructured materials offer the potential significant improvement on the photocatalytic activity as compared to conventional powders. Then, because of this reason, in this study, attempts have been made to fabricate thick  $\text{TiO}_2$  coating by thermal spray process using nanostructured powders as feedstock materials. Since preservation of the original properties of the feedstock materials is very important, cold spray method has been chosen to deposit the coating on the substrates due to its processing temperature which is below the melting temperature of  $\text{TiO}_2$ .

In order to achieve the objective to produce anatase  $\text{TiO}_2$  coating which work more effective for the degradation of harmful pollutants, a careful selection of synthesis method need to be chosen. However, feeding powders in submicrometer-sized have to be used to deposit cold spray coating using conventional powder feeder in order to feed them without blockage. Instead of using spray drying process which requires additional cost and may lead to change in the properties of the nanopowders, careful selection of synthesis method to produce  $\text{TiO}_2$  powders can be one of the solutions to produce agglomerated  $\text{TiO}_2$  powders which naturally united together due to van der Waals attraction. Natural agglomeration of nanoparticles of  $\text{TiO}_2$  powders up to submicrometer-sized can be achieved by addition of structure directing agent.

In this study,  $\text{TiO}_2$  coatings were successfully deposited by cold spray process using agglomerated powders which formed from primary particles of nanostructured materials. Factors

that contribute to the coating deposition have been investigated throughout of this study. The results revealed that the proper selections of synthesis methods, feedstock particle size, crystallinity of the powder, porosity contain in the powders and properties of the substrate materials affect the coating deposition by cold spray. From this study, the following factors can be concluded plays important role for the ceramic material deposition by cold spray process:

### **6.1.1 Feedstock particle size**

Suitable synthesis method is very crucial to determine the final phase content in the powder. Sulfate process has been chosen in this study as it shows higher possibility to produce higher amount of anatase phase instead of rutile phase. Moreover, this process also allows inhibiting the phase transformation from anatase to rutile which occurs at higher temperature as compared to chloride process. Design of the agglomerated nanostructured feedstock powder in submicrometer-sized with homogeneous particle distribution can be achieved by simple hydrolysis method as discussed in Chapter 2. The size of the feedstocks powder produced by this method not only provided effective supply in the powder feeder system which can prevent blockages from occur during the spraying process, but also can contribute to higher rate of successful deposition of  $\text{TiO}_2$  powder onto the substrate. Meanwhile, in case of  $\text{TiO}_2$  powder that synthesized by hydrothermal method, the produced powder were in dispersed distribution and also have broad particle distribution. This powder is not suitable for cold spray deposition as bigger particles tend to rebound upon the impact due excess of kinetic energy.

### 6.1.2 Porosity

Space between the nanoparticles or known as porosity plays significant role during the deposition of ceramic particles by cold spray process. Porosity in the powder functions as initiator for the particles to fragment/ breaking up upon the collision. Porosity in the as-synthesized TiO<sub>2</sub> powders can be controlled by proper selection of synthesis method, post heat treatment such as calcination process and also by addition of structure directing agent. This criterion has been discussed in details in Chapter 2, 3 and 4. In chapter 3, calcination at low temperature which is less than 500°C was conducted due to less progressive growth of crystallite size. The slow progressive growth contributed to less densification of particles which resulting in presence of some porosity in the powder. The porosity in the powder also can be controlled by addition of (NH<sub>4</sub>)<sub>2</sub>SO<sub>4</sub> during the synthesis. Higher mol % led to increase the nucleation rate during the synthesis resulting higher rate of agglomeration of the particles which reduce number of space between the primary particles. In case of high amount of porosity in the feedstock powder, it contributed to heavy breakage of agglomerates under extreme condition during cold spraying which in turns contribute to less tamping effect during the collision between the particle-particle interactions. On the other hand, if the powder contains less porosity as calcined at higher temperature, the dense particle experienced formation of stronger agglomerated particles led to fracture resistance upon impact onto the substrate.

### 6.1.3 Crystallinity

Coating deposition also was influenced by the crystallinity of the feedstock powder. This factor has been discussed in Chapter 2. The results obtained reveal that powder that has lower



crystallinity was easier to be deposited by cold spray. This is due to crystalline bridge that hold the particles is weaker than the powder that synthesized by hydrothermal method.

#### **6.1.4 Substrate materials**

This study shows that not only powder feedstock is important to deposit cold spray coating, but selection of suitable substrate material is also essential. It was found that higher hardness and surface roughness of the substrate provides easy interaction between the particle-substrate contact areas. Harder substrate material led to possibility of the TiO<sub>2</sub> particles to be deformed. On the other hand, a soft substrate damps the particle impact by consuming a significant part of the impact energy for its own deformation. Therefore, the spray particles rebounded instead of impinged onto the substrate.

## 6.2 Recommendations for Future Work

Some recommendations can be made from the results obtained and observations made during the studies. Further steps, new and modified procedures can be made such as:

- 1) Photocatalytic test of the as-prepared TiO<sub>2</sub> coating. Study the possibility of depositing cold sprayed TiO<sub>2</sub> coating for degradation of contaminants.
- 2) Addition of metal element such as aluminum, iron, nickel, vanadium etc. during the TiO<sub>2</sub> synthesis process. In this way, it can provide new opportunities for TiO<sub>2</sub> deposition by cold spray process on the metal substrates as the metal element would provide better plastic deformation for facilitation the adhesion of the ceramic particles. Moreover, some studies show that introduction of metal-ions into TiO<sub>2</sub> can improve the photocatalytic performance under visible-light due to effective charge transfer from the metal-ions to Ti-ions.
- 3) Details observation of TiO<sub>2</sub> coating by TEM analysis should be conducted in future study in order to clarify the bonding between the particles and substrate and also between the particle and particle by dislocation of particles which contribute to plastic deformation.

## 7 Contribution of Study

### 7.1 Contribution of This Study to the Research/ Academic Field

- 1) The agglomeration of nanosized particles into microscopic particle ranged which synthesis by simple hydrolysis method in this study as feedstock materials not only provide new opportunities to prepare cold spray coating but also can be future prospect spray materials for other types of thermal spray process to avoid blockage in the feeding system. Therefore, the need of spray drying and post treatment that require for removing the binder which has been used to bind the nanoparticles can be eliminated.
- 2) Moreover, the use of nanostructured powder as starting material to prepare TiO<sub>2</sub> coating in this study also can be preserved after the coating process. This result revealed that nanostructured anatase was present on the surface and cross-section of the TiO<sub>2</sub> coating as reveal by FESEM image at high magnification and also by XRD analysis. The nano-anatase TiO<sub>2</sub> coating is believed can perform well as photocatalyst as compared to micro-anatase TiO<sub>2</sub> or rutile TiO<sub>2</sub> coating.
- 3) This study is just a start for future studies regarding ceramic coating by cold spray process. The results obtained in this study shows that it is possible to deposit ceramic materials, which known quite difficult to be deposited by this coating process due to the brittle nature of the powders. However, at certain conditions, such as presence of nanostructured powders together with some amount of porosity which use to initiate the fracture upon the impact on the substrate, coating deposition can be possible to be formed

by cold spray. This result open new opportunities on potential applications of thick and large area for preparation of ceramic coating.

## **7.2 Contribution of This Study to the Industrial Field**

- 1) Promising results that reveal in this study shows that cold spray can be a good alternative to prepare anatase and nanostructured TiO<sub>2</sub> coating on ceramic tiles. This technology can be applied specifically in the field of construction especially in the urban areas as photocatalyst to clean the environment from pollutants. This technology not only applicable for outdoor applications such as for the wall of building but also for indoor application to preserve the indoor air quality such as in gymnasium, hospitals, smoking area in the train and etc.
- 2) The application of these micro-ranges sized of nanostructured powders can reduce the issues related to the human health risk involved in working with spraying of nanoparticles and offers more friendly working environment.

## 8 Publications List and Oral Presentations

### 8.1 List of Papers/Journals and Proceedings with Referee's Review

#### 8.1.1 List of Journals

1. **A. R. Toibah**, M. Sato, M. Yamada & M. Fukumoto, "Cold Sprayed TiO<sub>2</sub> Coatings from Nanostructured Ceramic Agglomerated Powders," *Materials and Manufacturing Processes*, 31: 1527-1534, 2016. DOI:10.1080/10426914.2015.1090587.
2. **Toibah Abd Rahim**, Keisuke Takahashi, Motohiro Yamada & Masahiro Fukumoto, "Effect of Powder Calcination on the Cold Spray Titanium Dioxide Coating," *Materials Transactions*, 57 ( No.08 ) : 1345-1350, 2016.

#### 8.1.2 List of Proceedings

1. **Toibah Binti Abd Rahim**, Manabu Sato, Motohiro Yamada, Masahiro Fukumoto, "Synthesis and Deposition Behavior of Cold-Sprayed Agglomerated TiO<sub>2</sub> Powders," 7th Asian Thermal Spray Conference, Xi'an, China, 23-25 SEPTEMBER 2015, pp. 28-29.
2. **Toibah Binti Abd Rahim**, Manabu Sato, Motohiro Yamada, Masahiro Fukumoto, "Synthesis Of Agglomerated TiO<sub>2</sub> Powder For Cold Spray Application", JAPAN THERMAL SPRAY SOCIETY, 2014 JTSS Fall Meeting, Aichi Japan, 5-6 NOVEMBER 2014, pp. 55-56.

3. Manabu Sato, **Toibah Binti Abd Rahim**, Yuta Watanabe , Motohiro Yamada, Masahiro Fukumoto, “ Effect Of Heat Treatment Of Titanium Oxide Powder On The Coating By Cold Spray Method”, JAPAN THERMAL SPRAY SOCIETY, 2014 JTSS Fall Meeting, Aichi Japan, 5-6 NOVEMBER 2014, pp. 63-64.

## 8.2 Oral presentations

1. **Toibah Binti Abd Rahim**, Manabu Sato, Motohiro Yamada, Masahiro Fukumoto, “Synthesis of Agglomerated TiO<sub>2</sub> Powder for Cold Spray Application”, Japan Thermal Spray Society, 2014 JTSS Fall Meeting, Aichi Japan, 5-6 NOVEMBER 2014.
2. Manabu Sato, **Toibah Binti Abd Rahim**, Yuta Watanabe , Motohiro Yamada, Masahiro Fukumoto, “Effect Of Heat Treatment Of Titanium Oxide Powder On The Coating By Cold Spray Method” , JAPAN THERMAL SPRAY SOCIETY, 2014 JTSS Fall Meeting, Aichi Japan, 5-6 NOVEMBER 2014.
3. **Toibah Binti Abd Rahim**, Takahashi Keisuke, Motohiro Yamada, Masahiro Fukumoto, “Effect Of Heat Treatment on Morphology and Crystallinity of Cold-Sprayed Nanostructured TiO<sub>2</sub> Coating”, 5th International Conference on the Characterization and Control of Interfaces for High Quality Advanced Materials (ICCCI 2015) , Kurashiki, Japan, 7-10 JULY 2015.

4. **Toibah Binti Abd Rahim**, Manabu Sato, Motohiro Yamada, Masahiro Fukumoto, “Synthesis and Deposition Behavior of Cold-Sprayed Agglomerated TiO<sub>2</sub> Powders”, 7th Asian Thermal Spray Conference, Xi’an, China, 23-25 SEPTEMBER 2015.
  
5. **Toibah Binti Abd Rahim**, Motohiro Yamada, Masahiro Fukumoto, “Synthesis And Properties of Agglomerated TiO<sub>2</sub> Powder Synthesized By Hydrolysis and Hydrothermal Methods for Cold Spray Coating”, The 5th International Conference on Solid State Science and Technology (ICSSST 2015), Langkawi, Malaysia, 13-15 DECEMBER 2015.

## 9 Acknowledgements

I would like express the deepest appreciation to my supervisors, Prof. Dr. Masahiro Fukumoto and Assistant Prof. Dr. Motohiro Yamada, whose expertise, generous guidance and full support, understanding and encouragement throughout my three years of study and research. Without their guidance and persistent help, this thesis would not have been possible. I am also largely indebted to their kindness and help during my living in Toyohashi, Japan.

I would like to thank my PhD thesis committee members, Prof. Masanobu Izaki, Associate Prof. Seiji Yokoyama and Associate Prof. Toshiaki Yasui, for their valuable discussions and suggestions for improvement of the thesis.

My sincere appreciation also goes to all the members of the Interface and surface Fabrication Laboratory, Department of Mechanical Engineering, Toyohashi University of Technology, for their help and cooperation during my study. I am highly indebted and grateful to all the cold spray group members: Watanabe-san, Sato-kun, Ishihara-kun, Yoshida-kun, Takahashi-kun, Tomida-kun, Nakanishi-kun and Mori-kun for their valuable discussion and help during my experimental works. I also wish to acknowledge the support received from the administration and technical staff of Toyohashi University of Technology during my PhD journey.

I would like express my sincere gratitude to my sponsors; Ministry of Higher Education Malaysia and Universiti Teknikal Malaysia Melaka for their financial support and giving me the opportunity to do the PhD.



It is my privilege to thank my dear husband, Mr. Khairul and my childrens; Irsyad, Irdina, Irfan and baby Zahin, for their constant encouragement, love and understanding throughout this PhD journey. Also, to all my family members and friends for all the motivation words and supports which help me to survive, not letting me give up and keep me going to achieve my dreams.